IEZ
Institut für Evolutionsbiologie
und Zooökologie

universitätbonn

Species Identification and Delimitation in Nemerteans

Dissertation

Zur Erlangung des Doktorgrades (Dr. rer. nat.)
der Mathematisch-Naturwissenschaftlichen Fakultät der
Rheinischen Friedrich-Wilhelms-Universität Bonn

vorgelegt von
Daria Krämer
aus Bergisch Gladbach

Bonn 2016

Angefertigt mit Genehmigung der
Mathematisch-Naturwisschenschaftlichen Fakultät der Rheinischen Friedrich-Wilhems-Universität Bonn

1. Gutachter: Prof. Dr. Thomas Bartolomaeus
Institut für Evolutionsbiologie und Ökologie, Universität Bonn

2. Gutachter: Prof. Dr. Per Sundberg
Department for Marine Sciences, University of Gothenburg

Tag der Promotion: 16.12.2016
Erscheinungsjahr: 2017

Für meine Geschwister Birgit und Raphael Krämer

Danksagung

Es ist fast unmöglich, hier allen Personen zu danken, aber ich gebe mein Bestes. Ein großes Dankeschön gilt Prof. Dr. Thomas Bartolomaeus, der mich in die Arbeitsgruppe aufgenommen und das Thema bereitgestellt hat. Der größte Dank gilt dabei Dr. Jörn von Döhren, der mich und diese Arbeit in den letzten Jahren betreut hat: Danke für jede Antwort auf jede Frage, für jede Diskussion und jede Aufmunterung (vor allem in den letzten Wochen)!

Besonders bedanken will ich mich bei Prof. Dr. Per Sundberg. Nicht nur für die Begutachtung dieser Arbeit, sondern auch für die Zeit in Göteborg. Ihm und den Mitgliedern seiner Arbeitsgruppe, allen voran Dr. Leila Carmona, Svante Martinsson, Dr. Matthias Obst, Prof. Dr. Christer Erséus und Prof. Dr. Urban Olsson bin ich aus tiefstem Herzen dankbar. Die Zeit hat mich unglaublich motiviert: Tack så mycket/muchas gracias for everything!

Nicht zu vernachlässigen sind für diese Zeit Eva Bäckström, Sonja Miettinen, Josefine Flaig, Florina Lachmann und Hasan Albahri: Ihr habt Göteborg für mich zu einem Zuhause gemacht! In diesem Zuge danke ich dem DAAD für das Stipendium, das mir das Arbeiten in Schweden überhaupt erst ermöglichte.

Zurück nach Bonn:

Ich möchte mich zu allererst bei Prof. Dr. Lukas Schreiber und Prof. Dr. Gerd Bendas für die Teilnahme an der Prüfungskommission bedanken!

Elise M. J. Laetz bin ich unglaublich dankbar, nicht nur für die Korrektur der englischen Sprache, sondern auch für die jahrelange Freundschaft!

Meinen Kollegen aus der der AG Bartolomaeus und AG Bakker danke ich für die angenehme Zusammenarbeit im Institut: Dr. Lars Podsiadlowski, Dr. Patrick Beckers, Dr. Markus Koch, Dr. Alexander Ziegler, Dr. Jörg Brün, Dr. Björn Quast, Sebastian Martin, Peter Lesny, Björn Müller, Dr. Ingolf Rick, Simon Vitt und Dr. Marion Mehlis danke ich für jedes offene Ohr, für jede Tafel Schokolade und jeden Ratschlag! Claudia Müller, Christiane Wallnisch, Tatjana Bartz, Kirsten Hennes und Anja Bodenheim danke ich, nicht nur wegen ihrer Unterstützung im Labor und bei allen möglichen organisatorischen Angelegenheiten, sondern auch für jedes Gespräch, jeden Keks und

jede amüsante Diskussion über meinen Kleidungsstil! Am meisten ertragen musste mich jedoch Dr. Ekin Tilic: Vielen Dank für deine Freundschaft und jeden „fetten Diss“!

Ein riesiger Dank gilt den Menschen aus meinem Leben außerhalb der Immenburg. Jana Groß, Jeanette Gajek, Rana Diegel, Henriette Krimphoff und Lara Seeger danke ich für jahrelange und neue Freundschaften und dafür, dass sie mir immer wieder zeigen was wirklich wichtig ist (und mich in den letzten Wochen mit Essen versorgt haben).

Meinen Geschwistern Birgit und Raphael und meinen Eltern Irene und Erwin möchte ich danken, da sie mich in einem liebevollen und geschützten Umfeld haben aufwachsen lassen. Ich bin dankbar für jede Unterstützung und jede Neckerei der letzten 28 Jahre!

Siegrid und Jochen Sechtem danke ich, da sie strenggenommen mit der Wattwanderung auf der Insel Föhr für meine erste meeresbiologische Exkursion, im Alter von sechs Jahren, verantwortlich waren.

Summary

The accurate identification and delimitation of species constitute the basis for assessing the biodiversity and phylogenetic relationships within the taxon Nemertea. However, working on nemertean taxonomy is challenging for many reasons. The external and internal morphology are relatively simple with only a few diagnostic characters. This makes it very difficult to identify species based solely on visual inspection. Additionally, the muddled taxonomic history of many genera and species hampers assigning identified species to the current systematic background.

As observed in many other taxa, the identification and delimitation of nemertean species has shifted from traditional morphological-based to molecular-based taxonomy. The usage of either methodology bears its own pitfalls. Most of our taxonomic knowledge is based on morphological data and relies on histological sections, which are difficult to compile and analyze. Additionally, the overall interpretation of morphological characters lacks a widely applied standard and is therefore subjective. DNA taxonomy holds great promise for faster species identification. This methodology is based on the comparison of sequence data, relying on the presence of a barcoding gap and high coverage of the target taxa within sequence databases. The latter is, however, not given in a majority of nemertean species, rendering a DNA-based approach for species identification problematic.

Within this thesis, I present three representative examples encountered in nemertean taxonomy. Chapters 2 and 3 concern the description of previously unknown species, one of which represents a cryptic species. Chapter 4 deals with the re-description of a nemertean species with a confusing nomenclatural history. With this thesis I give suggestions as to how species can be delimited, identified, and described in the future. I conclude that in most cases, an integrative taxonomic approach combining molecular data, external characters, and histological-based morphology constitute a stable background to safely delimit and identify nemertean species. The species descriptions presented herein show that if one method fails or is of limited conclusiveness, the application of the other approaches can assist to succeed in delimiting species boundaries. Molecular sequence data are of major importance

especially in terms of identifying and delimiting cryptic nemertean species. In these cases, molecular sequence data combined with external characters present a solid basis for species descriptions. Furthermore, molecular sequence data should always be included in species descriptions even if its relevance is not immediately apparent. As more data is assembled, it should and will provide a solid backbone for future barcoding identification and phylogenetic reconstructions. I suggest basing species re-descriptions on more than just one methodology in an integrative taxonomic approach. Including data from different methodological or biological backgrounds allows assessing species boundaries from multiple perspectives and additionally provides a link to the traditional knowledge of nemertean taxonomy.

Table of Contents

Chapter 1
General Introduction

1.1 Introduction

Species represent the most fundamental unit in all subfields of biology, including physiology, behavioral biology, phylogeography, ecology, evolution, and genetics (Agapow *et al.* 2004; De Queiroz 2005, 2007). From the traditional point of view, species represent the basic group within the hierarchy of taxonomic categories i.e. genera, families, orders, and classes (Linnaeus 1753, 1758; Darwin 1859; De Queiroz 2005, 2007). Currently, species are considered the only unit within the hierarchy that represents both, a taxonomic category and a "naturally occurring particular" (Mayden 1977: 387). Species therefore signify the only taxonomic category which can be observed in nature and for which objective criteria can be defined (Mayr 1943, 1969; De Queiroz 2005).

The importance of the term "species" is contrasted by the absence of a general consensus of what a species truly represents (Agapow *et al.* 2004; De Queiroz 2007). Since speciation is an ongoing process, when attempting to delineate and identify a species, one must be aware that this unit is constantly evolving and therefore changing (De Queiroz 2007). In other words, it is "more or less impossible for humans to perceive entire species simply by looking at them" (De Queiroz 2007: 879). This is reflected by more than 20 different species concepts which emphasize different criteria as important prerequisites for identifying and delineating an organism or a group of organisms into a species (Mayden 1997; De Queiroz 2005).

The Ecological Species concept (EcSC) for example, regards species as similar individuals occupying the same ecological niche or adaptive zone (van Valen 1976). In addition to being a separately evolving metapopulation lineage, it also has to occupy a different niche in order to be considered species (De Queiroz 2007: 882). The phylogenetic species concept (PSC) defines species as the smallest group of self perpetuating organisms and specifies these according to four further properties: (1) Smallest group of self perpetuating organisms with a unique composition of characters,

termed Diagnosable Version of the PSC (Nelson & Platnick 1981; Cracraft 1983; Nixon & Wheeler 1990); (2) smallest group of self perpetuating organisms that form the least inclusive monophyletic group of individuals sharing derived character states, termed Monophyletic Version of the PSC (Rosen 1979; Donoghue 1985; Mishler 1985); (3) smallest group of self perpetuating organisms with a temporal series of populations in between two speciation events, termed Hennigian Version of the PSC (Meier & Willmann 2000; Balakrishnan 2005); (4) smallest group of self perpetuating organisms sharing genes which are derived from a common ancestral allele, termed Genealogical Version of the PSC (Baum & Shaw 1995). The most widely adopted concept is the Biological Species Concept (BSC) which defines a species as a group of successfully interbreeding individuals which are reproductively isolated from other such groups (Mayr 1942).

As different species concepts rely on different criteria, De Queiroz (2007) proposes a unified species concept. He emphasizes that all concepts share a common element, namely that species are "separately evolving (meta) population lineages", which is the only necessary prerequisite to defining a species. All criteria advocated by the different species concepts, such as differences displayed by genetic and ecological data or reproductive isolation constitute evidence in assessing species boundaries (De Queiroz 2007). Definitions, however, only make sense, if they provide criteria to recognize or identify the defined. Since separately evolving metapopulation lineages refer to a historical process, this definition, although unifying species concepts, does not provide sufficient criteria to indicate species-specific isolation and thus the existence of a species. All other species criteria of the different species concepts can thus be regarded as important operational criteria (De Queiroz 2007: 882). If fulfilled, they are lines of evidence or indicators for species. The choice of a specific species concept will therefore depend on the criteria needed to identify a species and thus follows a strictly pragmatic approach. It nevertheless holds true that the more secondary criteria are observable, the stronger the evidence for a species.

In the course of discovering biodiversity, assigning a scientific name to a species provides an important reference system to communicate our knowledge between the different disciplines of biology (Wheeler 2004; Dayrat 2005). In addition to naming a species, recognizing, identifying, classifying, and describing them represents the

framework for systematists and taxonomists (Simpson 1961; Mayr 1969; Wilson 1985; Padial *et al.* 2010). In this context, many of the criteria suggested by the different species concepts might not be observable or, in the case of the BSC, require long-term studies. Taxonomists therefore primarily rely on morphological data to be able to assign individuals to a species by visual inspection (Padial *et al.* 2010). Observable variation in morphology also provides circumstantial evidence for reproductive isolation (Martinsson 2016). In many cases, species are identified based on an integrative taxonomic approach, which can include all types of data from life-history data to characters that are of ecological, chemical, or ultrastructural nature (Will *et al.* 2005). However, recognizing species, identifying which criteria are considered important in their delimitation and describing them still relies on the taxa investigated and the taxonomists working on them (Sundberg *et al.* 2016).

In this thesis, I present three examples of how to recognize, delimitate, and describe species within the taxon Nemertea. The chapters included herein represent typical scenarios encountered in nemertean taxonomy: Chapter 2 deals with the description of a previously unknown species, Chapter 3 concerns the description of cryptic species and Chapter 4 deals with the redescription of species. With this thesis I discuss how species can successfully be delimited, identified, and described in the future. I further suggest which data have to be included for each of these situations.

1.2 Introduction Nemertea

The spiralian taxon Nemertea is a comparably small group of soft-bodied, vermiform animals with approximately 1,300 species currently accepted (Gibson 1995; Kajihara *et al.* 2008). Nemerteans possess an eversible proboscis situated in a fluid-filled cavity, which can be rapidly employed to catch annelids or small crustaceans (Gibson 1972, 1982; McDermott & Roe 1985; Thiel & Reise 1993; Thiel 1998). Most nemerteans are free-living, nocturnal predators that can be found in a broad spectrum of marine habitats. A few species are also known to occur in freshwater and terrestrial environments (Gibson 1972, 1982). Some species have been described as entocommensal (*Malacobdella* Blainville, 1827 living within bivalves) or epibiotic predators (*Carcinonemertes* Coe, 1902 living on brachyuran crabs and feeding on its

host's eggs) (Gibson 1967, 1972, 1982; Gibson & Jennings 1969; Wickham 1979, 1980).

As in many other taxa, studying nemerteans primarily involves the exploration of species diversity and the phylogenetic relationships among species (for nemertean phylogenies see: Thollesson & Norenburg 2003; Andrade *et al.* 2012, 2014; Kvist *et al.* 2014; for other taxa see: Weigert *et al.* 2014; González & Giribet 2015; Hallas & Gosliner 2015). Both approaches depend on an accurate taxonomic work which includes the identification and description of species. Despite this, working on nemertean taxonomy is challenging for many reasons. First, nemertean morphology is relatively simple, with very few accessible diagnostic characters (Strand & Sundberg 2005a; b; Chen *et al.* 2010; Sundberg *et al.* 2010; Fernández-Álvarez & Machordom 2013 Knowlton 2000; Strand & Sundberg 2005; Chen *et al.* 2010; Sundberg *et al.* 2010; Fernández-Álvarez & Machordom 2013). A considerable number of unrecognized cryptic species, which are morphologically indistinguishable, is thereby suspected to be present in this group (Appeltans *et al.* 2012). Second, a vast majority of nemertean species were described during the 18th and 19th centuries. During that time, especially during the early 18th century, species descriptions mainly consisted of a few notes on the external morphology and lack a clear diagnosis (Gibson 1985, 1995). Third, in most cases neither type localities were mentioned nor type material has been deposited. Most species descriptions are therefore linked to numerous problems complicating their identification and classification. Many identities of nemertean species and more inclusive taxa are muddled due to a series of synonymizations and reinstatements of taxonomic names conducted in the past. A majority of those decisions lack profound documentation, leaving present day researchers with numerous names and no reference to type material, type localities, or molecular data.

1.3 Nemertean morphology

Nemerteans exhibit a huge variety of coloration and coloration patterns and display a diversity of body sizes (Figure 1.1). They can vary from a few millimeters in interstitial forms such as *Ototyphlonemertes* species Diesing, 1863 up to 30m in length as observed in *Lineus longissimus* (Gunnerus, 1770), the longest invertebrate ever recorded. In

general, most species vary from a few cm up to 30cm in length (Gibson 1972, 1982). The anterior region (head region, cephalic lobe) can either be clearly demarcated and is much wider than the rest of the body (Figure 1.1 C) or (bluntly) pointed and of the same width as the rest of the body (Figure 1.1 A, C) (Gibson 1972, 1982, Sundberg *et al.* 2009a, 2016). The head region can further be discriminated from the rest of the body by the mouth opening and/or the proboscis pore which are visible as slits ventrally or at the anterior-most tip of the head (Figure 1.1 A: *Arenogigas armoricus* Krämer & von Döhren, 2015). The cephalic lobe is further distinguishable by the presence of lateral horizontal cephalic slits (*Cerebratulus* Renier, 1804, *Micrura* Ehrenberg, 1828, Figure 1.1 B: *Notospermus geniculatus* (Delle Chiaje, 1828) and *Lineus* spp. Sowerby, 1806) or transversal furrows (Figure1.1 B: *A. armoricus*, Figure 1.1. C: *Carinina ochracea* Sundberg *et al.*, 2009 and *Tubulanus sp.* Renier, 1804) (Figure 1.1). Many species also possess eyes, which are variable in number and arranged in different patterns near the margin of the cephalic lobe. The posterior end is pointed (Figures 1.1, 1.2), bears a caudal cirrus (in *Cerebratulus* and *Micrura*) or a caudal sucker (Figure 1.1. A: *Malacobdella grossa* (Müller, 1776)) (Gibson 1972, 1982, Sundberg *et al.* 2009a, 2016). Depending on the age and the intensity of the coloration of a specimen, some internal structures such as the brain, alimentary canal, larger blood vessels, reproductive system, or the proboscis apparatus are visible through the body wall (Figures 1.1, 1.2).

The **body wall** generally constitutes the epidermis, followed by the dermis and the body wall musculature. The epidermis consists of multiciliated columnar cells, a variety of glandular and sensory cells, and a basiepithelial nerve plexus (Norenburg 1985 and references therein; Beckers 2011; Beckers *et al.* 2013). The dermis consists of a layer of extracellular matrix (*ecm*) which can be arranged as a simple basal lamina or as a prominent layer interspersed by glandular cells (Bürger 1895; Pedersen 1968; Gibson 1982; Norenburg 1985). Interiorly, the dermis borders the body wall musculature, which consists of genus-specific arrays of circular, longitudinal, diagonal and dorsoventral musculature. The stratification of the body wall musculature constitutes an important diagnostic trait for the classification of nemerteans (Gibson 1972, 1982).

The **proboscis apparatus** is situated dorsal to the alimentary canal and consists of three major components: the proboscis, which is surrounded by the rhynchocoel and opens anteriorly to the exterior via the third component, the rhynchodaeum (Figure 1.2).

The proboscis apparatus and the alimentary canal are either anteriorly fused or are completely separated from one another. The latter condition is present in palaeo- and heteronemerteans and some polystiliferous hoplonemerteans. The proboscis apparatus opens at the proboscis pore, which is situated at anterior most part of the head. The mouth opening is situated posteriorly to the proboscis pore and opens at the ventral side of the head. The former condition is present in monostiliferous and most polystiliferous hoplonemerteans. The rhynchodaeum and the alimentary canal lead into a short chamber, the atrium, which opens as a single pore to the exterior at the tip of the head (Gibson 1972, 1982). The rhynchodaeum, however, constitutes a simple, ciliated tube that opens at the proboscis pore. The rhynchodaeum is absent in *Malacobdella* in which the proboscis opens into the dorsal wall of the foregut. The rhynchocoel begin with the proboscis insertion and ends blindly. The proboscis itself constitutes a long muscular organ formed by the invagination of the anterior body wall. It is therefore similarly layered as the body wall. The unarmed proboscis of palaeo- and heteronemerteans appears uniform throughout its length whereas the armed hoplonemertean proboscis is morphologically divisible into three regions. The anterior region constitutes a thick-walled tube, followed by the stylet bulb region, and a posterior blind-ending tube. The stylet bulb region consists of a muscular diaphragm that is adorned with the proboscis armature. The latter can comprise a single stylet on a cylindrical base (in Monostilifera) or several small stylets embedded on a stylet cushion (in Polystilifera). In the inverted state, the bulb region is anteriorly surrounded by accessory pouches containing reserve stylets. The armature is absent in *Malacobdella* (Figure 1.2) (Gibson 1972, 1982).

The **alimentary canal** constitutes a ciliated tube situated ventrally to the proboscis apparatus extending the full length of the body. The alimentary canal is functionally and morphologically divisible into different regions. In hetero- and palaeonemerteans the mouth opens into a stomach that leads into the intestine. In hoplonemerteans, the alimentary canal consists of an esophagus (a short tube connecting the atrium with the stomach), a stomach, and a pyloric tube which opens into the dorsal wall of the intestine. The intestine may constitute a simple tube as in some palaeonemerteans or bear multiple, laterally extending diverticula as in many hoplo-, heteronemertean and the remaining palaeonemertean species. In most

hoplonemerteans the intestine additionally possess a blind-ending, anteriorly extending intestinal pouch (intestinal cecum) (Gibson 1972, 1982).

The **reproductive system** is constituted by serially arranged, spherical gonads which are restricted to the intestinal region (Figure 1.2). In sexually mature specimens, the gonads open via short ducts to the exterior. The distal parts of the gonoducts are exteriorly visible as serially arranged pores (gonopores). With the exception of a few ovoviviparous and hermaphroditic species, most nemerteans are oviparous and are of separate sexes (Gibson 1972, 1982; Friedrich 1979; von Döhren *et al.* 2010; von Döhren 2015).

In its basic structure, the **blood vascular system** consists of a pair of lateral longitudinal blood vessels, transversally interconnected by an anterior cephalic and a posterior anal lacuna (Figure 1.2). This basic pattern can be found in many cephalothricid nemerteans (Palaeonemertea) but differs in other taxa and therefore constitutes another diagnostic trait. In many hoplo- and heteronemerteans a third longitudinal vessel is present, which penetrates the ventral rhynchocoel wall. The three main longitudinal vessels can be regularly linked by transverse connectives that alternate with the lateral gut diverticula in some Hoplonemertea and Heteronemertea (Bürger 1895; Gibson 1972, 1982).

The **excretory system** constitutes protonephridia, which are located within the foregut region. In its basic structure, the excretory system consists of a pair of branched tubes, in close relation to the blood vascular system. The excretory duct opens via a single or several nephridiopores to the exterior (Figure 1.2) (Gibson 1972, 1982; Bartolomaeus & von Döhren 2010)

The **nervous system** can be divided into a central nervous system and a peripheral nervous system (*sensu* Beckers *et al.* 2013). The central nervous system constitutes a brain, consisting of paired, bi-lobed cerebral ganglia and a pair of lateral nerve cords (Figure 1.2). The brain lobes are transversally interconnected by a dorsal and a ventral commissural tract. The ventral lobes are confluent with the lateral nerve cords. Brain lobes and nerve cords are of medullary organization consisting of a central fibrous region (neuropil) surrounded by a layer of neuronal cell somata. The central nervous system is always enclosed by a layer of *ecm* (outer neurilemma) and in some genera by another, more proximal *ecm* layer (inner neurilemma) separating neuronal cell somata

from the neuropil. The peripheral nervous system is represented by several minor nerves and nerve plexus. These constitute cephalic, proboscidial, and gastric nerve complexes which originate from brain margins and commissural tracts. Nerves are characterized by neurite bundles surrounded by *ecm* whereas a plexus is characterized by a meshwork of neurites. The position of the nervous system in relation to the body wall layers represents an important diagnostic trait for nemertean classification (Bürger 1888, 1895, Gibson 1972, 1982; Beckers 2011; Beckers *et al.* 2013; Beckers & von Döhren 2016).

Sensory organs comprise eyes, cerebral, frontal, lateral, and epidermal sensory organs (Figure 1.2). Eyes are of the pigment-cup type and restricted to the cephalic lobe, but are absent in most paleo- and several heteronemerteans. Cerebral organs are paired neuroglandular structures that are found in close relation to the nervous and vascular systems. They open to the exterior via a ciliated canal. Cerebral organs are absent in some palaeo- and hoplonemertean species. The frontal organ is comprised of one (Hoplonemertea) or three (Heteronemertea) epidermal, ciliated pits that lead into the mucous secreting cephalic glands. The composition and position of sensory organs is taxon specific and constitutes an important diagnostic trait (Gibson 1972, 1982).

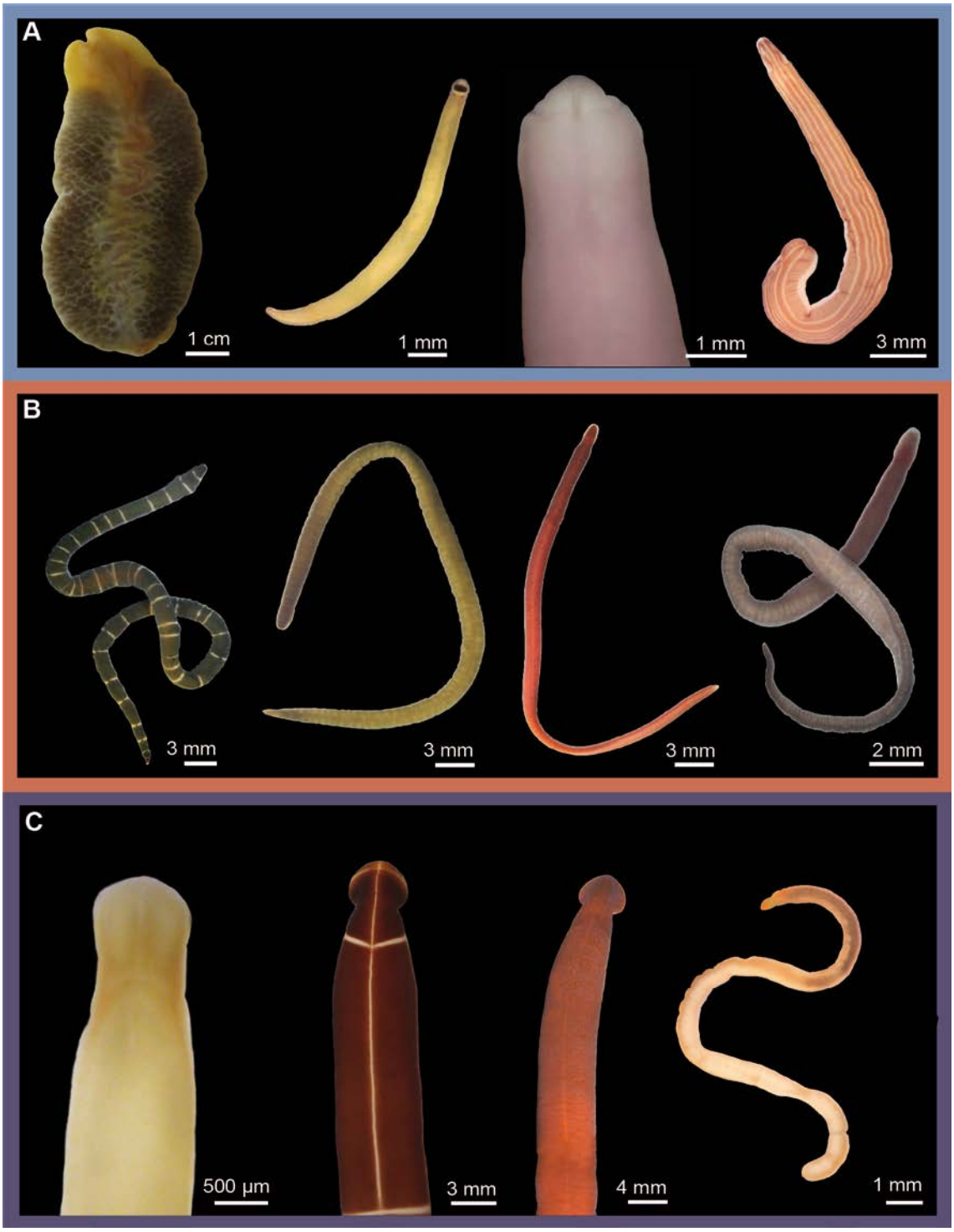

Figure 1.1. Nemertean diversity. **(A)** *Malacobdella grossa*, *Tetrastemma melanocephalum* (Johnston, 1837), *Arenogigas armoricus*, and *Drepanophorus spectabilis* as examples for monostiliferous and polystiliferous hoplonemerteans. **(B)** *Notospermus geniculatus*, *Lineus viridis* (Müller, 1774), *Lineus ruber* (Müller, 1774), and *Lineus clandestinus* Krämer *et al*., 2016 as examples for heteronemerteans. **(C)** *Carinina ochracea*, *Tubulanus superbus* (Kölliker, 1845), *Tubulanus polymorphus* Renier, 1804, and *Cephalothrix linearis* (Rathke, 1799) as examples for palaeonemerteans. Color scheme corresponds to Figure 1.3 (Photo credit for *Tubulanus superbus* and *Carinina ochracea*: AG Bartolomaeus).

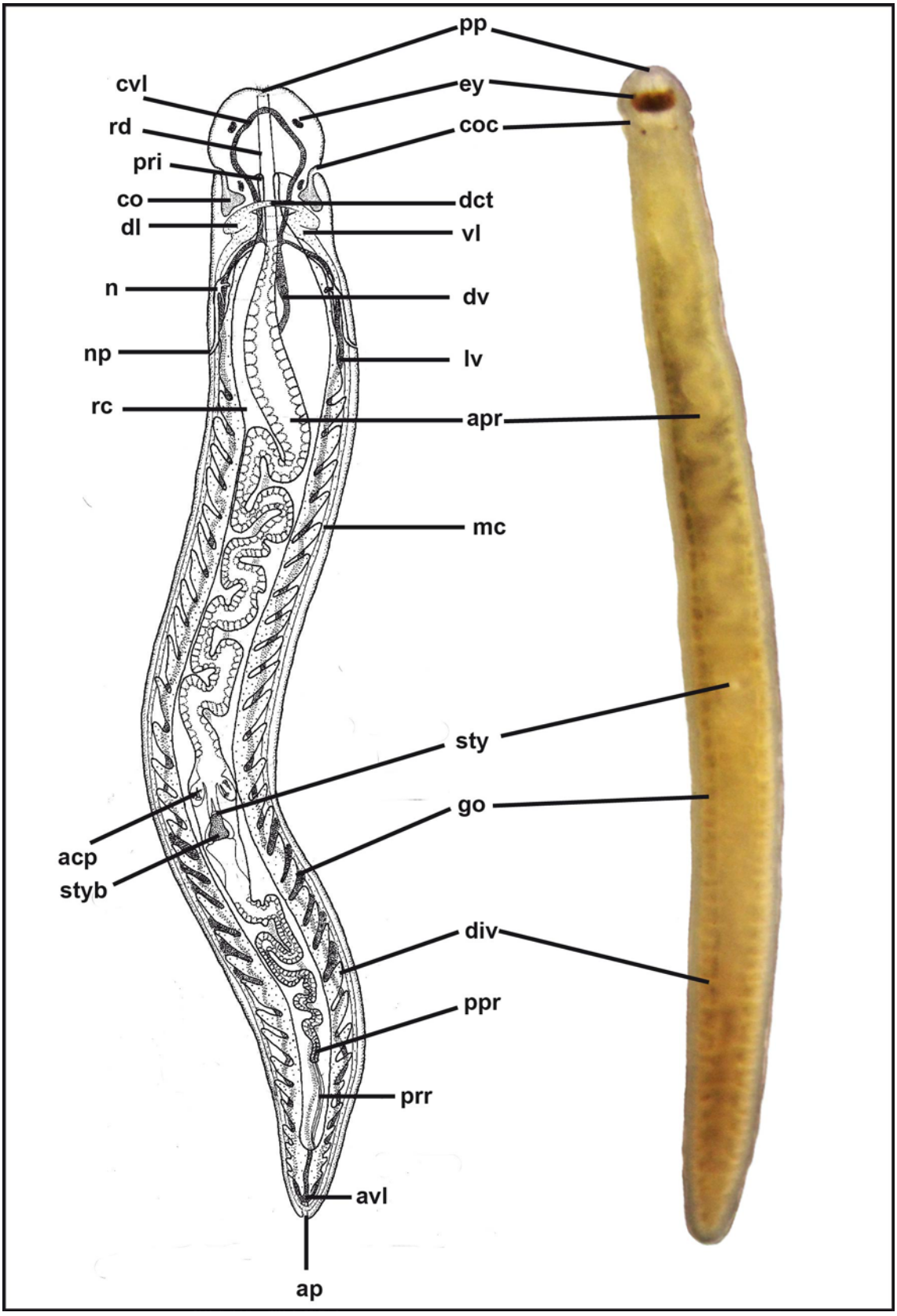

Figure 1.2 Schematic drawing of a hoplonemertean to show the arrangement of different organ systems (modified after Westheide & Rieger 2007) in comparison to a habitus image of

Tetrastemma melanocephalum. Abbreviations: **acp**, accessory stylet pouch; **ap**, anal pore; **apr**, anterior proboscis; **avl**, anal vascular loop; **co**, cerebral organ; **coc**, canal of cerebral organ; **cvl**, cephalic vascular loop; **dct**, dorsal commissural tract of brain; **div**, gastric diverticula; **dl**, dorsal brain lobe; **dv**, dorsal vessel; **ey**, eye; **go**, gonad; **lv**, lateral vessel; **mc**, medullary cord; **n**, nephridium; **np**, nephridal porus; **pp**, proboscis pore; **ppr**, posterior part of proboscis; **pri**, proboscis insertion; **prr**, proboscis retractor muscles; **rc**, rhynchocoel; **rd**, rhynchodaeum; **sty**, stylet; **styb**, stylet bulb; **vl**, ventral brain lobe.

1.4 Nemertean systematics

The internal morphology constitutes the basis for the traditional classification of nemerteans. The position and composition of several internal characters is therefore assessed through histological sectioning.

The structure of the proboscis apparatus, its connection to the digestive system, and the position of the nervous system, represent the basis for the traditional classification of nemerteans into the more inclusive groups of Anopla and Enopla (Stiasny-Wijnhoff 1923; Wijnhoff 1936; Coe 1943; Gibson 1972, 1982). The former includes Heteronemertea and Palaeonemertea whereas the latter contains Hoplonemertea and Bdellonemertea (i. e. *Malacobdella* which is based on its morphology considered as derived monostiliferous hoplonemertea (Thollesson & Norenburg 2003 and references therein)). In all enoplan representatives, the mouth opens anterior to the brain lobes. Within most hoplonemerteans the proboscis and digestive system open via an atrium as a single pore to the exterior. The proboscis itself is armed with a single stylet in monostiliferous hoplonemerteans (Monostilifera) or with a cushion equipped with several stylets in polystiliferous hoplonemerteans (Polystilifera). In anoplan nemerteans the mouth is situated below or posterior to the cerebral ganglia. The alimentary canal and the proboscis apparatus open separately, and the proboscis lacks armament (Stiasny-Wijnhoff 1923; Wijnhoff 1936; Coe 1943; Gibson 1972, 1982). Apart from this, information on the structure of the body wall, digestive tract, blood-vascular, excretory system, as well as, the composition of sensory organs serve as the traditional basis for classifying nemerteans at the family-, genus- or species level (Bürger, 1895, Coe 1904, 1905, Gibson 1972, 1982).

As in many other taxa, the advent of molecular methods has shifted the discussion on nemertean systematics. Most recent phylogenetic reconstructions

primarily rely on molecular approaches rather than on morphological data (Giribet 2015; Sundberg 2015). While many current phylogenetic reconstructions focus on assessing the positions of nemerteans within Spiralia (Turbeville *et al.* 1992; Turbeville 2002; Struck & Fisse 2008; Bleidorn *et al.* 2009; Hejnol *et al.* 2009; Podsiadlowski *et al.* 2009; Nesnidal *et al.* 2013; Dunn *et al.* 2014; Laumer *et al.* 2015), an increasing number of phylogenetic estimations target internal relationships among nemerteans. During the last 20 years, phylogenetic reconstructions developed from single-gene-based estimations using 16S or 18S sequences (Sundberg & Saur 1998; Sundberg *et al.* 2001) to multi-gene-based estimations including an increasing number of genes (Thollesson & Norenburg 2003; Andrade *et al.* 2012, 2014, Kvist *et al.* 2014, 2015). These studies aim at assessing a stable phylogeny of nemerteans, which could potentially provide a secure backbone for nemertean classification (Sundberg 2015). Therefore, phylogenetic analyses are increasingly included in current descriptions.

Phylogenetic reconstructions are partly congruent with the traditional classification of nemerteans mentioned above. Heteronemerteans and hoplonemerteans (including polystiliferous and monostiliferous nemerteans) are always recovered as monophyletic (Andrade *et al.* 2012, 2014, Kvist *et al.* 2014, 2015). Bdellonemertea (i. e. *Malacobdella*) nests within Monostilifera making Enopla synonymous with Hoplonemertea (Thollesson & Norenburg 2003). *Hubrechtella* species Bergendahl, 1902, which were traditionally considered as representatives of the putative palaeonemertean family Hubrechtiidae, are either recovered as sister to hoplonemerteans (Kvist *et al.* 2014, 2015) or sister to heteronemerteans (Thollesson & Norenburg 2003; Andrade *et al.* 2012, 2014). The latter grouping is further supported by the type of larvae, the planktonic pilidiophora, which is exclusive for most heteronemerteans and *Hubrechtella* (and *Hubrechtia* Bürger, 1892) (Thollesson & Norenburg 2003; Schwartz 2009). This is why several authors refer to this cluster as Pilidiophora (Thollesson & Norenburg 2003; Andrade *et al.* 2012, 2014; von Döhren 2015; Beckers & von Döhren 2016). The group containing Hoplonemertea and Pilidiophora is additionally referred to as Neonemertea by the same authors (Figure 1.3). Depending on the data set and analytical method used (Bayesian inference, parsimony, or Maximum Likelihood), palaeonemerteans (excluding *Hubrechtella*) are either monophyletic (Andrade *et al.* 2012, 2014) or paraphyletic (Thollesson &

Norenburg 2003; Kvist *et al.* 2014, 2015). *Tubulanus* (including *Callinera grandis* Bergendahl, 1903) is recovered as sister to Cephalothricidae (Thollesson & Norenburg 2003; Andrade *et al.* 2012; Kvist *et al.* 2014, 2015). *Carinina ocrachea* and *Carinoma* sp. Oudemans, 1885 either appear as basally branching palaeonemerteans (Andrade *et al.* 2012; Kvist *et al.* 2014, 2015) or as sister to Neonemertea (Thollesson & Norenburg 2003).

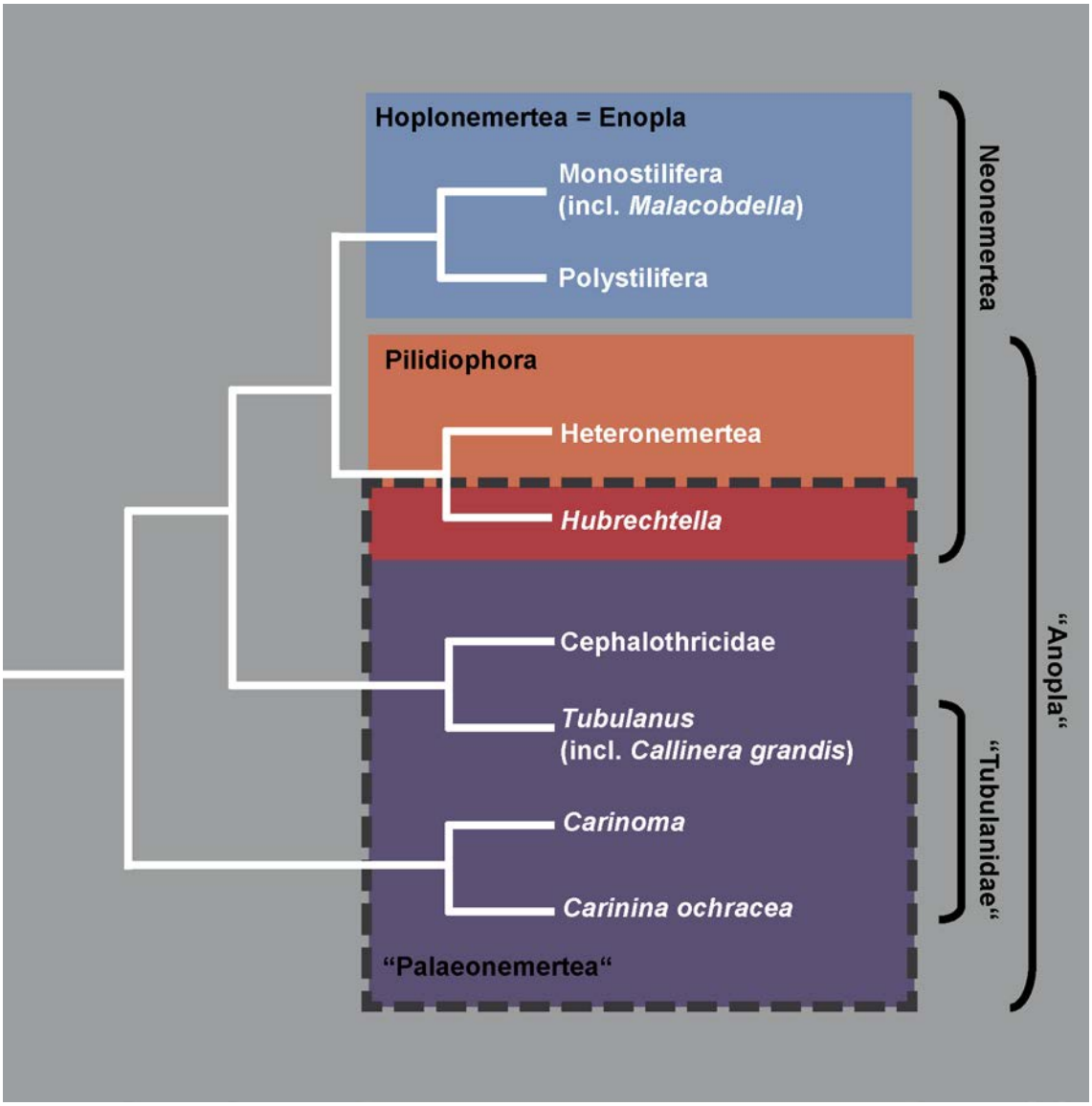

Figure 1.3 Current nemertean phylogeny summarized and redrawn after Andrade *et al.* (2012, 2014) and Kvist *et al.* (2014, 2015).

1.5 Species descriptions in nemerteans

Today, there are basically three different approaches that attempt to account for accurate species identification, classification, and descriptions of nemerteans. The first approach came into practice in the 19th century (see: Bürger, 1888, 1890, 1895; Coe 1904, 1905) and aims at detailed descriptions of the external and internal morphology primarily assessed through histological sectioning (Chapters 2-4).

The second approach relies on the more recent methodologies that utilize molecular sequence data for DNA taxonomy, DNA barcoding, and phylogenetic analyses. This involves the detection of species boundaries based on computer assisted algorithms, assigning species to a potential taxonomic unit, and then sorting them into the current phylogenetic and systematic background (Sundberg *et al.* 2009b, 2010; Chen *et al.* 2010; Leasi & Norenburg 2014; Chapters 2-4).

The third kind of descriptions constitutes an integrative taxonomic approach. Specimens are identified using molecular approaches and then compared to the identity revealed by traditional morphology or *vice versa* (Maslakova & Norenburg 2008; Sundberg *et al.* 2009a; Kajihara *et al.* 2011, 2015; Strand *et al.* 2014; Chernyshev *et al.* 2015; Hiebert & Maslakova 2015; Chapter 2 & 4). Some species boundaries are additionally assessed through additional data, such as life-history or larval development (Hiebert & Maslakova 2015).

However, most species descriptions are solely based on morphological data (Norenburg 1993; Frutos *et al.* 1998; Chernyshev 2003a; b, 2013; Kajihara *et al.* 2003; Ritger & Norenburg 2006) or, as recently suggested, on molecular data combined with notes on external characters (Strand & Sundberg 2011; Sundberg *et al.* 2016; Chapter 3).

In the following series of chapters, species boundaries and identities are assessed through the combination of different data sets in an overall integrative taxonomic approach. Different sets of molecular markers as well as data on internal and external morphology are therefore combined to assess species boundaries from different perspectives. The usability of each data set will be critically evaluated in the subsequent General Discussion.

Chapter 2

Arenogigas armoricus, a New Genus and Species of a Monostiliferous Hoplonemertean (Nemertea) from the North-West Coast of France

Daria Krämer* and Jörn von Döhren

University of Bonn, Institute of Evolutionary Biology and Ecology,

An der Immenburg 1, 53121 Bonn, Germany

*Corresponding author. E-mail: dkraemer@evolution.uni-bonn.de

This is the author's version of the article originally published in Zoological Science 32: 605-614 (2015)
doi: 10.2108/zs/140266

Key words:

Nemertea, Enopla, Monostilifera, Arenogigas armoricus, morphology, taxonomy, France

Abstract

A new genus and species of an endobenthic, unusually large eumonostiliferous hoplonemertean, *Arenogigas armoricus* gen. et sp. nov., is described from an intertidal sand flat in Pouldohan Bay near Concarneau, France. Morphological characters of the species and genus include a prominent connective tissue that divides the anterior longitudinal musculature, an extremely branched vascular system, the absence of a pre-cerebral septum, a pair of eyes situated at the anterior tip of the head, small cerebral organs positioned far anterior to the brain, 10 proboscidial nerves, and nine accessory stylet pouches.

2.1 Introduction

Nemertea is a spiralian taxon of unsegmented, soft bodied, vermiform animals, predominantly inhabiting marine environments. It comprises about 1280 described species of mainly epibenthic predators (Kajihara *et al.* 2008). Monostilifera, the largest taxon within Nemertea comprises approximately 45% of all described nemertean species (Gibson 1995; Kajihara *et al.* 2008). This taxon is characterized by a single stylet-bearing proboscis apparatus, which is used to pierce the cuticle of prey organisms such as small crustaceans and annelids (McDermott & Roe 1985). While most nemertean species measure less than 20 cm, most monostiliferous hoplonemerteans are comparably small, ranging in body length from millimeters up to approximately 12 cm (Gibson 1972, 1982; Turbeville 2007). Few exceptions in Monostilifera are among others *Tetranemertes antonina* (Quatrefages, 1846) or *Empectonema gracile* (Johnston, 1837), which can attain from 0.5 m up to 1 m in length, while remaining comparably slender with only a few in millimeters in width (Bürger, 1897-1907).

An unusually large monostiliferous hoplonemertean (approx. 40 cm in length, 3–9 mm in width) was found buried in 0.5 m depth in an intertidal sand flat near Concarneau, France. The uncommon endobenthic lifestyle as compared to other hoplonemertean species (Norenburg 1985) and the large body size lead to the assumption that the specimen represents a species new to science.

The result of a phylogenetic analysis based on partial sequences of the cytochrome *c* oxidase subunit I (COI), 16S rRNA, and 28S rRNA genes conducted herein is only of limited conclusiveness due to the sparsely available sequence data for this group. Therefore, making statements on the systematic status of the newly described species based on molecular markers is at best preliminary. The result obtained from the analysis of the molecular markers hints at an affinity of the newly described species to other members of the genus *Poseidonemertes* Kirsteuer, 1967. Observations on the internal morphology revealed prominent connective tissue (*sensu* Turbeville & Ruppert 1985; Turbeville 1991) splitting the anterior longitudinal muscle layer into two layers. This character is shared by only a small group of nemerteans within Monostilifera that have been classified as Poseidonemertidae Chernyshev, 2002 (Kajihara *et al.* 2001; Chernyshev 2002a). However, examination of the morphological characteristics found

in the new species show a combination of characters that is not exactly represented by any described poseidonemertid species. The composition of internal and external characteristics found in the specimen from France show closest similarities to '*Paranemertes*' *californica* Coe, 1904 which also has been suspected to be a member of the family Poseidonemertidae Chernyshev, 2002 instead of being a member of the genus *Paranemertes* Coe, 1901 (Kirsteuer 1974; Chernyshev 2002a). The anatomy of the newly described species from the coast of France is clearly in accordance with the emended diagnosis given for Poseidonemertidae (Chernyshev, 2002). However, since characters of the specimen from France decidedly differ from any of the diagnoses of the poseidonemertid genera we have decided to assign the animal to the new genus and species *Arenogigas armoricus* gen. et sp. nov.

2.2 Material and Methods

2.2.1 Specimens

Arenogigas armoricus was found buried in 0.5 m depth in an intertidal sand flat in Pouldohan Bay near Concarneau, Brittany France during low tide (Fig. 1). While trying to extract the animal from the sediment, it everted its proboscis, of which the anterior part was severed. Additionally, the specimen was torn into two pieces. The posterior end was measured but not photographically documented or fixed for further processing. The proboscis was examined under the compound microscope. Unfortunately, since there was no camera mounted on the microscope no images for documentation could be taken. Therefore, measurements of the central stylet and its basis could not be obtained. Subsequently, the proboscis was macerated in 1% KOH for several months to make the stylets accessible. The anterior region was anaesthetized in 7% $MgCl_2$ mixed with sea water at equal volumes, fixed in Bouin's solution after Dubosq-Brasil and photographically documented. The specimen was embedded in paraplast. Sections of 5-µm thickness were made that were stained with the Azan-method. Sections were analyzed with an Olympus BX-51 microscope equipped with an Olympus slide ver. 2.2 and photographed with an Olympus cc12 camera mounted on the microscope. Afterwards, images were aligned with IMOD (Kremer *et al.* 1996) and IMOD align

(http://www.q-terra.de/biowelt/3drekon/guides/imod_first_aid.pdf). The image series is deposited at Morph D Base. Figure 2.4: 3D-reconstruction of the circulatory system was performed with Fiji ver. 1.48r/Trakem and Amira ver. 5.3.1 based on the aligned image series.

2.2.2 DNA extraction and PCR amplification

A small piece of the specimen was preserved in absolute ethanol for DNA extraction with DNeasy Blood and Tissue kit (Qiagen®) following the manufacturer's instructions. Three loci were amplified: the partial mitochondrial genes coding for the cytochrome *c* oxidase subunit I (COI) and 16S rRNA, as well as the partial nuclear 28S rRNA gene. All primers used for the amplification and sequencing reactions are listed in Appendix I: Supplementary Table 1. PCR reactions were conducted with the Ex Hot Start Polymerase TaKaRa™ or HotMaster *Taq* polymerase (Invitrogen™) kits. Thermal cycling was initiated with 2 min at 94°C, followed by 40 cycles (30 sec at 94°C, 60 sec at 53/45°C (COI/16S), 60 sec at 72°C), and ending with a 2 min final elongation at 72°C. For 28S, thermal cycling was initiated with 2 min at 94°C, followed by 35 cycles (60 sec at 94°C, 45 sec at 64°C, 90 sec at 72°C) ending with 7 min final elongation at 72°C. PCR products were purified with NucleoSpin® Extract II-Kit (MACHEREY-NAGEL GmbH & Co. KG) following the instructions of the manufacturer. Purified PCR products were sent to LGC Genomics© for Sanger sequencing (Sanger *et al.* 1977), using PCR primers as well for sequencing. All new sequences are deposited in GenBank. Accession numbers for COI, 16S, and 28S are listed in Appendix I: Supplementary Table 2.

2.2.3 Sequence analysis and phylogenetic analysis

To enable a molecular characterization of *Arenogigas armoricus* a phylogenetic analysis based on the three amplified markers was conducted including sequence data of several hoplonemertean species including mono- and polystiliferan species. The palaeonemertean *Cephalothrix rufifrons* (Johnston, 1837) was used as outgroup. Species

included in the analysis are listed in Appendix I: Supplementary Table 2 with their GenBank accession numbers and references. Sequences were edited and concatenated using Bioedit ver. 7.1.3.0 (Hall 1999). A multiple sequence alignment of COI, 16S and 28S was performed with MAFFT v. 7 (Katoh & Standley 2013) with G-INS-I strategy using the following parameters: gap penalty of 1.53/3 (COI, 16S/ 28S); scoring matrix for nucleotide sequences of 200PAM/K = 2; offset value = 0.0. A maximum-likelihood analysis was performed with RAxML v. 8 (Stamatakis 2014) using the GTR model of sequence evolution and the CAT model of rate heterogeneity (Stamatakis 2006). One hundred bootstrap replicates were conducted to evaluate nodal support.

2.3 Results

2.3.1 Taxonomy

***Arenogigas* gen. nov**

Type species. *Arenogigas armoricus* sp. nov., fixed by the original designation.

Etymology. The generic name is masculine in gender, a composite of the Latin arena ("sand") and gigas ("giant"), referring to the unusual large size for a hoplonemertean. The specific name of the new species, armoricus, an adjective, refers to Armorica, the Latin name of the region between the Seine and Loire rivers in France where the species was found.

Diagnosis. Endobenthic, monostiliferous hoplonemerteans of large size: 30–40 cm in length, 3 mm (cephalic lobe) to 9 mm (caudal region) in width; dark red, fluid-filled rhynchocoel, presumably reaching to posterior end of body; proboscis well developed, anterior chamber with three muscle layers (outer circular, middle longitudinal, inner circular), proboscidial nerve plexus comprising 10 nerves, armature comprising a single central stylet and nine accessory stylet pouches; longitudinal body wall musculature anteriorly divided by thick layer of connective tissue; pre-cerebral septum absent; head

retractor muscles derived from inner portion of the longitudinal musculature; foregut divisible into esophagus, stomach, and long pylorus; short intestinal cecum lacking intestinal pouches but with short lateral diverticula; circulatory system consisting of cephalic loop and extensively branching blood vascular system throughout whole body, mid-dorsal vessel with single vascular plug; cerebral ganglia small, dorsal ganglion shifted ventrolaterally close to ventral ganglia, paired ganglia positioned ventrolaterally to each side of rhynchocoel, with neither neurochord cells nor accessory nerves; frontal organ absent; voluminous, diffuse cephalic glands present, extending in front of brain; eyes two, situated ventrally, deeply embedded within musculature at anterior tip of head, not visible from exterior; small, saclike cerebral sensory organs, situated far anterior to brain, opening laterally into cephalic furrow; excretory system present within foregut region and intestinal region; sexes presumably separate.

***Arenogigas armoricus* sp. nov.**

Type specimen. Holotype anterior part of a sexually mature female, series of transverse sections, 69 slides (cephalic region: MNHN-AO-1181-1 to AO-1181-69; https://www.morphdbase.de/?D_Kraemer_20150722-M-6.1, intestinal region: www.morphdbase.de/?D_Kraemer_20150730M-8.1), tissue in absolute ethanol of holotype (MNHN-AO1181-71) and paratype (MNHN-AO-1181-70) deposited at the Muséum national d'Histoire naturelle, Paris.

Type locality. Intertidal sand flat (Figure 2.1), Pouldohan Bay, France. The bay is characterized by poorly sorted sandy sediment with a high organic fraction showing anaerobic conditions within a few centimeters depth.

Figure 2.1 The type locality of *Arenogigas armoricus* gen. et sp. nov., the intertidal sand flat of Pouldohan Bay near Concarneau, France, during low tide

Description

External features. Addition of lengths of the two parts of described specimen resulted in minimum body length of approximately 40 cm. Body width varying in different body regions. Cephalic lobe measuring 3 mm in width and 2.5 mm in length (from cephalic furrows to tip of head). Body broadening to 4 mm in postcephalic region. Posterior end measuring 14 cm in length, broadened in paddle-like manner, measuring 9 mm at its widest point and tapering down to 3 mm to form blunt tip. Head bluntly pointed and demarcated from trunk by a single cephalic furrow encircling head on dorsal and ventral sides like curly brackets (Figure 2.2 A, C, D). Cephalic furrow situated in front of brain lobes. Rhynchopore situated subterminally and opening at level of cephalic furrow. Anteriorly, groove extending from rhynchopore for 2.5 mm in relaxed specimen (Figure 2.2 C). Color of living animal uniformly brick red. Dark red rhynchocoelic fluid leaking

out after rupture, leading to fading of red coloration into pale pink. In fixed specimen, pale pink coloration retained (Figure 2.2 A, C, D). Except for digestive tract, no eyes or internal organs visible through body wall (Figure 2.2 A).

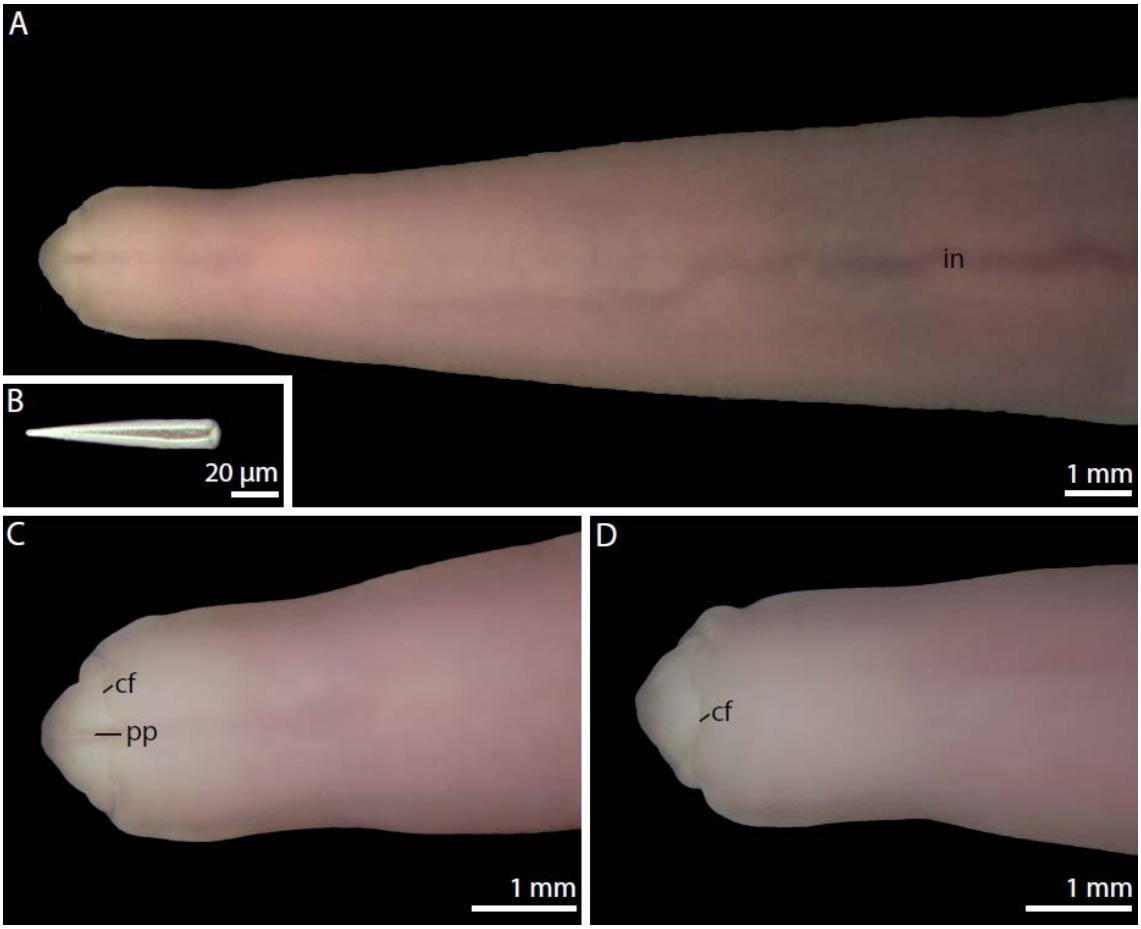

Figure 2.2 *Arenogigas armoricus* gen. et sp. nov., holotype (MNHN-AO-1181-71). Habitus images of fixed specimen and one macerated accessory stylet. **(A)** Ventral view of anterior body showing the intestine shining through the body wall. **(B)** Accessory stylet. **(C)** Ventral view of the head showing the proboscis pore and the cephalic furrow. **(D)** Dorsal view of the head showing the cephalic furrow. Abbreviations: **cf**, cephalic furrows; **in**, intestine; **pp**, proboscis pore.

Body wall. Epidermis containing very few glandular cells of which dominant type being flask-shaped mucous glands (Figure 2.3 C, D). Dermis *sensu* Norenburg (1985) appearing as prominent layer, measuring half of height of circular muscle layer (Figure 2.3 A, D). Body wall musculature consisting of outer circular and inner longitudinal

muscle layers. Longitudinal muscle layer anteriorly divided by thick layer of connective tissue (Figure 2.3 A, D). Outer longitudinal muscle layer appearing thin, whereas inner layer being more pronounced, with musculature appearing densely packed (Figure 2.3 A, D, E). Within inner longitudinal muscle layer, another subdivision visible; Outer portion of musculature densely packed with submuscular glands (Figure 2.3Figure 2.3 A). Layer of separating extracellular matrix becoming more prominent between cerebral organs and rear of brain; measuring same height as combined outer circular and outer longitudinal muscle layers (Figure 2.3 A, D). Connective tissue traversed by multiple blood vessels, diffuse submuscular glands and muscle fibers. Precerebral septum absent. Outer longitudinal musculature reaching to head tip but not contributing to head retractors. Proboscis insertion and head retractor muscles originating from inner layer of longitudinal muscles (Figure 2.3 A, F). Head retractors discernible as small bundles surrounding rhynchodaeum, being more densely packed above rhynchodaeum (Figure 2.3 F). At level of anterior intestinal diverticula, extracellular matrix layer disappearing; inner and outer longitudinal muscle layers located in juxtaposition (Figure 2.3 H). Dorsoventral muscles present, clearly discernible in intestinal region (Figure 2.3 E).

Proboscis apparatus. Proboscis pore situated subterminally in front of cephalic furrow (Figure 2.2 A, C, Figure 2.3 B), leading into thin walled, ciliated rhynchodaeum that lacks glandular cells (Figure 2.3 F). Prominent rhynchodaeal sphincter formed by thick layer of circular muscles. Proboscis insertion positioned anterior to brain, consisting of longitudinal muscles that branch off from inner longitudinal body wall musculature (Figure 2.3 A). Holotype injured and partly everted its proboscis while collecting. Lengths of proboscis and rhynchocoel thus unobtainable. Rhynchocoel lined with thin, barely visible, proximal longitudinal, and distal, more pronounced outer circular muscle layers. Rhynchocoelic musculature more pronounced in its posterior course (Figure 2.3 E, H). In everted state, proboscis layered as follows: anterior proboscis epithelium arranged into papillae followed by thick layer of extracellular matrix with embedded layer of circular muscles. Pronounced longitudinal muscle layer bearing 10 proboscis nerves. Circular neural sheath connecting proboscidial nerves, dividing longitudinal musculature in pronounced outer and thin inner layers. Additionally, barely visible inner circular muscle layer present (Figure 2.3 D). Proboscis armature consisting of single

central stylet and nine accessory stylet pouches each containing 2–3 reserve stylets. Central and accessory stylets (Figure 2.2 B) were straight with smooth surface. Stylet armature only observed *in vivo*, not photographically documented. Stylet bulbous macerated; therefore no data available for basis of central stylet.

Alimentary canal. Esophagus opening from ventral rhynchodaeal wall in front of rhynchodaeal sphincter. Esophagus lined by unciliated, thin epithelium lacking gland cells, extending to ventral commissural tract of brain (Figure 2.3 A). Anterior esophagus appears flattened, but widening in diameter in its posterior course. In front of stomach it is of same height as inner longitudinal musculature. Shape of esophagus resembling round tube with weakly folded epithelium. At height of brain ventral commissural tract, transition to stomach marked by epithelium being thrown into several deep folds and high abundance of gland cells (Figure 2.3D). Stomach widening increasingly, assuming almost same width as proboscis. In its posterior course, stomach leading to pyloric canal. Pyloric canal about 3.5 times longer than stomach. Pyloric epithelium sparsely ciliated, with well developed wall containing glandular cells. Pylorus, opening into dorsal wall of intestine. Short intestinal cecum present with pair of short lateral diverticula originating from pylorus–intestine junction (Figure 2.3 H). Lateral, anteriorly protruding intestinal pouches absent. Epithelium of intestine and cecum characterized by higher abundance of gland cells and yellowish inclusions. At junction between pylorus and intestine, gut epithelium becoming thicker and thrown into shallow folds. Intestinal canal widening increasingly in its posterior course, forming unbranched lateral diverticula extending distally to lateral medullary nerve cords.

Circulatory system. Cephalic loop positioned posterior to eyes and dorsal to proboscis pore (Figure 2.3 B) giving rise to two lateral, longitudinal vessels, positioned lateral to rhynchodaeum. At level of esophagus; numerous smaller blood vessels originating from two longitudinal and cephalic vessels by multiple branching, interconnected in an irregular manner resulting in extensive capillary network within body wall (Figure 2.3 A, D, Figure 2.4). Thus, main lateral longitudinal blood vessels not discernible. Strong capillarization within layer of connective tissue, separating longitudinal musculature and inner portion of the inner longitudinal muscles. Posterior to brain, extracellular matrix surrounding medullary nerve cords also penetrated by several capillaries (Figure

2.3 E). Single mid-dorsal vessel present dorsal to intestine, extending all length of section series, entering the rhynchocoel wall, forming single vascular plug at level of brain commissural tracts (Figure 2.3 D, H). Mid-dorsal vessel presumably originating from left side of vascular system. Connection to one of right lateral vessels not observed (Figure 2.4). Full extension of blood vascular system not accessible in holotype due to lack of more caudal region.

Nervous system. Brain situated far posterior to rhynchopore at level of anterior stomach (Figure 2.3 D), comparably small, not exceeding thickness of inner longitudinal muscle layer in diameter. Posterior part of brain divided into dorsal and ventral pair of lobes of similar size. Dorsal lobes shifted close to ventral lobes; both lobes situated ventrolaterally to rhynchocoel, interconnected by thin, dorsal commissural tract followed by thicker ventral commissural tract (Figure 2.3 D). Dorsal lobes ending blindly, ventral lobes confluent with lateral medullary nerve cords and situated in layer of loose extracellular matrix, proximal to longitudinal muscle layer (Figure 2.3 E). Medullary cords traversed by myofibrils and interconnected by several commissural plexus dorsal and ventral to rhynchocoel (Figure 2.3 E). Additionally, several nerves emanating regularly from cords, extending laterally into longitudinal musculature. Neuronal cell somata of medullary cord and neuropil not separated by inner neurilemma. Neuronal cell somata encircling neuropil in U-shaped manner (Figure 2.3 E). Three different types of cell somata distinguishable. First type (s1) characterized by small cell body containing small, red-stained nucleus. Majority of cell somata comprised of second type (s2), showing enlarged cell body and large nucleus stained in purple. Third type (s3) measures twice the size of s2, located in periphery of medullary cords. Neither accessory lateral nerve nor neurochord cells or neurochords observed. Inner neurilemma missing (Figure 2.3 D, G). Same three types of neuronal cell somata, as already described for the medullary cords, present in brain. S1 showing high abundance around dorsal brain lobe. S2 encircling dorsal and ventral lobe, whereas enlarged s3 cells situated in brain periphery (Figure 2.3 G). Brain neurochord cells absent. Several cephalic nerves originating from dorsal and ventral brain lobes protruding anteriorly towards head tip (Figure 2.3 A). Small indistinct nerve leading from cerebral organs to brain. Origin of cerebral organ nerves from brain not detected.

Proboscis innervated by pair of nerves, originating from ventral cephalic lobes; two nerves extending anteriorly towards proboscis insertion; splitting into ten nerves innervating proboscis. Proboscidial nerves interconnected by circular neural sheath. Additionally, each proboscidial nerve giving rise to nerve fibers radiating to outer part of proboscidial longitudinal muscles (Figure 2.3 D). Two gastric nerves running parallel to digestive tract, closely connected with pyloric epithelium and interconnected by transverse commissures. Origin of gastric nerves from brain not determined.

Frontal organ and cephalic glands. Frontal organ not discernible. Voluminous, diffuse cephalic glands posteriorly extending in front of brain opening via barely visible epidermal pits (Figure 2.3 A). Cephalic glands barely distinguishable from longitudinal musculature within tip of head (Figure 2.3 C). Submuscular glands discernible at level of esophagus, occupying outer portion of inner longitudinal musculature and being scattered within layer of connective tissue (Figure 2.3 A).

Sensory organs. Pair of pigment-cup ocelli present but not externally visible (Figure 2.2, Figure 2.3 B), situated ventrally at anterior tip of head in front of cephalic vascular loop, and deeply embedded within longitudinal musculature. Pigmented cup oriented towards the ventrolateral side of animal. Sack-like, small cerebral sensory organs positioned far anterior to brain, measuring less than half of brain lobes in diameter (Figure 2.3 C). Each cerebral sensory organ connected to exterior by unbranched, ciliated canal, opening laterally into cephalic furrow. Within cerebral organs, canal ending blindly in glandular tissue.

Excretory system. Nephridial system present in foregut region. Nephroducts closely apposed dorsally to medullary lateral nerve cords and blood vessels embedded in parenchymatous tissue (Figure 2.3 E). Neither extension of excretory system nor number of nephridial units detectable in the holotype. Efferent ducts and nephridiopores also not found.

Reproductive system. Sexes presumably separate (only a female was found). In vivo, serially arranged gonads filled with yellowish eggs. In holotype, further details regarding arrangement of gonads not gained.

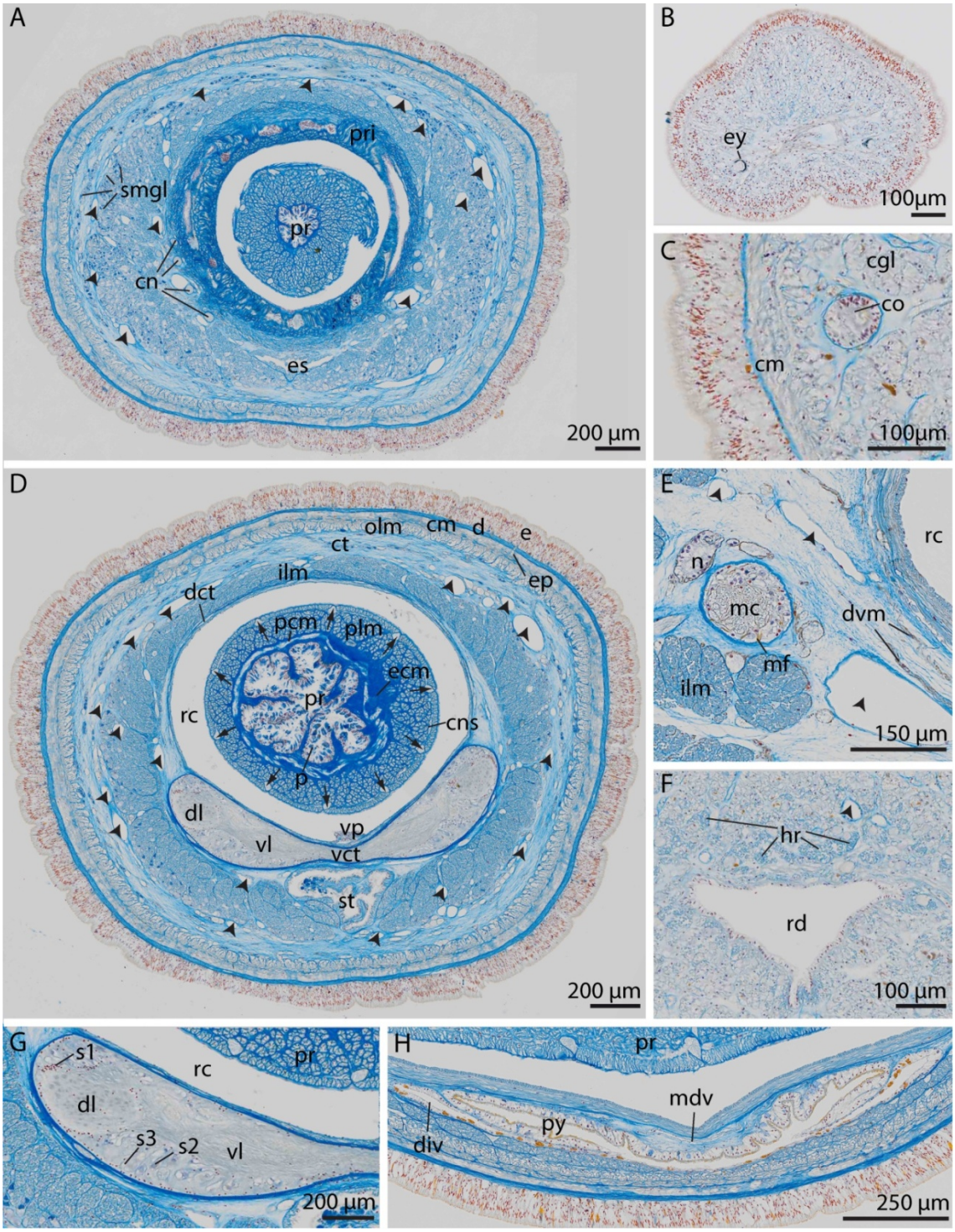

Figure 2.3 *Arenogigas armoricus* gen. et sp. nov., holotype, cross sections, Azan. **(A)** MNHN-AO-1181-38 Transverse section through the proboscis insertion derived from the inner longitudinal musculature and the strong vascularization of the body wall. **(B)** MNHN-AO-1181-4 Transverse section through the head tip showing the position and orientation of the eyes. **(C)** MNHN-AO-1181-16 Transverse section through cerebral organ. **(D)** MNHN-AO-1181-43 Transverse section through the cerebral region to show the position of the dorsal and ventral brain lobes, as well as the division of the longitudinal musculature into inner and outer layers.

(E) www.morphdbase.de/?D_Kraemer_20150730-M-8.1 Transverse section through the medullary cord within the intestinal region to show the location of the nephridium. **(F)** MNHN-AO-1181-16 Transverse section through the precerebral region to show the head retractors. **(G)** MNHN-AO-1181-43 Transverse section through the brain lobes to show the composition of neuronal cell somata. **(H)** www.morphdbase.de/?D_Kraemer_20150730-M-8.1 Transverse section through pylorus-intestine junction. Abbreviations: **cgl**, cephalic gland; **cm**, circular musculature; **cn**, cephalic nerves; **cns**, circular neural sheath; **co**, cerebral organ; **ct**, connective tissue; **d**, dermis; **dct**, dorsal commissural tract; **div**, paired lateral, cecal diverticula; **dl**, dorsal lobe; **dvm**, dorsoventral musculature; **e**, epidermis; **ecm**, extracellular matrix layer (within proboscis); **es**, esophagus; **ey**, eyes; **hr**, head retractors; **ic**, intestinal cecum; **ilm**, inner longitudinal musculature; **mc**, medullary cord; **mdv**, mid-dorsal blood vessel; **mf**, myofibril; **n**, nephridium; **olm**, outer longitudinal musculature; **p**, papillae; **pcm**, proboscis circular musculature; **plm**, proboscis longitudinal musculature; **pr**, proboscis; **pri**, proboscis insertion; **py**, pylorus; **rc**, rhynchocoel; **rd**, rhynchodaeum; **st**, stomach; **s1–s3**, neuronal cell somata, type 1–3; **vct**, ventral commissural tract; **vl**, ventral lobe; **vp**, vascular plug; **arrows**, proboscidial nerves; **arrowheads**, circulatory system.

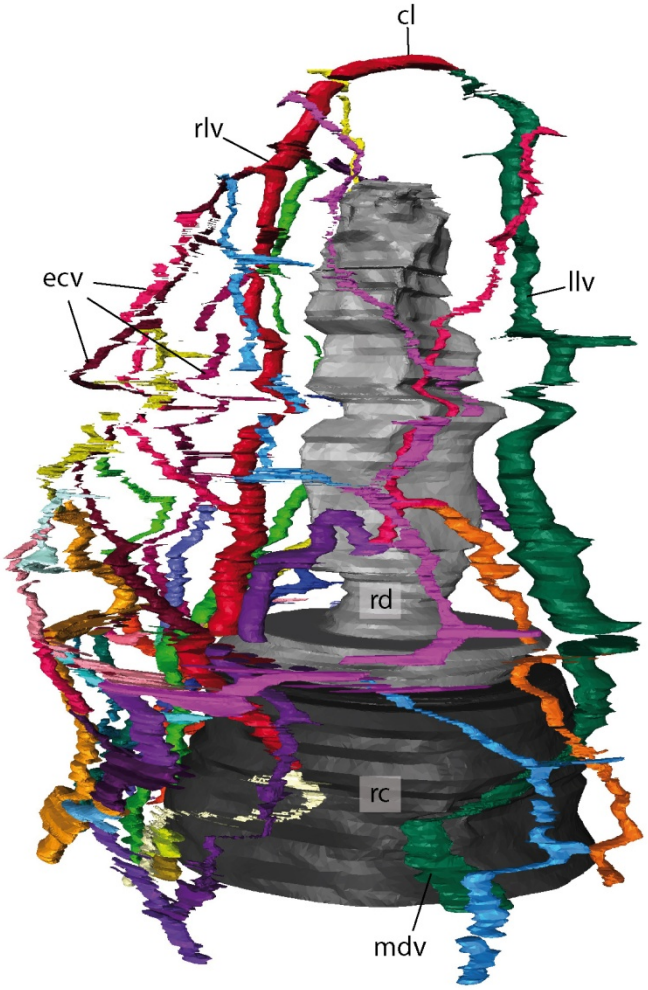

Figure 2.4 *Arenogigas armoricus* gen. et sp. nov., holotype (MNHN-AO-1181-1 to AO-1181-69, https://www.morphdbase.de/?D_Kraemer_20150722-M-6.1), right half of circulatory system, ventral view, snapshot 3d-reconstruction (213 slides). Abbreviations: **cl**, cephalic loop; **ecv**, extra-cerebral vessel; **llv**, left lateral vessel; **mdv**, mid-dorsal blood vessel; **rc**, rhynchocoel; **rd**, rhynchodaeum; **rlv**: right lateral vessel.

2.3.2 Molecular phylogeny

The data set used for the ML analysis consisted of three aligned subsets: COI (580 nucleotides (nt)), 16S (371nt) and 28S (936nt). The concatenated alignment of all markers contained 1886nt. The resulting tree shows the monophyly of all included monostiliferous (72%) and polystiliferous hoplonemerteans (99%). The clade which has been termed Eumonostilifera based on the bilayered rhynchocoel (Chernyshev 2003c) is supported by a bootstrap value of 74%. Within eumonostiliferans, the tree does not give a clear resolution concerning Ototyphlonemertidae, Emplectonematidae, and Poseidonemertidae. The results show a clear affiliation of *Arenogigas armoricus* to three *Poseidonemertes* species supported by a bootstrap value of 100% (Figure 2.5).

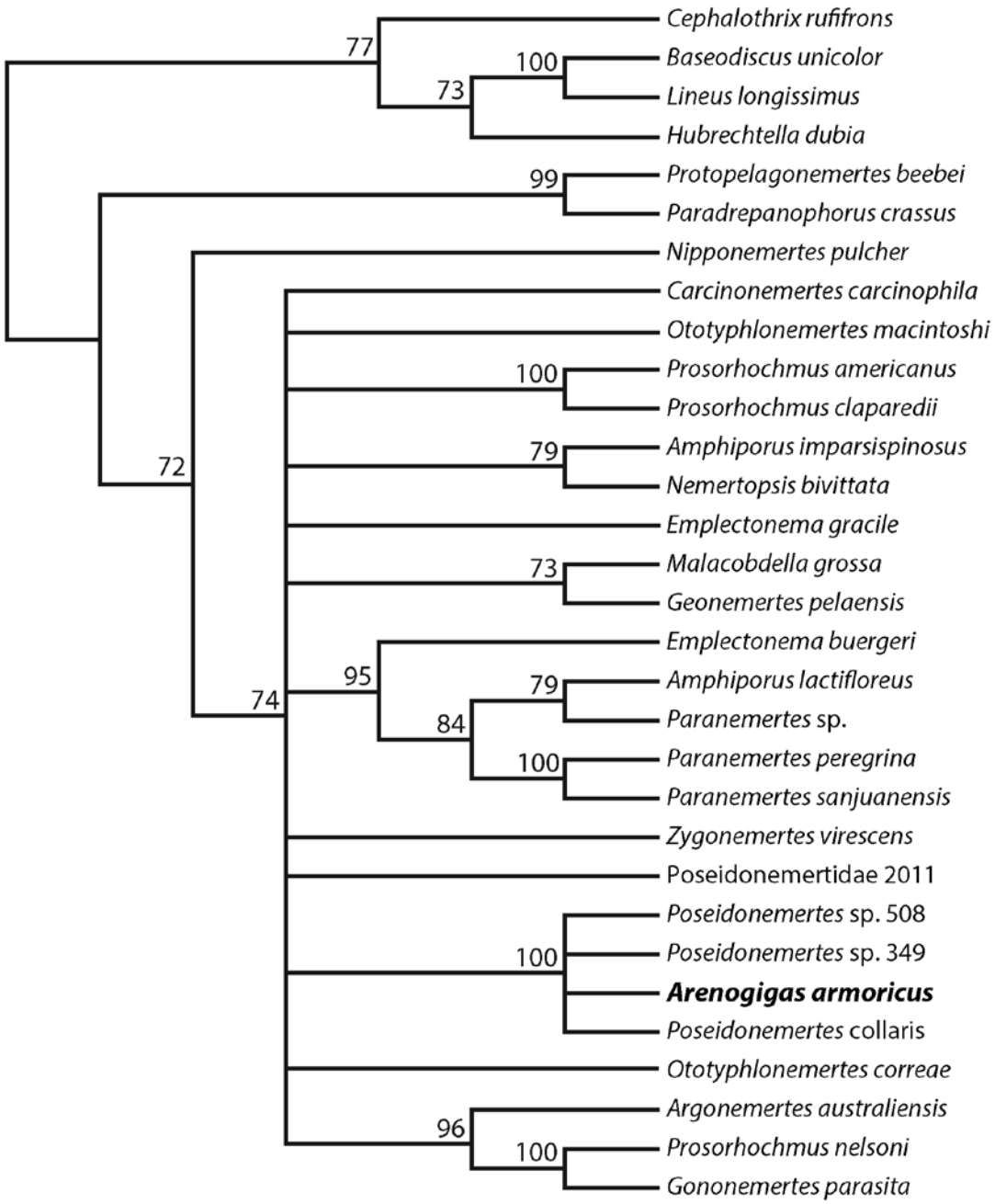

Figure 2.5 Best tree from maximum likelihood analysis (RAxML, GTR + CAT (Stamatakis, 2014)) of combined 16S rRNA, 28S rRNA, and COI mtDNA. Numbers above branches indicate bootstrap percentages (> 70%) from 100 replicates.

2.4 Discussion

The new species *Arenogigas armoricus* possesses an anteriorly bilayered longitudinal muscle layer separated by connective tissue that is interspersed with a profusely branched blood vascular system. Although the extension of the rhynchocoel along the body length could not be determined in the specimen described it is obvious that the insertion of the proboscis is formed by longitudinal fibers that are exclusively derived from the inner layer of the split longitudinal musculature (i.e. a precerebral septum is absent *sensu* Kirsteuer, 1974). The species possesses a short intestinal cecum with one pair of comparably short lateral diverticula at the level of the insertion of the pylorus into the intestine. The number of proboscis nerves in the anterior chamber of the proboscis amounts to 10 and there are nine accessory stylet pouches in the analyzed specimen. Among monostiliferous hoplonemerteans an anteriorly divided longitudinal muscle layer is present in only a small number of species (Kajihara *et al.* 2001) most of which have been classified as Poseidonemertidae (Chernyshev 2002a, 2005). Although there is some reservation concerning the monophyly of Poseidonemertidae (Chernyshev, pers. comm.) the division of the longitudinal musculature by a layer of connective tissue has been regarded as an apomorphic character of this family containing the mostly monotypic genera *Alaxinus*, *Aenigmanemertes*, *Correanemertes*, *Diopsonemertes*, *Fasciculonemertes*, *Diplomma*, *Poseidonemertes*, *Tetranemertes*, *Kirsteueriella*, and the species '*Paranemertes*' *californica* (Chernyshev 2002a; Kajihara *et al.* 2011). In the members of the '*Amphiporus hastatus* group', which have provisionally been assigned to Poseidonemertidae the type of tissue separating the longitudinal muscle layers is unknown (Kajihara *et al.* 2001; Chernyshev 2005).

The result of our molecular analysis clearly shows a robustly supported (bootstrap value = 100), close affinity of *A. armoricus* to the majority of the poseidonemertid representatives included in the analysis (*Poseidonemertes collaris*, *Poseidonemertes* sp. 349, and *Poseidonemertes* sp. 508). The only other poseidonemertid representative (Poseidonemertidae 2011, provided by A. V. Chernyshev) does not unambiguously form a monophyletic assemblage with the *Poseidonemertes* clade. For the following reasons, however, the result of the molecular analysis has to be taken with considerable reservation: (1) The species included in the analysis are restricted to three members of

the type genus (*Poseidonemertes*) and an allegedly non-congeneric poseidonemertid species (Poseidonemertidae 2011). The taxon sampling thus only represents a small fraction of the putative poseidonemertid radiation. On the other hand, this result underpins the notion of Chernyshev (pers. comm.) that Poseidonemertidae are potentially non-monophyletic. (2) No representative species of the remaining genera included in Poseidonemertidae (*sensu* Chernyshev, 2002) were included in the analysis. This makes statements about potential closer affiliations to any of the remaining poseidonemertid genera impossible. (3) The high number of poorly supported nodes and the incongruence of the tree topology with published results re-illustrates the recently identified limits of the molecular markers used (Andrade *et al.* 2012). Thus, drawing conclusions merely based on molecular data has to be regarded as premature. Instead, the limited taxon sampling regarding poseidonemertid species only allows for stating an affiliation of *A. armoricus* with Poseidonemertidae, thus providing additional support from molecular data to the conclusions drawn from the presence of a split longitudinal muscle layer that is separated by connective tissue (Kajihara *et al.* 2001; Chernyshev 2005). From a taxonomic point of view, an affiliation of *A. amoricus* to *Poseidonemertes* seems unwarranted, due to several morphological differences between this genus and *A. armoricus*, which include the absence of a precerebral septum and a profusely branched blood vascular system that are not present in the genus *Poseidonemertes*. In poseidonemertid genera, a strongly branched vascular system as seen in *A. armoricus* has only been reported in *Kirsteueriella biocellata* (Coe, 1944), '*Paranemertes*' *californica* Coe, 1904, and two members of the '*Amphiporus hastatus* group': *Amphiporus hastatus* McIntosh, 1874 and *Amphiporus korschelti* Friedrich, 1940 (Kirsteuer 1974; Kajihara *et al.* 2001; Chernyshev 2002a). Of these, only *A. korschelti*, *K. biocellata*, and *P. californica* correspond to *A. armoricus* in possessing a proboscis insertion exclusively formed by fibers of the inner layer of the longitudinal muscle layer (precerebral septum is absent *sensu* Kirsteuer, 1974). In addition to the endobenthic life-style within sandy substrates, *A. armoricus* shows morphologically more similarities to *K. biocellata* and *P. californica*. The eyes are located at the extreme tip of the head, deeply embedded in the head musculature and the small, sack-like cerebral organs are positioned far anterior to the brain. A short intestinal cecum with a single pair of diverticula which arise from the junction of the pylorus and intestine and

the lack of cecal pouches, as observed in *A. armoricus* has also been reported for *K. biocellata* (Coe 1944). For *P. californica*, the cecum is reported to exhibit few pairs of cecal pouches although it does not become entirely clear how many pairs are located anterior of the junction of pylorus and midgut (Coe, 1904, 1905). The presence of 10 proboscis nerves, a much thicker connective tissue layer separating the longitudinal muscle layers, a more profusely branched blood vascular system in which main vessels are indiscernible, and the comparably large size of *A. armoricus*; however, represent distinct differences from the respective characters reported in *K. biocellata* (Coe, 1944). The number of proboscis nerves, the thickness of the connective tissue layer, the degree of branching of the blood vessels, and the large body size are rather in accordance to what has been described and illustrated in *P. californica* (Coe, 1904). *P. californica* and *A. armoricus* on the other hand, differ regarding the amount of accessory stylet pouches. Whereas a maximum number of six has been described in *P. californica*, nine can be found in the new species (Coe 1904, 1905). Based on our observations we conclude that *A. armoricus* anatomically corresponds most closely to *P. californica*. Contrastingly, the phylogenetic analysis conducted in this study shows no close relation of the new species to *Paranemertes peregrina* Coe, 1901, the type species of the genus *Paranemertes*. An assignment to this genus has therefore to be regarded as problematic. As already concluded by Kirsteuer (1974), some *Paranemertes* species differ from the type species of this genus, *Paranemertes peregrina*, by having an anteriorly divided longitudinal musculature and should therefore be excluded from the genus *Paranemerte*s. Chernyshev (2002) transferred '*Paranemertes*' *biocellatus* Coe, 1944 to a newly established genus, *Kisteueriella*, but did not include *P. californica* in it. Although arguments for this decision are not explicitly stated in the text the differences between *K. biocellata* and *P. californica* regarding the extend of connective tissue separating the longitudinal muscle layers in the anterior region and the degree of branching of the blood vessels in the same region are considered valid to support this decision. Since for neither *Kirsteueriella* nor *Paranemertes* species with a divided longitudinal musculature, molecular data are available an assignment of *A. armoricus* to either of these genera based on molecular evidence is impossible. Furthermore, the poorly resolved status of Poseidonemertidae including several species inquirendae and the lack of broad coverage in molecular data do not permit for any well founded

hypotheses on the evolution and hence the systematics of this taxon to be stated. In the past this lack of information has led to generic and familial assignments that have turned out to be incorrect from a phylogenetic point of view (Maslakova *et al.* 2005; Andrade *et al.* 2012; Kvist *et al.* 2014). It is likely that this also holds true for *P. californica*, the species *A. armoricus* corresponds to most closely. As pointed out by Chernyshev (2002) the former species should not be assigned to the genus *Paranemertes* but is rather a member of Poseidonemertidae. Nevertheless, we refrain from revising the status of *P. californica* until more data, particularly molecular markers, are available.

Due to the unique composition of characters found in *A. armoricus* and the lack of molecular data from the majority of poseidonemertid genera we consider the erection of a new species and genus (viz. *Arenogigas armoricus* gen. et sp. nov.) as inevitable. Although the decision of erecting a new genus contributes to the inflation of the number of monotypic genera within Nemertea, we consider this necessary for the reasons stated above and are confident that some poseidonemertid species, presently considered as species *inquirendae*, will be assigned as members of the genus *Arenogigas* in the future.

2.5 Acknowledgements

We are grateful to Thomas Bartolomaeus who found the new species and to Prof. Dr. Alexei Chernyshev who gave substantial support in characterizing the new species and for providing the sample of Poseidonemertidae 2011. We are thankful to Lars Podsiadlowski who provided substantial support with the molecular analysis and Nils Krüger who sampled and sequenced *Prosorhochmus claparedii* and to Anja Bodenheim, Claudia Müller and Christiane Wallnisch for technical assistance. Thanks to Cédric Hubas of the Muséum national d'Histoire naturelle in Paris for type material deposition. The authors are grateful to Irene Krämer who helped by translating the Russian literature. The authors are also grateful to the staff of the Station de Biologie Marine et Marinarium de Concarneau in France for providing facilities and accommodation during the collection trip.

Chapter 3

Unraveling the *Lineus ruber/viridis* species complex (Heteronemertea, Nemertea)

Daria Krämer*, Christian Schmidt, Lars Podsiadlowski, Patrick Beckers, Lisa Horn and Jörn von Döhren

University of Bonn, Institute of Evolutionary Biology and Ecology,

An der Immenburg 1, 53121 Bonn, Germany

*Corresponding author. E-mail: dkraemer@evolution.uni-bonn.de

This is the author's version of the article originally published online in Zoologica Scripta June 21th 2016
doi:10.1111/zsc.12185

Abstract

Lineus ruber (Müller, 1774) and *Lineus viridis* (Müller, 1774) are among the longest known and most abundant intertidal nemertean species found on both sides of the North Atlantic. Due to easy maintenance in captivity, both species have been well studied concerning morphology, reproduction, development and ecology. Originally described as two separate species in the 18th century, they were subsequently synonymised and considered colour varieties of a single species. It was not until the mid-20th century that complementary redescriptions, including information on reproduction and development, re-established the specific identities of *L. ruber* and *L. viridis*. With the advent of molecular markers in nemertean systematics, however, doubt was again cast on their specific identities. To solve one of the longest standing problems in nemertean systematics, we assembled a comprehensive data set combining external morphology and three genetic markers (mitochondrial cytochrome *c* oxidase subunit I, 16S rRNA and nuclear internal transcribed spacer region) from 160 specimens of *L. ruber* and *L. viridis* collected at six sampling sites along the continental coast of
Western Europe. The data set was analysed with tree-based and non-tree-based species delimitation methods. The results from all methods used confidently delimit three separate clades. A distinct barcoding gap was detected in our data set which thus provides a framework to unequivocally identify specimens as members of any of the three species. Comparison of our findings with published data enables us to assign one lineage to *L. ruber* and one to *L. viridis*. We designated neotypes for both species. The third clade is very similar to *L. viridis*, only distinguishable by a conspicuous, iridescent

ventral fold in some male specimens This lineage shows a syntopic distribution along western European coasts and represents a species new to science and is described as *Lineus clandestinus* sp. n. based on its external characters and the analyses of the molecular data provided in this study.

3.1 Introduction

Nemertea (Rhynchocoela) is a clade of unsegmented, mostly marine spiralian worms that comprises approximately 1300 described species (Gibson 1995; Kajihara *et al.* 2008). As vagile nocturnal predators equipped with a venomous, eversible proboscis, they are suspected to elicit a major predatory influence on respective local prey communities (McDermott & Roe 1985; Thiel & Reise 1993; Thiel 1998; Thiel & Kruse 2001; Caplins *et al.* 2011; Whelan *et al.* 2014; and references therein). Its putative basal position within Trochozoa gives Nemertea a key role for the understanding of the evolution of Spiralia (Haszprunar 1996; Turbeville 2002; Edgecombe *et al.* 2011). Thus, nemertean species represent interesting, though until today largely neglected, objects of study in several disciplines of biology including morphology, ecology, physiology, genetics, evolutionary development and phylogenetics.

The heteronemertean species *Lineus ruber* (Müller, 1774) and *Lineus viridis* (Müller, 1774) are among the most abundant and most widespread nemertean species with a circumpolar distribution in the Northern Hemisphere (Gibson 1982, 1995). They have been well investigated regarding many aspects of nemertean biology (Rogers *et al.* 1995a and references therein; McDermott 2001; von Döhren & Bartolomaeus 2006, 2007; Beckers *et al.* 2011; von Döhren 2011; von Döhren *et al.* 2012; Martín-Durán *et al.* 2015). However, historically there has been much uncertainty about the identity of these species. Although each having been originally described as distinct species they have long been considered colour varieties, synonymised as either *L. ruber* or *L. gesserensis* (Gibson 1995). This has to be accredited to the original description by Müller which does not contain sufficient information about diagnostic characters or type localities for either species (Müller 1774; Gibson 1982, 1995). It was not until the 20th century when the two species were separated independently by Schmidt (Schmidt 1964, for an English list and summary of the preceding publications) and Gontcharoff (1951, 1959, 1960) based not only on colouration but also on distinct differences in reproduction biology and life-history strategies. With her comprehensive studies in Roscoff, France, Gontcharoff (1951, 1959, 1960) provided complementary descriptions of *L. ruber* and *L. viridis* making delimitation and identification of the two species possible. Although no official neotype material was deposited, reference to these two

Lineus species was subsequently made based on the findings of Gontcharoff (1951) (Gibson 1995).

Even though having been successfully employed to detect and delimit new, cryptic species in various nemertean taxa (Strand & Sundberg 2005a; Sundberg *et al.* 2009b, 2010; Chen *et al.* 2010; Fernández-Álvarez & Machordom 2013; Leasi & Norenburg 2014; Alfaya *et al.* 2015; Hao *et al.* 2015; Kang *et al.* 2015), more recently employed methods of molecular systematics have remained inconclusive regarding the specific identities of *L. ruber* and *L. viridis*. While data on several isoenzyme loci in animals from France, Great Britain and the United States detected a third species among European *L. ruber* and *L. viridis* specimens (Rogers *et al.* 1995), comparative data on the 16S rRNA gene from Scandinavian and British specimens again advocated synonymy of *L. viridis* with *L. ruber* (Sundberg & Saur 1998).

The present study aimed to resolve this long-standing problem with a combined, multiple method approach and a dense, comprehensive specimen sampling. To gain information on distribution and genetic population structure in Europe, collecting was conducted at the north and northwest coasts of France and the German North Sea coast. We performed phylogenetic analyses based on gene fragments of the cytochrome *c* oxidase subunit I (COI), 16S rRNA (16S) and the nuclear internal transcribed spacer region (ITS). The COI data set was further subjected to several tree-based and non-tree-based species delimitation methods to identify the number of species among the sampled specimens (for other nemertean species, compare: Sundberg *et al.* 2009b; Chen *et al.* 2010; Kvist *et al.* 2014; Leasi & Norenburg 2014; Alfaya *et al.* 2015; Faasse & Turbeville 2015; Hao *et al.* 2015; Kang *et al.* 2015). Our results show a separation of the sampled specimens into three distinct clades of which two can be assigned with high confidence to either *L. ruber* or *L. viridis sensu* Gontcharoff (1951). The third clade represents a species new to science and is herein described as *Lineus clandestinus* sp. n.

3.2 Material and Methods

3.2.1 Specimens and sampling sites

One hundred and sixty specimens were collected during 2010 and 2013 from six localities from the north and northwest coasts of France (Concarneau, Île de Groix, Roscoff, Wimereux), and the German North Sea coast (Helgoland, Sylt) (Figure 3.1, Appendix II: Supplementary Table 3). All nemerteans were collected during low tide beneath rocks and stones lying on sand or shell gravel. For identification, individuals were anaesthetised in 7% $MgCl_2$ mixed with sea water at equal volumes and photographed with a digital camera (Canon EOS 600D) mounted on a dissection microscope (Zeiss Stemi 2000). A tissue sample of each individual was preserved in absolute EtOH (99.9%) for DNA extraction, whereas the anterior ends of some individuals were fixed in Bouin's solution for histological cross-sectioning (azan staining). Specimens were classified into *L. ruber* and *L. viridis* based on their colouration according to the description given by Gontcharoff (1951). Specimens of *Ramphogordius sanguineus* (Rathke, 1799) and *Riseriellus occultus*, Rogers *et al.* 1993 that were used as out-group species in the phylogenetic analyses were collected at Concarneau in 2012 and 2011, respectively. All specimens were identified based on differences in their behaviour when disturbed as described by Gontcharoff (1951) and Rogers *et al.* (1993). Specimen IDs used herein were created as follows: pre-identification of species (Lv, *L. viridis*; Lr, *L. ruber*; Ro, *R. occultus*; Rs, *R. sanguineus*), a sequential number, abbreviation of the sample site (Con, Concarneau; Hl, Helgoland; Idg, Île de Groix; Rsc, Roscoff; Sy, Sylt; Wi, Wimereux) and the last two digits of the year of sampling (Appendix II: Supplementary Table 3).

3.2.2 Nucleic acid purification and PCR amplification

DNA was extracted with DNeasy Blood and Tissue kit (Qiagen®) following the manufacturer's instructions. Three loci were amplified: the partial COI and 16S rRNA and ITS (ITS1, 5.8S rDNA and ITS2). All primers used for the amplification and sequencing reactions are listed in Appendix II: Supplementary Table 4 (Folmer *et al.* 1994; Palumbi 1996). For COI and 16S, either TaKaRa™ Ex Hot Start polymerase or

Hot-Master Taq polymerase (Invitrogen™) was used. Polymerase chain reactions (PCRs) for ITS were performed with TaKaRa™ LA Hot Start polymerase. Thermal cycling was initiated with 2 min at 94 °C, followed by 40 cycles (30 s at 94°C, 60 s at 53 °C (COI/ITS)/51°C (16S) and 60 s at 72°C), and terminated with a 2-min final elongation at 72°C. PCR products were purified with NucleoSpin® Extract II-Kit (MACHEREY-NAGEL GmbH & Co. KG) following the instructions of the manufacturer. Purified PCR products were sent to LGC Genomics© for Sanger sequencing, using forward and reverse primers for sequencing (Sanger *et al.* 1977). The entire data set is deposited in GenBank with specimen IDs and accession numbers for COI, KM878335–KM878496; 16S, KM878497– KM878518; and ITS, KM878519–KM878539 (Appendix II: Supplementary Table 3).

3.2.3 Sequence analysis

Sequences were edited with BioEdit version 7.0.9. and aligned using MAFFT version 7 with G-INS-I strategy using default parameters: scoring matrix for nucleotide sequences of 200PAM/K = 2; gap opening penalty of 1.53; and offset value of 0.0 (Hall 1999; Andrade *et al.* 2012; Katoh & Standley 2013). The amount of heterozygotes within the ITS region was below 1%. Sites containing ambiguous information were excluded.

3.2.4 Non-tree-based species delimitation

To assess the composition and number of species, pairwise distances were calculated using uncorrected p-distances implemented in MEGA version 5.2.1 based on the COI gene of all collected *L. ruber* and *L. viridis* specimens (Tamura *et al.* 2011).

A haplotype network was estimated using statistical parsimony implemented in TCS version 1.21 with the connection limit set to 95% (Templeton *et al.* 1992; Clement *et al.* 2000; Hart & Sunday 2007) which is the most commonly threshold used for COI sequences of nemerteans (see Sundberg *et al.* 2009b; Chen *et al.* 2010; Kang *et al.* 2015).

A barcoding gap was identified using the Automatic Barcode Gap Discovery (ABGD) (Puillandre *et al.* 2012). The nucleotide divergence threshold (NDT) was set to 95% and applied to the COI alignment using the R-script written by Tang *et al.* (2012).

3.2.5 Phylogenetic analyses and tree-based species delimitation

For phylogenetic analyses based on the combined COI (523nt), 16S (431nt) and ITS (1006nt) data, five *Lineus ruber* and 15 *Lineus viridis* were selected to represent all sample sites and the most frequent haplotypes of each group/network detected by non-tree-based species delimitation methods. Additionally, COI and 16S data were combined with sequence data taken from GenBank (Appendix II: Supplementary Table 5), whereas ITS was analysed separately. Phylogenetic trees were reconstructed using maximum likelihood (ML) based on the general time-reversible model and a gamma distribution with a proportion of invariant sites (GTR+G+I) implemented in MEGA version 5.2.1 (Nei & Kumar 2000; Tamura *et al.* 2011). The model for phylogenetic reconstruction was selected by MrModeltest version 2.3 based on the Akaike information criterion (Nylander 2004). Branch support was estimated using 500 bootstrap replicates. Bootstrap values ≥ 80% were considered robust support. *Riseriellus occultus* was used for out-group rooting.

To test for the number of species obtained by non-treebased methods, the Bayesian implementation of the Poisson tree process model (bPTP) for species delimitation (Zhang *et al.* 2013) was applied to the COI data set. Therefore, a phylogenetic input tree was reconstructed based on the complete COI data set (161 sequences, 523nt) with the settings outlined above.

3.3 Results

3.3.1 Specimen numbers per sampling site

A total of 160 *Lineus ruber* and *Lineus viridis* specimens were collected at six sampling sites. Larger numbers of specimens were collected from Sylt, Germany (n = 72), Roscoff, France (n = 44), and Wimereux, France (n = 21), while the remaining sample sites together contribute only approximately 17% of the analysed specimens to the

analyses: Helgoland, Germany (n = 9); Île de Groix, France (n = 8); and Concarneau, France (n = 6) (Figure 3.1, Appendix II: Supplementary Table 3).

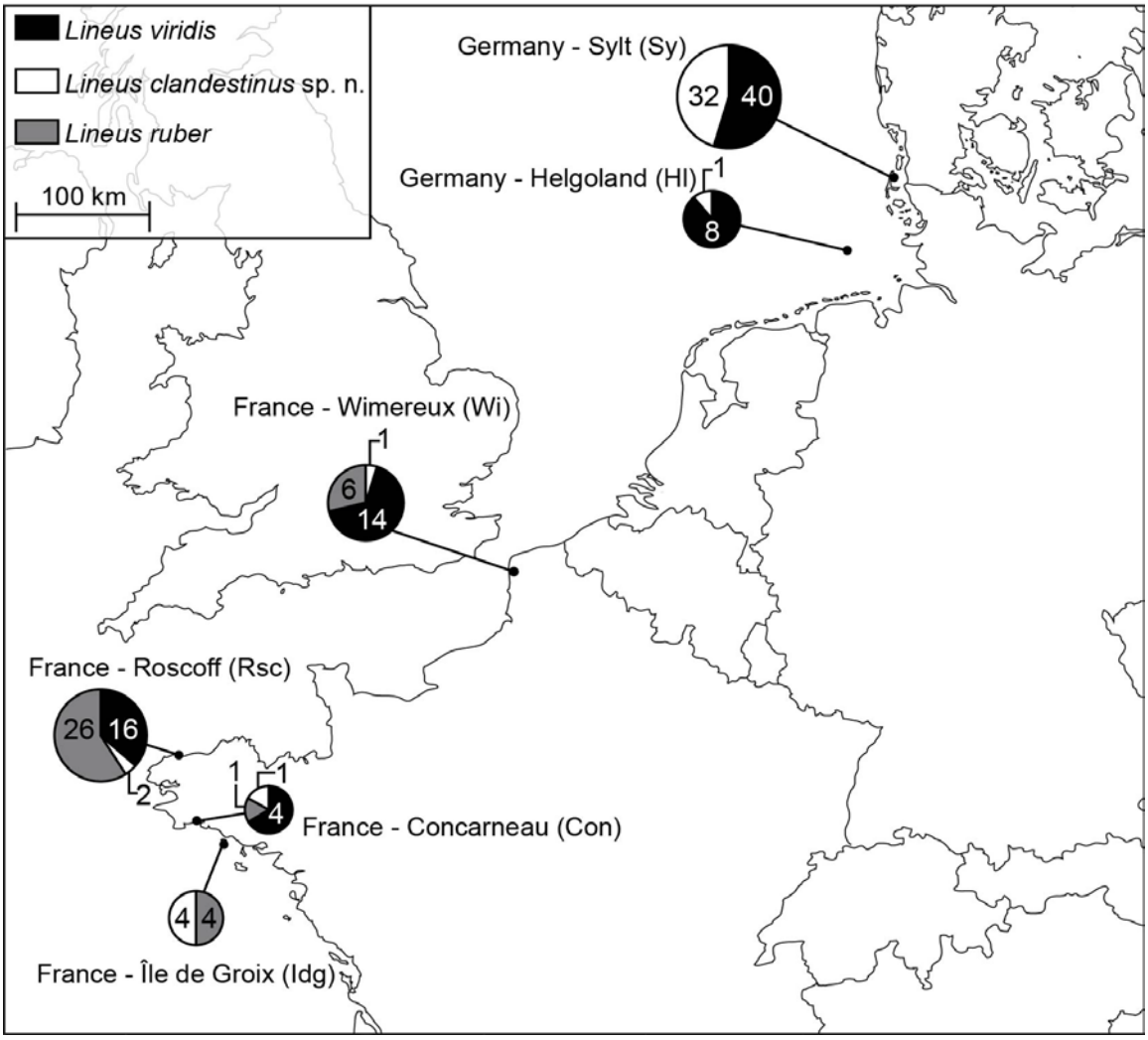

Figure 3.1 Map showing sampling sites in Europe and total number of collected specimens for each species

3.3.2 Distribution and non-tree-based species delimitation

We obtained COI sequences for each collected specimen (160 sequences) which resulted in an alignment of 523nt in length. The statistical parsimony analysis of the COI data set under the 95% connection limit yields three unconnected haplotype networks (Figure 3.2, Appendix II: Supplementary Table 3). While in two networks body colouration of the specimens varies over a considerably wide range of green to red

shades, the remaining network contains only specimens with red to reddish-brown pigmentation (Figure 3.8, Figure 3.9). The latter network is therefore assigned to *L. ruber*, according to the description given by Gontcharoff (1951) (Figure 3.2 C, Figure 3.8 B). Specimens exhibiting the dark green colour that has been described for *L. viridis* by Gontcharoff (1951) were only found in one of the remaining networks. As a consequence, this network is termed *L. viridis* (Figure 3.2 A, Figure 3.8 A). The third network contains specimens with highly variable body colouration but also individuals with a conspicuous ventral fold. The latter are exclusively found in this network which is termed *Lineus clandestinus* sp. n. (for description see below) (Figure 3.2 B, Figure 3.9 A, B).

The *L. ruber* network includes 37 specimens (approx. 23% of all collected specimens) representing nine different haplotypes (Figure 3.2 C). All specimens of this network were collected at French sampling sites, with 70% of the specimens grouped in this network originating from Roscoff. There is a single, highly frequent haplotype found in 19 of 37 specimens, two medium-frequency haplotypes found in four and six specimens, respectively, and six low-frequency haplotypes, two of which represented by two specimens and four represented by one specimen. Most of the haplotypes are interconnected by a single mutational step. Only one haplotype found in a single specimen from Roscoff is separated by three substitutions from its nearest neighbouring haplotype (Figure 3.2 C).

The *L. viridis* network contains 82 specimens (approx. 51% of all collected specimens) in 16 distinct haplotypes from all locations except the southernmost sampling site, Île de Groix (Figure 3.2 A). There are three highly frequent haplotypes detected in 10, 20 and 21 specimens, respectively. Three haplotypes with medium frequency are present in four, six and eight specimens. Ten haplotypes show a low frequency with two haplotypes occurring in two specimens each while the remaining eight have been found in only a single specimen. Most haplotypes are separated from the closest neighbouring haplotype by a single nucleotide substitution. One haplotype found in a specimen from Wimereux is separated from the next by two mutational steps, while another haplotype found in one specimen from Roscoff is separated from the nearest haplotype by three substitutions (Figure 3.2 A).

The *L. clandestinus* network contains 41 specimens (approx. 32% of all collected specimens) from all of the six sampling sites (Figure 3.2 B). This network comprises five haplotypes. The vast majority of 32 specimens (78%) originate from Sylt. In this haplotype network, there is a single dominant highly frequent haplotype present in 36 specimens (90%). One haplotype was found in two specimens while the remaining three haplotypes are represented by one specimen each. The lowest frequency haplotypes are separated from the dominant haplotype by one mutational step (Figure 3.2 B).

When comparing the three networks, the least population structure is seen in the *L. clandestinus* with five haplotypes and 88% of the specimens showing the same haplotype. In *L. viridis*, there are 16 haplotypes of which the three most frequent haplotypes have been found in 25%, 24% and 13% of the specimens comprising the network. Regarding genetic population structure, the *L. ruber* network is slightly less structured than the network of *L. viridis* with nine haplotypes and 51% of the specimens exhibiting the most frequent haplotype; 53 mutational steps are needed to connect *L. viridis* and *L. clandestinus*. The resulting haplotype network is connected to the *L. ruber* network via 62 mutational steps (data not shown).

The ABGD and NDT also identified three groups within the COI data set (Table 3.2). Pairwise distances reveal low intraspecific divergences varying from 0% to 1.53% in *L. virdis*, 0% to 0.96% in *L. ruber* and 0% to 0.38% in *L. clandestinus*. Thus, differences in genetic population structure of the haplotype networks are also reflected in the intraspecific variation in the uncorrected p-distance values. Interspecific uncorrected p-distances are highest between *L. viridis* and *L. ruber* with 12.95% to 14.15%, and lowest between *L. viridis* and *L. clandestinus* with 10.71% to 11.47% sequence divergence. Pairwise distances between *L. clandestinus* and *L. ruber* show divergences varying from 11.85% to 12.62% (Table 3.1).

Table 3.1 Summary of uncorrected p-distances (%) for all COI sequences.

	L. viridis	*L. ruber*	*L. clandestinus*	*R. sanguineus*
L. viridis	0-1.53			
L. ruber	12.95-14.15-	0.-0.96		
L. clandestinus	10.71-11.47	11.85-12.62	0-0.38	
R. sanguineus	15.11-15.87	14.34-14.91	15.11-15.30	-
R. occultus	17.02-17.59	15.87-16.44	15.30-15.49	16.25

Table 3.2. Number of entities (#E)/haplotypes (#H) obtained by tree-based, non-tree-based species delimitation, and phylogenetic analyses.

TCS	**ABGD**	**NDT**	**ML**	**bPTP**
#E:3				
#H:				Estimated #E: 3-20 (Ø: 4.79)
L. clandestinus: 5				Accptance rate: 0.41588
L. ruber: 9				Merge: 50096
L. virdis: 16	#E: 3	#E 3	#E: 3	Split: 49904

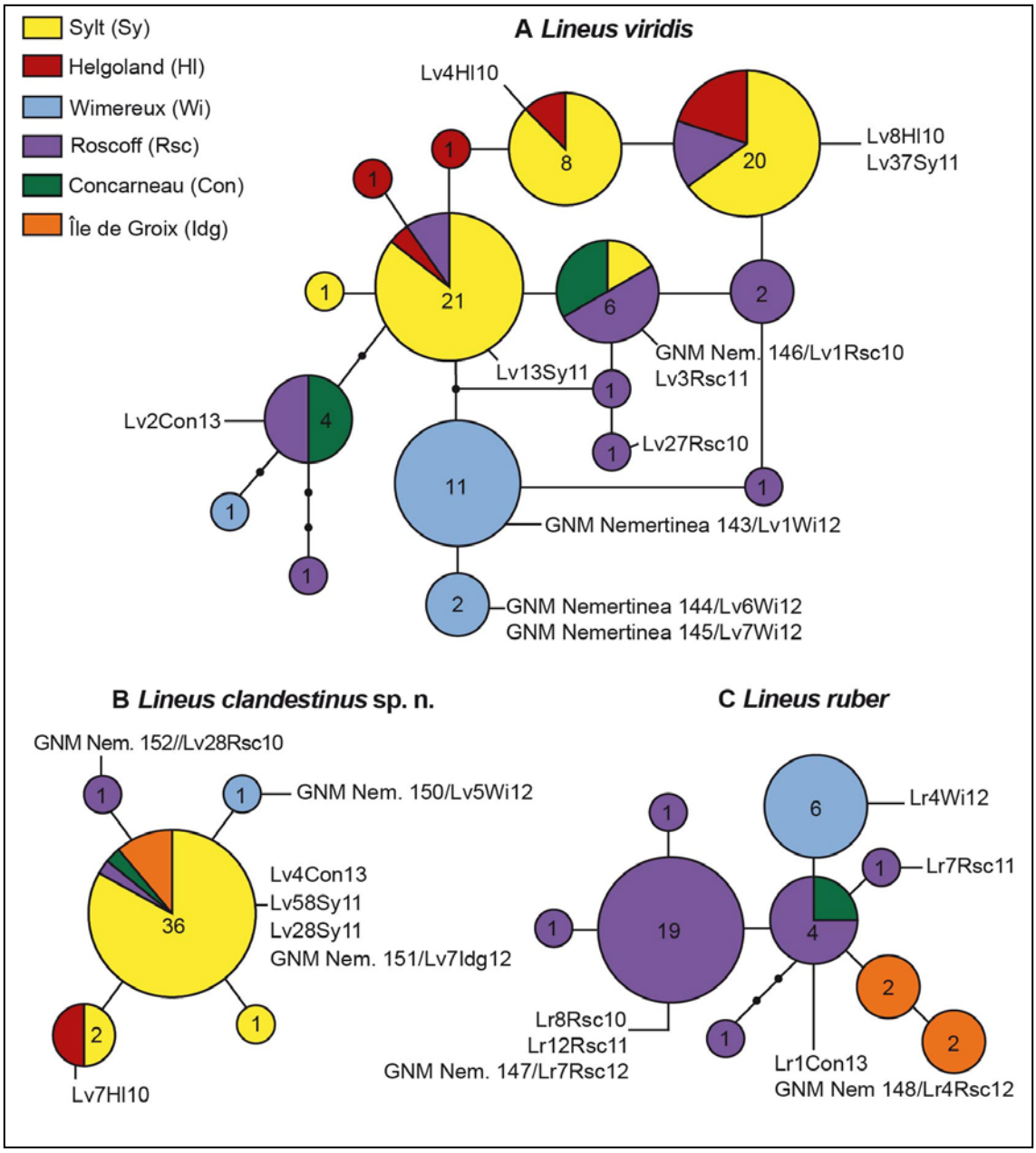

Figure 3.2 The statistical parsimony haplotype network based on the mitochondrial DNA cytochrome *c* oxidase subunit I gene for **(A)** 82 *Lineus viridis*, **(B)** 41 *Lineus clandestinus* and **(C)** 37 *Lineus ruber* specimens, coloured by geographic distribution. The connecting limit is set to 95%. Minimal distance between *L. viridis* and *L. clandestinus*: 53 steps, *L. clandestinus* and *L. ruber*: 62 steps. An empty line connecting haplotype pie charts represents a single mutational change; each black dot on a line represents one additional mutational change. Numbers within pie charts represent the number of specimens within each haplotype. Specimen IDs indicate museum material and specimens used for the phylogenetic analyses.

3.3.3 Phylogenetic analyses and tree-based species delimitation

The maximum-likelihood analysis of the complete COI data set shows the analysed specimens contained in three separate lineages that all have highly robust nodal support (bootstrap value: 99%). The out-group species, *Ramphogordius sanguineus* (Rs1Con12) and *Riseriellus occultus* (Ro1Con11), group outside of the *Lineus* lineage. Two of the lineages, *L. viridis* and *L. clandestinus*, are more closely related to moderately robust nodal support (bootstrap value: 89%). The third lineage, *L. ruber*, is sister to the other two clades with slightly less robust nodal support (bootstrap value: 73%) (Figure 3.3). Included published sequence data assigned to *L. viridis* or *L. ruber* (HQ858579, FJ839919, EF124970, EF124974, AJ436936, KC812596, KC812597 and GU392024) show affiliation to *L. viridis*, whereas *L. ruber* specimens (DQ911370, KC812595) from the UK and Chile group with *R. sanguineus* (Rs1Con12) (Sundberg & Saur 1998; Thollesson & Norenburg 2003; Sundberg & Strand 2007; Schwartz 2009; Podsiadlowski *et al.* 2009; Strand & Sundberg 2011; Andrade *et al.* 2012; Strand *et al.* 2014). Only one specimen from the UK which was identified as *L. ruber* (KC812602) groups within the clade labelled as *L. ruber* (Figure 3.4, Appendix II:Supplementary Table 5) (Strand *et al.* 2014).

The phylogenetic analysis based on 431-nt-long alignment of 16S resulted in robust nodal support values for *L. viridis* (100%), *L. clandestinus* (94%) and *L. ruber* (99%) (Figure 3.5). The sister group relationship of *L. viridis* and the new species is robustly supported with a bootstrap value of 99%. Specimens assigned to *L. viridis* from the USA (EF124886) group with individuals from *L. viridis*, as already shown by our COI analysis (EF124974, Figure 3.5). Specimens from Sweden which had been identified as *L. ruber* based on the reddish colouration group with either *L. viridis* (AF103759) or *L. clandestinus* (AF103758). *L. ruber* from Wales (DQ911371), which is identical to *L. ruber* DQ911370 used for the COI analysis, groups with *R. sanguineus* (Rs1Con12), that is congruent with our phylogenetic analysis based on COI. The only GenBank sequence from *L. ruber* grouping with *L. ruber* individuals of the present study originates from a specimen collected in Wales (AF103757) (Figure 3.4, Figure 3.5, Appendix II:Supplementary Table 5).

The ITS alignment has a length of 1006 nucleotides and shows an identical topology with an identical composition of specimens as the COI- and 16S-based trees:

the analysed specimens cluster in the same three major clades (Figure 3.6). Nodal support for each clade is highly robust (each bootstrap value: 100%). The sister group relationship of *L. viridis* and *L. clandestinus* shows lower nodal support than in the phylogenetic analysis of the COI alignment (bootstrap value: 66%) (Figure 3.6).

The phylogenetic analysis of the combined data set including COI, ITS and 16S of the sampled specimens iterates the results from the analyses of the isolated markers both in topology and in specimen composition, albeit with generally higher nodal support values. The bootstrap support is 100% each for lineages of *L. viridis*, *L. clandestinus* and *L. ruber*. The sister group relationship of *L. viridis* and *L. clandestinus* is supported with a bootstrap value of 95% (Figure 3.7).

Results from the bPTP approach slightly differ from all other results and suggested 3–20 (mean 4.79) independent entities (Table 3.2).

Results from all methods applied analyses clearly support the existence of *L. clandestinus* as the third species within the *L. ruber/viridis* species complex. We describe *L. clandestinus* sp. n. and designate neotypes for *L. ruber* and *L. viridis* as there is no type material available for both species. We base the descriptions on external characters and DNA sequences of the type material (deposited at the Göteborgs Naturhistoriska Museum (GNM), MorphDBase and GenBank) and additional examined specimens (deposited at GenBank).

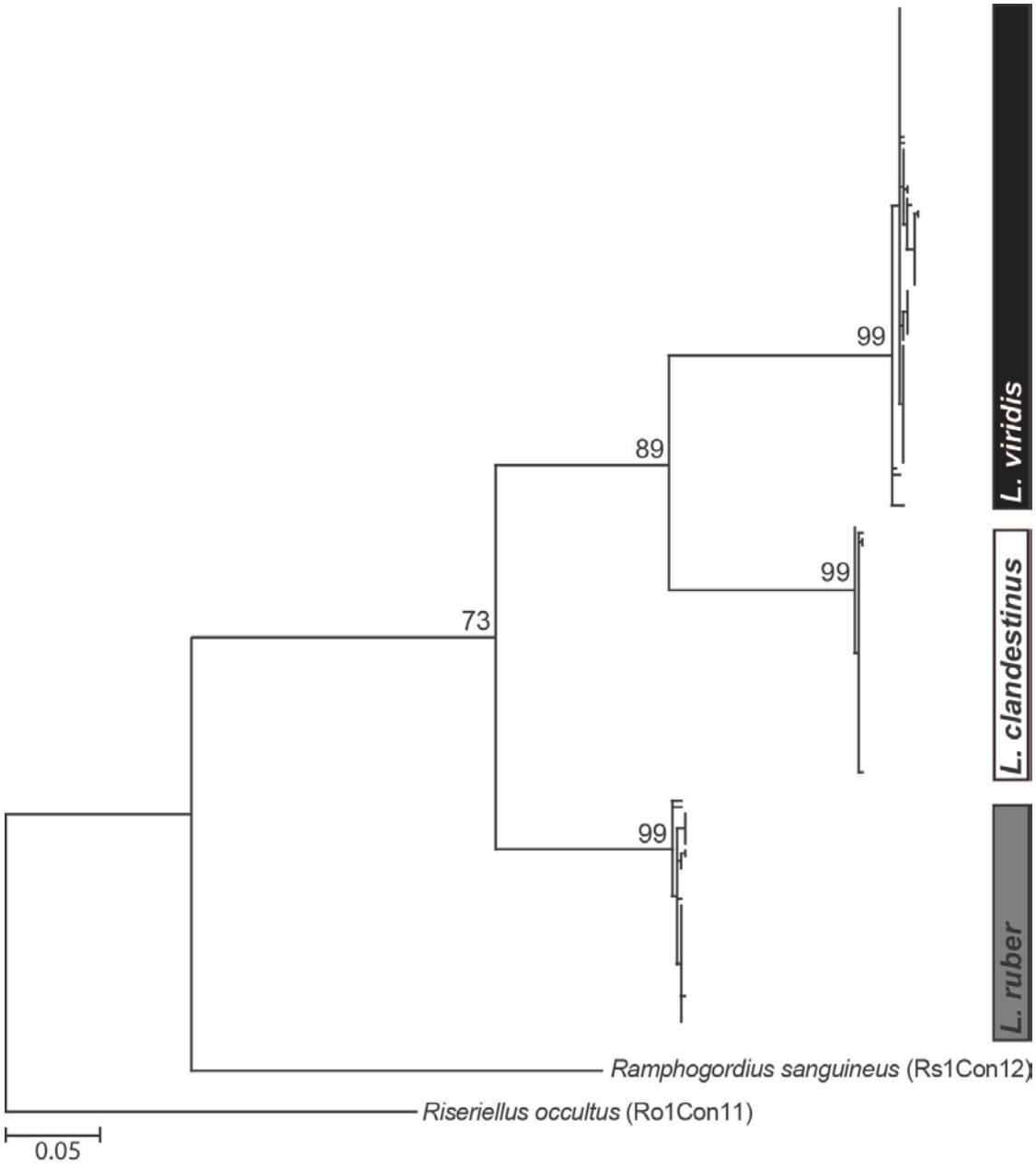

Figure 3.3 Maximum likelihood tree of all *Lineus ruber*, *Lineus viridis*, *Lineus clandestinus*, and *Ramphogordius sanguineus* specimens specimens based on COI mtDNA (162 sequences). Numbers above nodes indicate bootstrap support from 500 replicates for each clade. Inner resolutions are not shown due to low bootstrap support. *Riseriellus occultus* (Ro1Con11) was used for outgroup rooting.

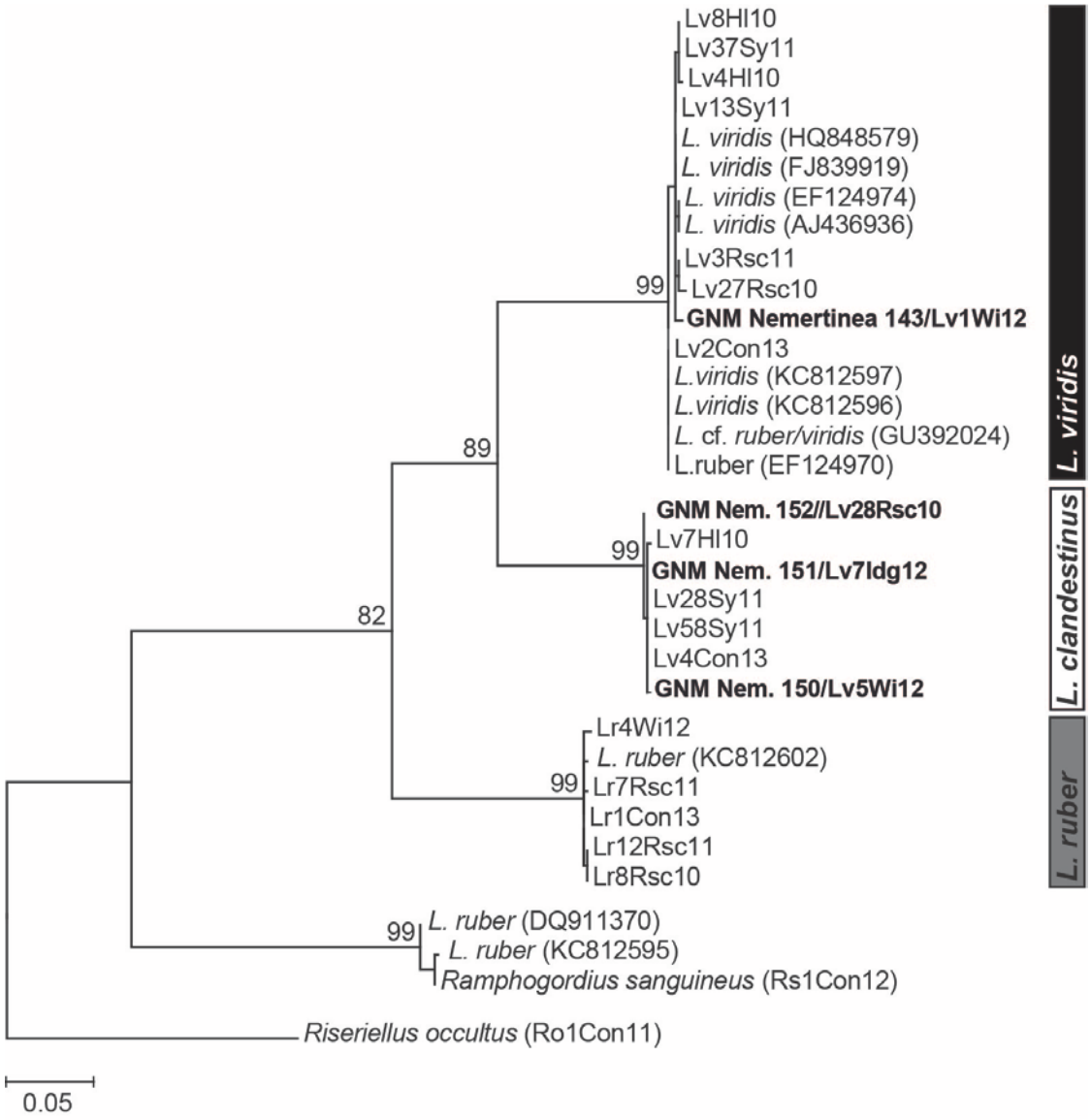

Figure 3.4 Maximum likelihood tree of selected *Lineus ruber*, *Lineus viridis*, *Lineus clandestinus*, and *Ramphogordius sanguineus* specimens based on COI mtDNA. Numbers above nodes indicate bootstrap support from 500 replicates for each clade. Inner resolutions are not shown due to low bootstrap support. *Riseriellus occultus* (Ro1Con11) was used for outgroup rooting. Bold type indicates material deposited at GNM.

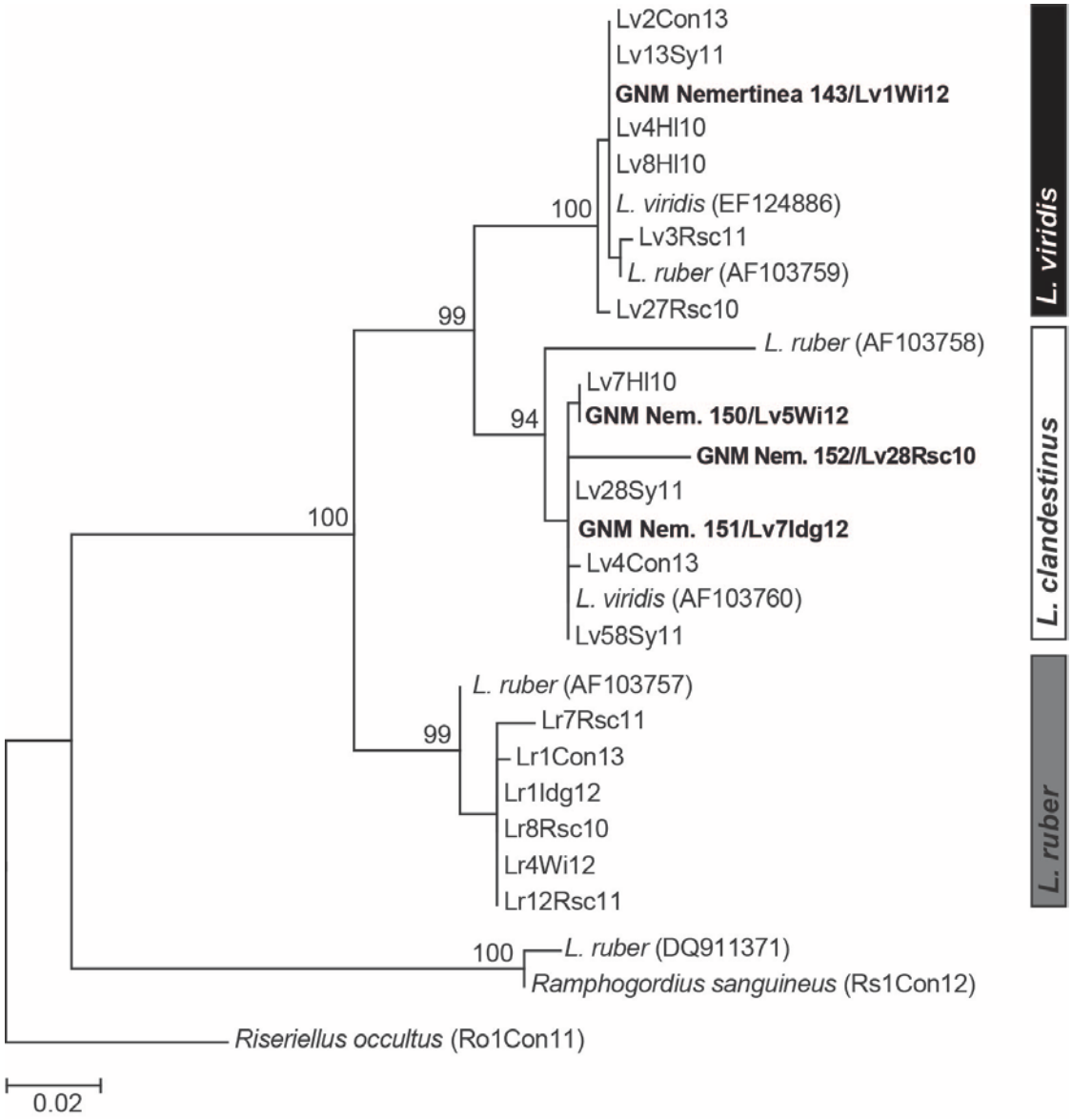

Figure 3.5 Maximum likelihood tree of selected *Lineus ruber*, *Lineus viridis*, *Lineus clandestinus*, and *Ramphogordius sanguineus* (Rs1Con12) specimens based on 16S rRNA. Numbers above nodes indicate bootstrap support from 500 replicates for each clade. Inner resolutions are not shown due to low bootstrap support. *Riseriellus occultus* (Ro1Con11) was used for outgroup rooting. Bold type indicates material deposited at GNM.

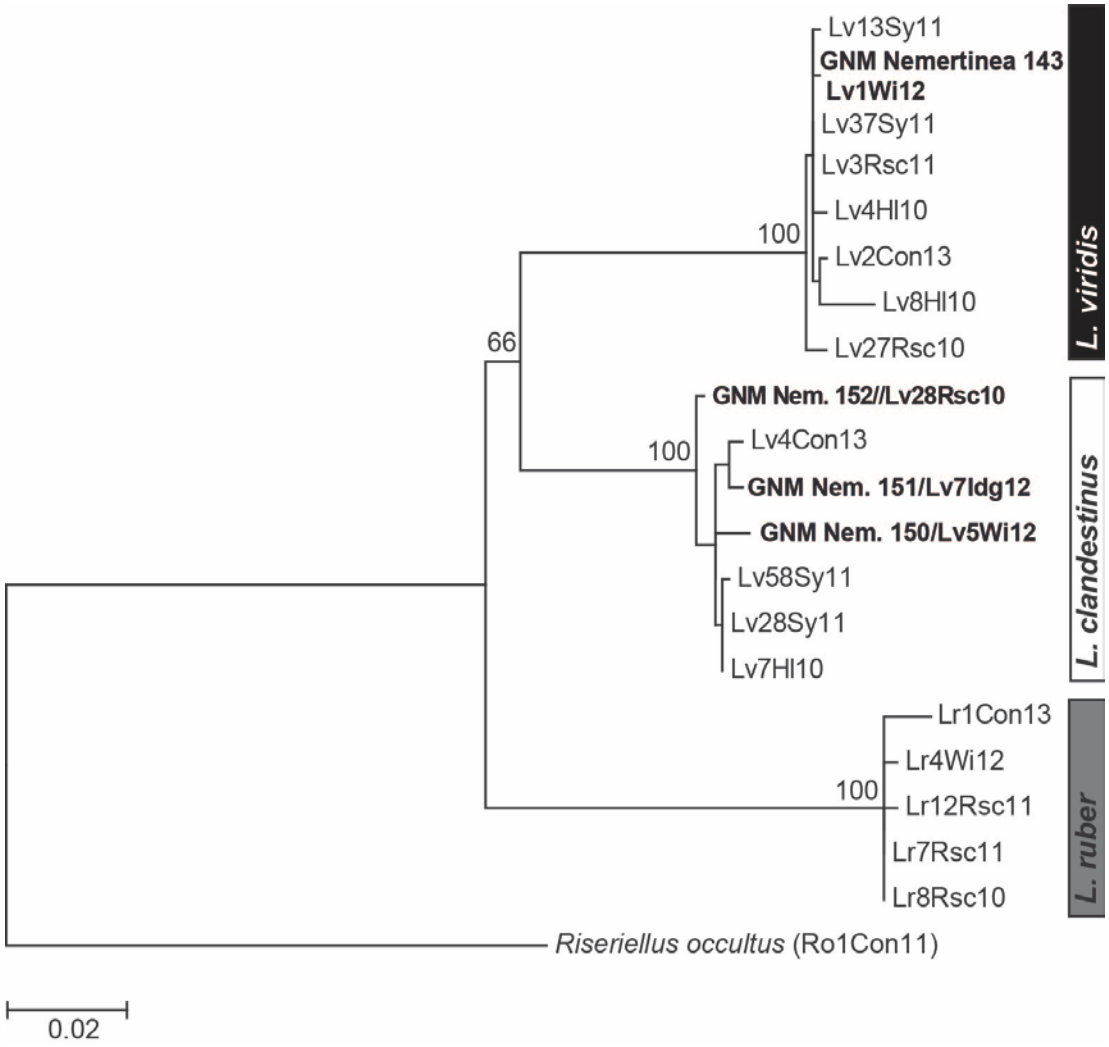

Figure 3.6 Maximum likelihood tree of selected *Lineus ruber*, *Lineus viridis*, and *Lineus clandestinus* specimens based on ITS rRNA. Numbers above nodes indicate bootstrap support from 500 replicates for each clade. Inner resolutions are not shown due to low bootstrap support. *Riseriellus occultus* (Ro1Con11) was used for outgroup rooting. Bold type indicates material deposited at GNM.

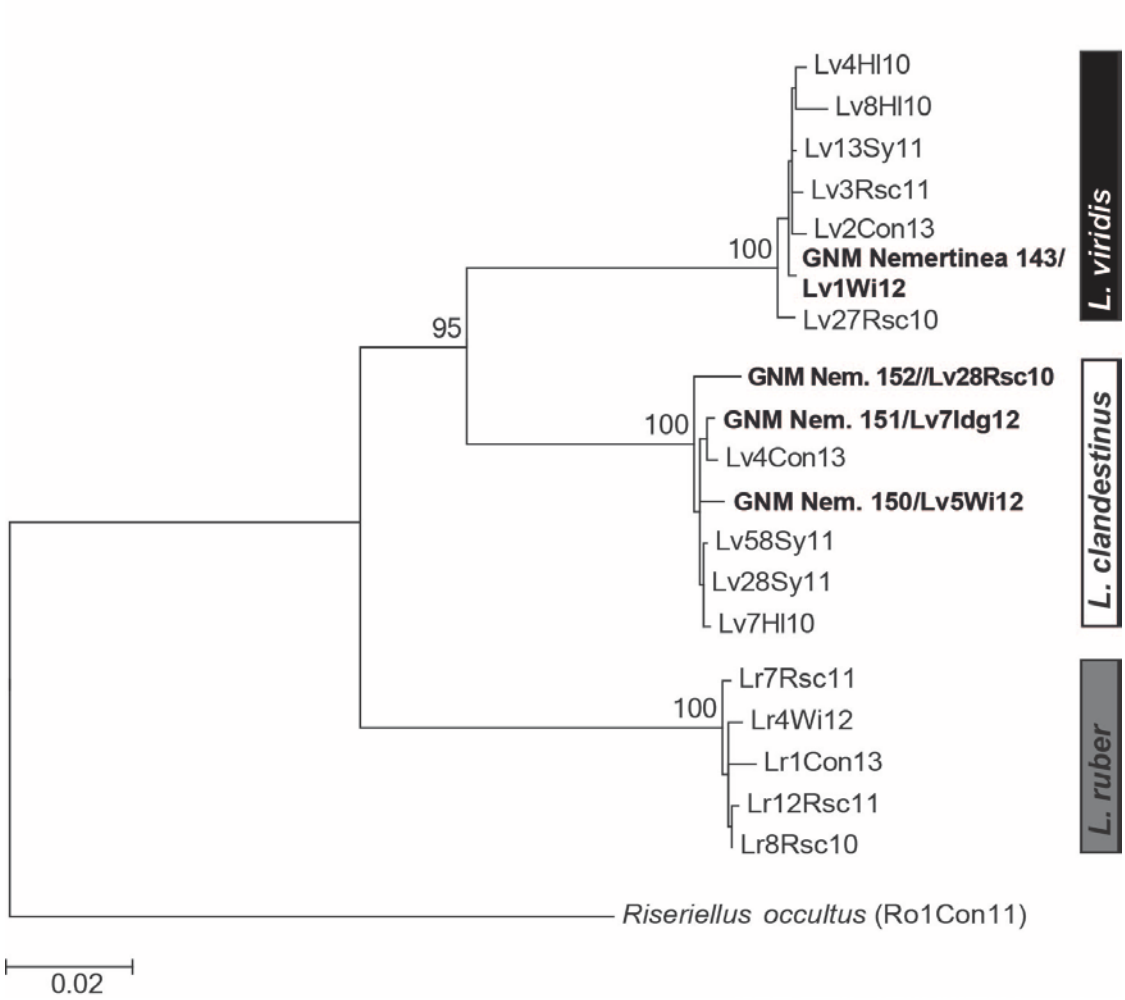

Figure 3.7 Maximum likelihood tree of selected *Lineus viridis*, *Lineus clandestinus* and *Lineus ruber* specimens based on combined COI mtDNA, 16S rRNA, and ITS rRNA. *Riseriellus occultus* (Ro1Con11) was used for outgroup rooting. Numbers above nodes indicate bootstrap support from 500 replicates for each clade. Inner resolutions are not shown due to low bootstrap support. Bold type indicates material deposited at GNM.

3.3.4 Taxonomy

Family LINEIDAE McINtosh, 1873-1874

Genus *Lineus* Sowerby, 1804

Lineus ruber

For list of synonyms see Bürger 1904 (p. 101) and Gibson 1995 (pp. 373–374)

Neotype designated here. FRANCE Roscoff intertidal zone in front of marine biological station (48°43041.59″N 3°59020.73″W), lower intertidal during diurnal low tide, coarse sediment underneath stones, tissue in ethanol (GNM Nemertinea 147/Lr7Rsc12 (Figure 3.8 B), GenBank accession number: KM878482 (COI)).

Voucher material. FRANCE Roscoff intertidal zone in front of marine biological station (48°43041.59″N 3°59020.73″W), lower intertidal during diurnal low tide, coarse sediment underneath stones, tissue in ethanol (GNM Nemertinea 148/Lr4Rsc12 (Figure 3.8 B), GenBank accession number: KM878464 (COI);

Sixty-one slides of histological transverse sections, anterior part of specimen sliced until nephridial, system, 5 µm, azan staining (GNM Nemertinea 149/Lr6Rsc10, first 52 slides: www.morphdbase.de/?D_Kraemer_20160122-S-3.1).

Other material. Roscoff intertidal zone in front of marine biological station (48°43041.59″N 3°59020.73″W), lower intertidal during diurnal low tide, coarse sediment underneath stones, histological transverse sections, anterior part of specimen sliced until nephridial system, 5 lm, azan staining (www.morphdbase.de/?D_Kraemer_20160125-S-7.1);

FRANCE Roscoff intertidal zone in front of marine biological station (48°43041.59″N 3°59020.73″W), lower intertidal during diurnal low tide, coarse sediment underneath stones, 23 specimens with sequence data deposited at GenBank (Appendix II: Supplementary Table 3);

FRANCE Wimereux, Pointe aux Oies (50°45046.47″N 1°3601.52″E), intertidal zone during diurnal low tide in front of marine biological station, three specimens with sequence data deposited at GenBank (Appendix II: Supplementary Table 3);

FRANCE Concarneau, Cabellou Plage (47°51019.08″N 3°54058.55″W), intertidal zone, coarse sediment underneath stones during diurnal low tide, one specimen from Concarneau with sequence data deposited at GenBank (Appendix II: Supplementary Table 3);
FRANCE Île de Groix, Pointe Saint-Nicolas (47°37043.85″N 3°29011.15″W), upper littoral during diurnal low tide, four specimens with sequence data deposited at GenBank (Appendix II: Supplementary Table 3).

Description. Length 14 mm to 43 mm (mean 23 mm), width 1 mm. Body characterised by brown to red shades. Ventral side always lighter in colouration, slightly translucent: gastric pouches visible through body wall. Head bluntly pointed with triangular-shaped pigmentation (Figure 3.8 B, Lr8Rsc10). Brain distinguishable as reddish bilobed structure through dorsal and ventral body wall (Figure 3.8 B, GNM Nem. 147/ 148). Mouth appearing as whitish slit, positioned behind cephalic lobe and brain (Figure 3.8 B, GNM Nem. 147). Eyes situated at lateral margins of pigmented part of cephalic lobe (Figure 3.8 B, GNM Nem. 148, Lr8Rsc10, Lr4Wi12, Lr12Rsc11). Variable number of ocelli (four to 13) unequally distributed on each side (Figure 3.8 B). Visibility of eyes and brain depending on pigmentation; in darkly pigmented individuals, eyes and brain not distinguishable (Lr1Con13). Sexually mature specimens with dorsally flattened body, without modified ventral side (Figure 3.8 B, GNM Nem. 147).

Lineus viridis

For list of synonyms see Bürger 1904 (p. 104) and Gibson 1995 (p. 374)

Neotype designated here. FRANCE Roscoff intertidal zone in front of marine biological station, lower intertidal during diurnal low tide (48°43041.59″N 3°59020.73″W), coarse sediment underneath stones, tissue in ethanol (GNM Nemertinea 142/Lv2Rsc12 (Figure 3.8 A), GenBank accession number: KM878416 (COI)).

Voucher material. FRANCE Wimereux, Pointe aux Oies (50°45046.47″N 1°3601.52″E), intertidal zone during diurnal low tide in front of marine biological station, cephalic region of juvenile in ethanol (GNM Nemertinea 143/ Lv1Wi12 (Figure 3.8 A), GenBank accession numbers: KM878399 (COI), KM878513 (16S), KM878522 (ITS));

Whole female except for small part from posterior end used for DNA extraction (GNM Nemertinea 144/ Lv6Wi12 (Figure 3.8 A), GenBank accession number: KM878396 (COI));

Whole female except for small part from posterior end used for DNA extraction (GNM Nemertinea 145/ Lv7Wi12, GenBank accession number: KM878396 (COI));

FRANCE Roscoff intertidal zone in front of marine biological station (48°43041.59″N 3°59020.73″W), lower intertidal during diurnal low tide, coarse sediment underneath stones, 79 slides of histological transverse sections, anterior region sliced until nephridial system, 5 µm, azan staining (GNM Nemertinea 146/Lv1Rsc10, GenBank accession number: KM878392 (COI), first 30 slides: www.morphdbase. de/?D_Kraemer_20160124-S-6.1).

Other material. FRANCE Roscoff intertidal zone in front of marine biological station (48°43041.59″N 3°59020.73″W), lower intertidal during diurnal low tide, coarse sediment underneath stones, 34 slides of histological transverse sections, anterior part of female sliced until nephridial system, 5 lm, azan staining (Lv2Rsc10, GenBank accession number: KM878387 (COI), www.morphdbase.de/?D_Kraemer_20160120-M-9.1).

GERMANY Sylt, 'Odde Watt' List (55° 1048.62″N 8°25045.53″E), intertidal zone during nocturnal low tide, 40 specimens with sequence data deposited at GenBank (Appendix II: Supplementary Table 3);

GERMANY Helgoland, Helgoländer Sockel (54°110 18.18″N 7°52016.42″E), upper littoral during diurnal low tide, eight specimens with sequence data deposited at GenBank (Appendix II: Supplementary Table 3);

FRANCE Wimereux, Pointe aux Oies (50°45046.47″N 1°3601.52″E), intertidal zone during diurnal low tide in front of marine biological station, 11 specimens with sequence data deposited at GenBank (Appendix II: Supplementary Table 3);

FRANCE Roscoff intertidal zone in front of marine biological station (48°43041.59″N 3°59020.73″W), lower intertidal during diurnal low tide, coarse sediment underneath stones, 13 specimens with sequence data deposited at GenBank (Appendix II: Supplementary Table 3);
FRANCE Concarneau, Cabellou Plage (47°51019.08″N 3°54058.55″W), intertidal zone, coarse sediment underneath stones during diurnal low tide, four specimens with sequence data deposited at GenBank (Appendix II: Supplementary Table 3).

Description. Length from 13 mm up to 71 mm (mean 37 mm), width 1–2 mm. Body colouration variable: red, yellow or brownish yellow. Most specimens with dark-green colouration and violet hue anteriorly passing off to bright green towards posterior end (Figure 3.8 A, GNM Nem. 144/142). Ventral side always lighter in colouration. Brain distinguishable as reddish bilobed structure through dorsal and ventral body wall (Figure 3.8 A, GNM Nem. 143, Lv37Sy11). Mouth appearing as whitish slit, positioned behind cephalic lobe and brain. Number of eyes varying from two to eight, unequally distributed at lateral margins of pigmented part of cephalic lobe (Figure 3.8 A, GNM Nem. 143). Visibility of eyes and brain depending on pigmentation; in darkly pigmented individuals, eyes and brain not distinguishable (Figure 3.8 A, GNM Nem. 144/142, Lv13Sy11, Lv8Hl10). Sexually mature specimens with dorsally flattened body, without modified ventral side (Figure 3.8 A, GNM Nem. 144).

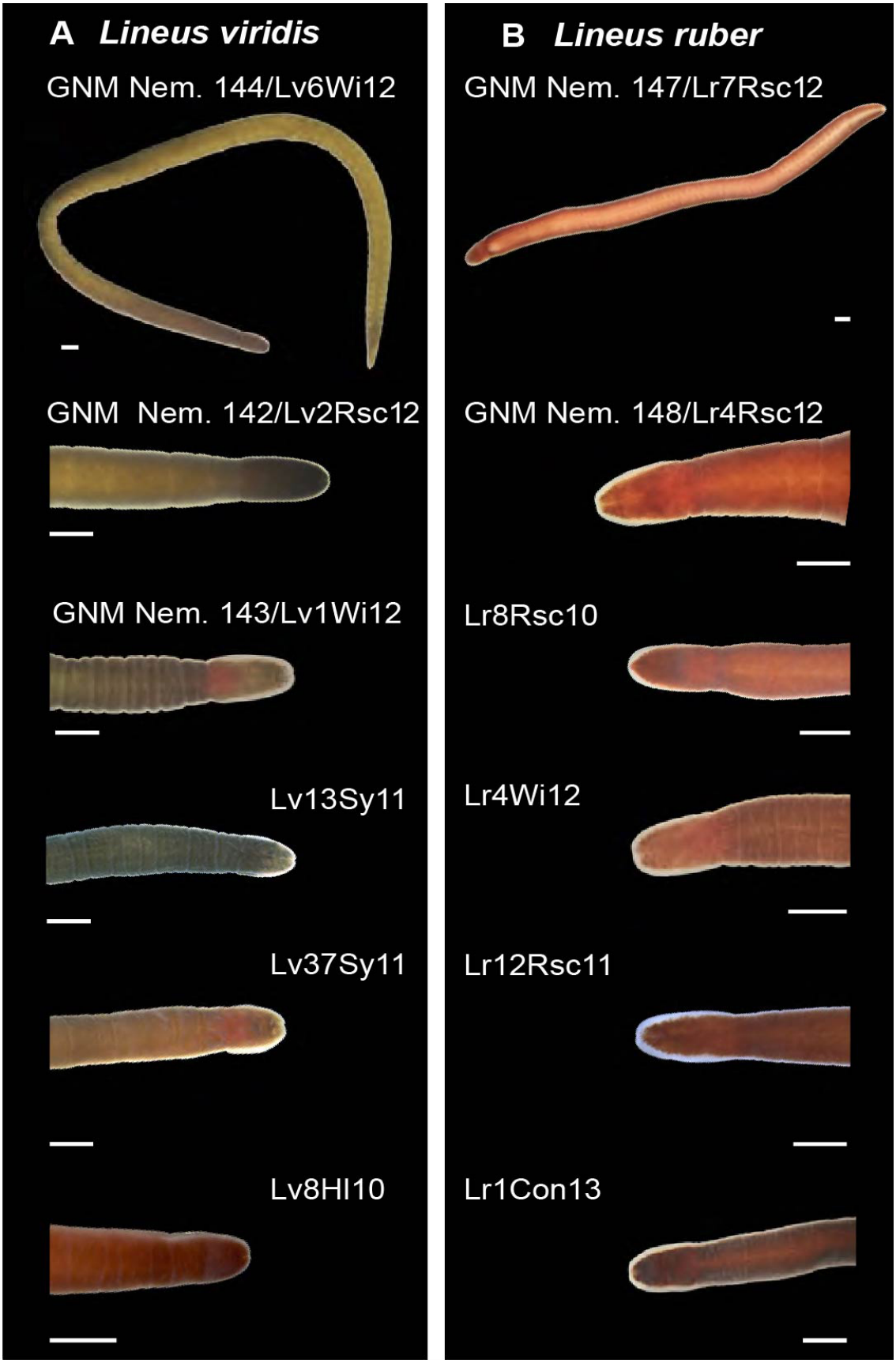
A Lineus viridis
GNM Nem. 144/Lv6Wi12
GNM Nem. 142/Lv2Rsc12
GNM Nem. 143/Lv1Wi12
Lv13Sy11
Lv37Sy11
Lv8HI10
B Lineus ruber
GNM Nem. 147/Lr7Rsc12
GNM Nem. 148/Lr4Rsc12
Lr8Rsc10
Lr4Wi12
Lr12Rsc11
Lr1Con13

Figure 3.8 Life habitus images of selected *Lineus viridis* and *Lineus ruber* specimens showing color diversity within each cluster. **(A)** Uppermost specimen showing exclusive dark green morphotype of *L. viridis* followed by specimens and their specimen IDs used in the phylogenetic analyses, scales: 1mm. **(B)** Uppermost specimen showing the red non-exclusive morphotype for *L. ruber* followed by specimens and their specimen IDs used in the phylogenetic analyses. Note that some specimens exhibit triangular shaped pigmented head (Lr8Rsc10, Lr7Rsc11). Scales: 1mm.

***Lineus clandestinus* sp. n.**

Holotype. FRANCE Wimereux, Pointe aux Oies (50°45046.47″N 1°3601.52″E), intertidal zone during diurnal low tide in front of marine biological station, cephalic region of female specimen in ethanol (GNM Nemertinea 150/Lv5Wi12 (Figure 3.9 A), GenBank accession numbers: KM878454 (COI), KM878533 (ITS), KM878501 (16S)).
Paratypes. FRANCE Île de Groix, Port Saint-Nicolas (47°37043.85″N 3°29011.15″W), upper littoral during diurnal low tide, tissue of female specimen in ethanol (GNM Nemertinea 151/Lv7Idg12 (Figure 3.9 D), GenBank accession numbers: KM878438 (COI), KM878499 (16S), KM878528 (ITS));
FRANCE Roscoff, intertidal zone in front of marine biological station (48°43041.59″N 3°59020.73″W), lower intertidal during diurnal low tide, coarse sediment underneath stones, cephalic region of juvenile in ethanol (GNM Nemertinea 152/Lv28Rsc10 (Figure 3.9 E), GenBank accession numbers: KM878455 (COI), KM878504 (16S), KM878529 (ITS));
Tissue of female specimen in ethanol (GNM Nemertinea 153/Lv3Rsc12, GenBank accession number: KM878457 (COI));
GERMANY Sylt, 'Odde Watt' List (55° 1048.62″N 8°25045.53″E), intertidal zone during nocturnal low tide, 85 slides of histological transverse section, anterior part of specimen sliced until nephridial system, 5 lm, azan staining (GNM Nemertinea 154/Lv56Sy11, GenBank accession numbers: KM878424 (COI), www.morphdbase.de/? D_Kraemer_20160123-S-4.1);
Ventral-fold morphotype: Series of histological transverse sections of mature male. Anterior part sliced till gonad region (66 slides) (GNM Nemertinea 155, www.morphdbase.de/?D_Kraemer_20160123-S-5.1).

Other Material. GERMANY Sylt, 'Odde Watt' List (55° 1048.62″N 8°25045.53″E), intertidal zone during nocturnal low tide, 32 specimens with sequence data deposited at GenBank (Appendix II: Supplementary Table 3);

GERMANY Helgoland, Helgoländer Sockel (54°11018.18″N 7°52016.42″E), upper littoral during diurnal low tide, one specimen with sequence data deposited at GenBank (Appendix II: Supplementary Table 3);

FRANCE Concarneau, Cabellou Plage (47°51019.08″N 3°54058.55″W), intertidal zone, coarse sediment underneath stones during diurnal low tide, one specimen with sequence data deposited at GenBank (Table S1);

FRANCE Île de Groix, Pointe Saint-Nicolas (47°37043.85″N 3°29011.15″W), upper littoral during diurnal low tide, three specimens with sequence data deposited at GenBank (Appendix II: Supplementary Table 3).

Etymology. The specific name *clandestinus* is a Latin adjective (concealed, secret) referring to the fact that the new species has been concealed among *Lineus ruber* and *Lineus viridis* for centuries.

Differential diagnosis

Description. Length from 11 mm to 48 mm (mean 26 mm), width 1 mm. Head bluntly pointed with cephalic slits reaching rear of brain. Brain distinguishable as reddish bilobed structure through dorsal and ventral body wall (Figure 3.9 A, C–G). Mouth appearing as whitish slit, positioned behind cephalic lobe and brain (Fig. 3A). Eyes situated at lateral margins of pigmented part of cephalic lobe (Figure 3.9 C, E–G). Number of eyes varying from three to seven ocelli, unequally distributed on each side. Visibility of eyes depending on pigmentation; in darkly pigmented individuals, eyes not distinguishable (Figure 3.9 D). Body colouration variable: red, brown, greenish or brownish yellow, therefore barely distinguishable from *Lineus rube*r or *Lineus viridis*. Some specimens with red head while rest of body greenish or brownish (Figure 3.9 A, E). Ventral side always lighter in colouration. Some sexually mature males with ventral fold: iridescent, long cilia bearing, concavely shaped-ventral side, gonads visible through ventral and dorsal body wall (Figure 3.9 A, B). Ventral fold extending from far behind cephalic lobe to caudal end, extending two-thirds of body length (Figure 3.9 A).

Figure 3.9 A-G *Lineus clandestinus* sp. n. Habitus images of holotype, paratypes, and specimens used for phylogenetic analyses. **(A)** *L. clandestinus* ventral fold morphotype (Lv28Sy11) showing extension of ventral fold and holotype (GNM Nemertinea 150/Lv5Wi12). **(B)** detailed view of ventral fold. **(C)** Anterior end of holotype from Wimereux (GNM Nemertinea 150/Lv5Wi12). **(D)** Anterior end of paratype from Île de Groix (GNM Nemertinea 151/Lv7Idg12). **(E)** anterior end of paratype from Roscoff (GNM Nemertinea 152/Lv28Rsc10). **(F)** Anterior end of specimen from Helgoland used for phylogenetic analyses. **(G)** Anterior end of specimen from Concarneau Lv4Con13 used for phylogenetic analyses. Scales: 1mm. Abbreviations: **br**, brain; **go**, gonads; **m**, mouth; **vf**, ventral-fold.

3.4 Discussion

3.4.1 Unravelling the *Lineus ruber/viridis* species complex: systematic implications

Nemertean species are generally considered to exhibit few specific morphological characters, the majority of which have been postulated to be prone to considerable homoplasy or intraspecific variation (Sundberg & Svensson 1994; Schwartz & Norenburg 2001; Sundberg & Strand 2010; Kvist *et al.* 2014). Therefore, some taxonomic confusion and a considerable number of unrecognised, that is cryptic, species have been suspected to be present in this group (Appeltans *et al.* 2012). To clarify these taxonomic issues, methods of molecular systematics including tree-based, non-tree-based species delimitation as well as phylogenetic analyses have been widely and successfully used (Strand & Sundberg 2005a; Sundberg *et al.* 2009b, 2010; Chen *et al.* 2010; Leasi & Norenburg 2014; Strand *et al.* 2014). The most commonly employed molecular markers to resolve nemertean systematics are fragments of the mitochondrial 16S rRNA and the COI gene (Sundberg & Saur 1998; Sundberg *et al.* 2009a; b, 2010; Chen *et al.* 2010; Leasi & Norenburg 2014; Strand *et al.* 2014). More recently, however, there has been some reservation to the exclusive use of mitochondrial markers to delimit species due to phenomena related to the mode of inheritance of the mitochondrial genome (Melo-Ferreira *et al.* 2005; Strand & Sundberg 2005a; Rubinoff *et al.* 2006; Vogler & Monaghan 2006; Ross *et al.* 2008; Sundberg *et al.* 2009b; Yao *et al.* 2010; Funk & Omland 2011; Hailer *et al.* 2012). To overcome this problem, the analysis of a second, independently recombining nuclear marker, the internal transcribed spacer region (ITS) has been suggested and recently applied to nemerteans (Sundberg *et al.* 2009a; Bucklin *et al.* 2011). Resolving the so-called *Lineus ruber/viridis* species complex, one of the longest lasting problems in nemertean taxonomy, with molecular data, has so far led to inconclusive results. While three clades were identified with isoenzyme data by Rogers *et al.* (1995), the analysis on the 16S rRNA of only a few *L. ruber* and *L. viridis* samples lumped the specimens analysed into a single lineage (Sundberg & Saur 1998). In addition to a broad methodological spectrum, our data set accounts for all the problems outlined above in that we performed dense sampling from different localities, used ITS as an additional, independently

recombining marker and included 16S, to relate our results to existing data of Sundberg & Saur (1998).

Except for the bPTP approach, results from all methods clearly state the existence of three clades, distinctly separated by the criteria of the respective method. Our results correspond with Rogers *et al.* (1995), who suggested a third cryptic species among *L. viridis* and *L. ruber* on British and northern French coasts. The inclusion of published 16S and COI data further supports Rogers *et al.*'s (1995) but also suggests the absence of *L. ruber* at the US North American Atlantic and Swedish North Sea coasts (Sundberg & Saur 1998; Thollesson & Norenburg 2003; Schwartz 2009). The notion of *L. ruber* and *L. viridis* (and *L. clandestinus*) comprising a single species can be rejected.

Examining the external morphology shows that the more distantly related clade (*L. ruber*) is largely invariant possessing a red to reddish-brown colouration and, in some specimens, a triangular-pigmented head. Furthermore, investigated egg clutches of females that group within this clade show a morphology that corresponds to Gontcharoff's (1951, 1960) descriptions for *L. ruber* (Krämer and von Döhren unpublished). The clade we named *L. ruber* herein is attributed to *L. ruber sensu* Gontcharoff (1951) mainly based on the narrow colour range of specimens but also on the morphology of the egg string produced by specimens of this clade. Specimens of *L. viridis* range in colouration from red to green, while egg clutches, and the development of the offspring inside corresponds to the description for *L. viridis* by Gontcharoff (1951) (Krämer & von Döhren unpublished). We conclude that the clade we named *L. viridis* herein is *L. viridis sensu* Gontcharoff (1951) as her redescription includes green colouration as diagnostic character. This is in line with findings of Rogers *et al.* (1995) who had also defined *L. viridis* based on Gontcharoff's (1951) description. In *L. clandestinus*, no purely green specimens were found. In this clade, however, specimens with a lighter-coloured, iridescent, ventral fold, which has not been described by Gontcharoff (1951), were observed occasionally. We suppose the function of the ventral fold to be a transitory structure related to reproduction as it is restricted to specimens with developing gonads (Schmidt, Krämer, Beckers & von Döhren, unpublished). The ventral fold was absent from all *L. viridis* and *L. ruber* specimens even when they were in a reproductively mature state. This was also not observed by Gontcharoff (1951, 1960), and the clutch of *L. clandestinus* has never been knowingly described, although

there is the possibility that information on it has unknowingly been included in previous studies on reproduction and development (Schultze 1853; Barrois 1877; Hubrecht 1886; Arnold 1898; Nusbaum & Oxner 1913; Gontcharoff 1951, 1960; Schmidt 1964 and references therein; Bartolomaeus 1984). We conclude that *L. clandestinus* is likely corresponding to the aberrant type *sensu* Rogers *et al.* (1995) and regard it as species new to science. Even though we cannot exclude the probability that *L. clandestinus* has been described in previous studies (Friedrich 1935; Cantell 1975; Chernyshev 2004), we decided against the re-establishment of any of the junior synonyms, as they have been used for *L. ruber* and *L. viridis* almost interchangeably. It would be impossible to assign any of the synonyms without doubt to any of the species. Additionally, more commonly used species names like *Lineus gesserensis* are either still valid (Gibson 2005) or lack molecular data preventing a direct comparison and assignment to any of the synonyms.

We decided to assign neotypes from Roscoff for *L. ruber* and *L. viridis* for three reasons: (1) there is no type material available from the original description by Müller in 1774 (Kristensen, R. M., pers. communication). (2) Insufficient information about the type locality in Greenland (Müller 1774) does not allow for the recollection of material from the *Locus typicus*. For these reasons, it is impossible to check whether the originally described *L. ruber* and *L. viridis* are truly separated species, if one species is a colour variant of the other, or even the cryptic species *L. clandestinus*. (3) Schmidt (Schmidt 1946, summarised in English in 1964) and Gontcharoff (1951, 1960) were the first to clearly state the separation of *L. ruber* and *L. viridis* into distinct species based on specimens collected from the Barents Sea, as well as from Roscoff. We therefore consider it as appropriate to assign neotypes for both species collected from Roscoff. We follow the precedent of *Micrura alaskensis* (Coe, 1901) which was originally described from Alaska. Data on morphology, COI and 16S sequences revealed five cryptic species of which one was redescribed as *Maculaura alaskensis* based on neotype material sampled from Oregon, USA (Hiebert & Maslakova 2015). Analogously to *L. ruber/viridis, M. alaskensis* was therewith neotypified from a non-type locality which is within the historically documented distribution range of the species.

By sight, individuals can only be unequivocally assigned to either *L. ruber*, *L. viridis* or *L. clandestinus* if specimens with triangular-pigmented head (*L. ruber*), the

dark-green (*L. viridis*) or the ventral-fold (*L. clandestinus*) morphotypes are encountered. Otherwise, identification can only be confirmed by comparing the sequence data provided in this study. *L. ruber*, *L. viridis* and the newly discovered species, *L. clandestinus*, are described based on external appearance and genetic markers (COI, 16S and ITS) from a comparably high number of specimens but not based on internal characters. Histology-based species descriptions might give a detailed overview of the internal characters employed to differentially diagnose the described species. Although these descriptions are still common practice within nemertean taxonomy (Chernyshev 2013; Chernyshev *et al.* 2015; Krämer & von Döhren 2015), they are of very limited use when describing and delimiting cryptic species, that is species that are morphologically indistinguishable (Strand & Sundberg 2011; Jörger & Schrödl 2013). In the *Lineus ruber/viridis* species complex, apart from the abovementioned differences in external appearance, there are no species-specific internal differences observed between *L. ruber*, *L. viridis* and *L. clandestinus* (Krämer, pers. observation). A histology-based description of internal characters in *L. clandestinus* will not fulfil the demand for its specific differentiation against *L. viridis* (or *L. ruber*). Therefore, the identity of *L. clandestinus* as an individual species separated from *L. ruber* and *L. viridis* is based on the evidence of it representing a reproductively isolated lineage from the analysis of the genetic markers employed herein. This is particularly evident for the samples from Roscoff where, based on our results, all three species occur syntopically with no molecular evidence for interbreeding.

We consider our decision to base the descriptions on external characters linked with DNA sequences as sufficient and in line with the opinion of most nemertean taxonomists and current approaches of describing and delineating (cryptic) species (Strand & Sundberg 2011; Jörger & Schrödl 2013; Hao *et al.* 2015; Kang *et al.* 2015; Sun *et al.* 2015; Sundberg 2015; Sundberg *et al.* 2016). Nevertheless, we decided to deposit histological section series at Göteborgs Naturhistoriska Museum (GNM) and MorphDBase to facilitate investigation of the internal morphology in the future. But we consider it as sufficient to base identification of *L. ruber*, *L. viridis* and *L. clandestinus* on the sequence data provided in this study and the voucher specimens deposited at

GNM which will serve as a backbone for fast and reliable species identification (Strand & Sundberg 2011).

3.4.2 Outlook

The network analysis based on COI shows that the newly described species, *L. clandestinus*, is present in all sampling sites, while L. ruber is restricted to the French sampling sites. *Lineus viridis* has not been found at Île de Groix, the southernmost sampling site, which may be due to the low number of samples collected there. The sample size from Helgoland and Sylt confidently shows the absence of *L. ruber* from the German North Sea coast. Conceivable reasons for the absence of *L. ruber* from this area are related to the differences between habitats present in the intertidal zone along western European coasts. Atlantic and Channel coast habitats (Île de Groix, Concarneau, Roscoff and Wimereux) are characterised by the presence of rocks, boulders, coarse sediment and a steep coastal slope with tidal ranges of up to 8 m (Menéndez & Woodworth 2010). North Sea shores on the other hand are characterised by a shallow coastal slope and predominantly sandy sediments. These differences result in different upper intertidal habitats with different abiotic regimes and biotic communities on the Atlantic and Channel coast shores as opposed to the German North Sea coast. Distribution data from the Atlantic coast indicate that *L. ruber* is found in the upper intertidal zone, while presumably both *L. viridis* and *L. clandestinus* are regularly found in the mid-intertidal zone. The distribution patterns hint at different habitat preferences of the three species (Gibson 1995; von Döhren & Krämer, unpublished). Arguably, in *L. ruber*, either prey preferences or oxygen demands of the developing offspring are not met in the more humid sandy habitats of the German North Sea coasts. Alternatively, displacement of *L. ruber* from the habitat caused by competition of *L. viridis* and *L. clandestinus* being better adapted to humid beaches could be a reason for the absence of *L. ruber*.

The circumstantial evidence for reproductive isolation of *L. viridis* and *L. clandestinus* by the molecular markers employed in this study poses another interesting question. So far, there are no known biological differences in the two species which share a syntopic distribution in nearly all sampled habitats. As the reproductive isolation

was not directly tested (i.e. mating of *L. viridis* and *L. clandestinus* in captivity) in this study, future research is warranted that focuses on the biological differences in the two species to find out what maintains the reproductive barrier between these species. There is first evidence that *L. viridis* and *L. clandestinus* on the coast of Sylt island (North Sea) might be isolated by their differing reproductive periods (Bartolomaeus, pers. observation). The low genetic structure observed in *L. clandestinus* which is arguably as widely distributed as the sibling *L. viridis* also needs an explanation. There might be a considerably lower mutation rate of COI in *L. clandestinus* or a more recent introduction of a few founder individuals of this species to the sampled locations. Although the latter phenomenon has been shown in nemerteans before (Fernández-Álvarez & Machordom 2013), more comprehensive sampling spanning a broader geographic range is needed to evaluate the alternative hypotheses.

3.5 Acknowledgements

The authors are grateful to Prof. Dr. T. Bartolomaeus and Prof. Dr. P. Sundberg who gave helpful and advisory support for this manuscript. We thank Prof. Dr. Hiroshi Kajihara, Prof. Dr. Alexei Chernyshev and the anonymous reviewer for helpful comments and edits which substantially improved this manuscript. We acknowledge Anja Bodenheim, Claudia Müller and Christiane Wallnisch for technical assistance. We thank Kennet Lundin of the Göteborgs Naturhistoriska Museum for the fast responses and for type material deposition. The authors are also grateful to the staff of the Wattenmeerstation, List, Sylt and Biologische Anstalt Helgoland of the AWI in Bremerhaven, the Station Marine de Wimereux, the Station Biologique de Roscoff and the Station de Biologie Marine et Marinarium de Concarneau in France for providing facilities and accommodation during the collection trips.

Chapter 4

Redescription of *Tubulanus polymorphus* Renier, 1804 (Palaeonemertea: Nemertea) leads to the re-establishment of *Tubulanus ruber* (Griffin, 1898)

Daria Krämer*, Patrick Beckers, and Jörn von Döhren

University of Bonn, Institute of Evolutionary Biology and Ecology,

An der Immenburg 1, 53121 Bonn, Germany

*Corresponding author. E-mail: dkraemer@evolution.uni-bonn.de

This chapter contains unpublished data on selected taxa

Keywords

Ribbon worms, integrative taxonomy, morphology, phylogeny.

Abstract

In the taxon Nemertea, the past decades have shown that the specific identity of some of the longest-known species is doubtful. As an example, *Tubulanus polymorphus* Renier, 1804 (Palaeonemertea) is reported to be widely distributed in the northern hemisphere including the west coasts of both Europe (Atlantic Ocean) and North America (Pacific Ocean). *Tubulanus polymorphus* is the type species of *Tubulanus*, and had originally been described from the Mediterranean Sea. Specimens from the Pacific coast of the USA and Canada had originally been described as a different species, *Carinella rubra* Griffin, 1898 mainly based on different colors and remote geographic ranges. *C. rubra* was later synonymized with *T. polymorphus*, apparently attributing the differences between Atlantic and Pacific specimens to intra-specific variation.

This study aims to clarify the identities of these species in an integrative taxonomic framework: Comparison of molecular (COI, 16S), morphological, and life-history data (habitat occupancy and reproductive biology) of specimens collected from San Juan Island, Washington state (USA, Pacific coast) and Roscoff, (France, Atlantic coast) reveals striking differences between the Atlantic and Pacific specimens. Morphologically, the specimens differ with respect to the body coloration, the structure of the nervous system, cerebral sensory organs, musculature, blood-vascular system,

and cephalic mucus glands. Phylogenetic analyses of the respective molecular markers together with other congeneric sequences indicate that the specimens from the North American Pacific and the European Atlantic coasts are not even close relatives. Instead, they are separately grouped into two clusters of species separated by a basal split within the genus *Tubulanus*.

Based on the differences detected in each data set we decided to re-describe the Atlantic specimens as *Tubulanus polymorphus* and reinstate the species *Tubulanus ruber* (Griffin, 1898) for individuals from the Pacific coast. Morphological as well as molecular data are publicly available and enable the reassignment of information published under the name *T. polymorphus* to one or the other species. The redescription of *T. polymorphus* or, more specifically, the redefinition of the type species, represents the prerequisite for an overdue revision of the genus *Tubulanus*.

4.1 Introduction

Ribbon worms (phylum Nemertea) comprise a group of mostly marine, epibenthic predators (Gibson 1972, 1982). A vast majority of the approximately 1300 known species was described during the 19th century based on a few notes on the external appearance (Strand & Sundberg 2005b; Kajihara *et al.* 2008; Sundberg *et al.* 2009b, 2016; Sundberg 2015). This practice renders accurate delimitation and assignments of (new) species on different taxonomic levels (from species to family level) problematic. Additionally, it has led to erroneous synonymization of some species in the past (Gibson 1995). With advanced methodology at hand, species descriptions became more precise with detailed information on internal and external morphology. Also, and more importantly, references to DNA sequences are now commonly included, which allow for faster and more precise species assignments and identification (Strand & Sundberg 2005b; Sundberg *et al.* 2009b, 2010, 2016; Sundberg 2015). In the past decade, these data have helped to resolve taxonomic confusion: In more than 100 species changes in validity, names and/or generic affiliations, and introduction of new genera were executed (Kajihara *et al.* 2008, 2011; Strand & Sundberg 2011; Hiebert & Maslakova 2015; Krämer & von Döhren 2015).

The palaeonemertean genus *Tubulanus* Renier, 1804, for example, is known for its questionable monophyletic status and confusing nomenclatural history (Andrade *et al.* 2012; Kvist *et al.* 2014, 2015; Kajihara *et al.* 2015). Thirty-five described species are currently included within the genus but several recent phylogenetic analyses have shown that *Tubulanus* is likely paraphyletic (Sundberg & Hylbom 1994; Gibson 1995; Ritger & Norenburg 2006; Kvist *et al.* 2014, 2015; Kajihara *et al.* 2015). Taxonomic confusion is also inherent at a more basic taxonomic level regarding the type species of *Tubulanus*, *Tubulanus polymorphus* Renier, 1804. *Tubulanus polymorphus* was originally described from the Mediterranean Sea in an unpublished work by Renier in 1804, followed by more detailed descriptions by Bürger (1892, 1895). A similar looking species was simultaneously described as *Carinella rubra* Griffin, 1898 from the Pacific coast of the USA (Griffin 1898). Based on their similar external characters *C. rubra* was synonymized with *T. polymorphus* by Coe in 1940, even though descriptions on the internal morphology indicated striking differences. Until the reinstatement of *T.*

polymorphus and Tubulanidae as valid taxon names by Melville (1986), specimens from the Pacific and European coasts were handled as one species and randomly referred to as *C. rubra*, *C. polymorpha*, or *T. polymorphus* by different authors (Bürger 1888, 1890, 1892, 1895, 1904; Joubin 1890; Riches 1893; Griffin 1898; Allen & Todd 1900; Coe 1940; Sheldon 1901; Coe 1901, 1904, 1905; Bergendal 1903; Punnett 1903; Wijnhoff 1912; Southern 1913; Friedrich 1936) (Appendix III: Supplementary Table 6). Since 1986 information on morphology, development, and molecular data had been published under the name *T. polymorphus*, irrespective of where specimens had been collected (Ricketts & Calvin 1948; Gontcharoff 1955; Hylbom 1957; Friedrich 1958; Corrêa 1964; Brusca & Brusca 1978; Melville 1986; Stricker 1987; Blake 1993; Stricker & Folsom 1998; Stricker *et al.* 2001; von Döhren *et al.* 2010; Andrade *et al.* 2012; Beckers *et al.* 2013; Mulligan *et al.* 2014; Hiebert 2015) (Appendix III: Supplementary Table 6). Thus, *T. polymorphus* was regarded as a common sublitoral species with a wide distribution in the northern hemisphere ranging from European (North Atlantic and Mediterranean Sea) to North American (North Pacific) coasts (Gibson 1982, 1995).

With a comprehensive data set, including molecular phylogeny based on COI and 16S, external and internal morphology, as well as information on habitat preferences and first observations on reproductive biology, we re-describe *T. polymorphus* based on specimens collected from the North American Pacific and European Atlantic coasts. With the aid of all data sets we were able to detect distinct differences between the Pacific and the Atlantic specimens that support the separate identity of the two original species. We decided to re-describe the Atlantic specimens as *Tubulanus polymorphus* and re-establish *Tubulanus ruber* as the species name for individuals collected from the Pacific.

4.2 Material and Methods

4.2.1 Specimens

Three specimens of *Tubulanus polymorphus* were collected in September 2011 and 2014 during diurnal low tides in the sublitoral zone close to the Marine Biological

Station of Roscoff, France. Specimens were found buried in sediment at 0.2-0.5 m depth in between the roots of *Zostera marina* Linnaeus, 1753. It was impossible to extract intact specimens from the sediment, therefore only anterior ends were collected. Specimens were anaestized in 7% $MgCl_2$ mixed with sea water at equal volumes and subsequently photographed with a digital camera (Canon EOS 600D) mounted on a dissection microscope (Zeiss Stemi 2000) and fixed in absolute ethanol for DNA extractions. One additional specimen was fixed for histological investigation and one for DNA extractions

Two specimens of *Tubulanus ruber* were collected during diurnal low tide within the mid intertidal zone of the rocky shore close to Cattle Point on San Juan Island, Washington, USA in 2007. Individuals were found underneath stones. Since no camera was available during the collection trip, no pictures were taken from the neotype material. Both individuals were used for histological (anterior end) as well as molecular investigations (posterior end).

4.2.2 Histology

The anterior ends of anaesthetized specimens were fixed overnight in Bouin's fluid (modified after Dubosq-Brasil). The tissue was dehydrated in an ascending ethanol series followed by methyl benzoate and butanol. Afterwards, the samples were pre-incubated with Histoplast (Thermo Scientific) and embedded in Paraplast (McCormick Scientific). Sections of 5 µm were made with a Leica RM2165 microtome and stained with the Azan-method. Sections were photographed with an Olympus BX-51 microscope equipped with an Olympus cc12 camera mounted on a dotSlide 2.2 system (Olympus). Images were aligned with Imod (Kremer *et al.* 1996) and imod align (http://www.q-terra.de/biowelt/3drekon/guides/imod_first_aid.pdf) and uploaded to MorphDBase (http://www.morphdbase.de).

4.2.3 Nucleic acid purification, PCR amplification, Sequence analysis, and Phylogeny

DNA was extracted with the Dneasy Blood and Tissue Kit (Qiagen) following the manufacturer's instructions. For phylogenetic analyses, cytochrome c oxidase subunit I (COI) and 16S rRNA (16S) were amplified using LCO1490/HCO1298 and ar-L/br-H primer pairs (Folmer *et al.* 1994; Palumbi 1996). Thermal cycling was initiated with 2 min at 94 °C, followed by 40 cycles (30 s at 94°C, 60 s at 51/53 °C (16S/COI) and 60 s at 72°C), and terminated with a 2-min final elongation at 72°C. PCR products were purified with NucleoSpin® Extract II-Kit (MACHEREY-NAGEL GmbH & Co. KG) following the instructions of the manufacturer. Purified PCR products were sent to LGC Genomics© for Sanger sequencing, using forward and reverse primers for sequencing (Sanger *et al.* 1977).

Sequences were edited with Bioedit Version 7.0.9. and aligned using MAFFT Version 7 with G-INS-I strategy using default parameters: scoring matrix for nucleotide sequences of 200PAM/K=2; gap opening penalty of 1.53; offset value of 0.0 (Hall 1999; Andrade *et al.* 2012; Katoh & Standley 2013).

To assess inter- and intraspecific variation of the two species in question uncorrected p-distances were calculated with MEGA version 5.2.1 based on the COI alignment (579nt) of all collected specimens and sequence data taken from (Thollesson & Norenburg 2003; Andrade *et al.* 2012; Kvist *et al.* 2014) (Table 1).

Phylogenetic trees were reconstructed based on the COI alignment and 16S data gained from the collected specimens as well as sequence data taken from GenBank (Appendix III: Supplementary Table 7). The brachiopod species *Terebratalia transversa* (Sowerby, 1846) was used as outgroup. Uncertain positions within the 16S alignment were removed with Gblocks version 0.91b (Castresana 2000) using default parameters for maximum number of contiguous non-conserved positions, minimum block length (10), allowed gap positions (none) and the usage of similarity matrices. Other parameters were changed to 13 for minimum number of sequences for conserved position and 21 for minimum number of sequences for a flanking position. The resulting alignment (261nt, 65% of the original 400 positions) was concatenated with COI and analyzed using maximum likelihood (ML) based on the General Time Reversible model and a

Gamma distribution with a proportion of invariant sites (GTR+G+I) implemented in MEGA Version 5.2.1 (Nei & Kumar 2000; Tamura *et al.* 2011). The model for phylogenetic analyses was selected by MrModeltest version. 2.3 based on the Akaike information criterion (Nylander 2004). Branch support was estimated using 500 bootstrap replicates. The same analysis was conducted with the original 16S alignment concatenated with COI.

4.3 Results

4.3.1 Taxonomy

Tubulanidae Bürger, 1904 (1874)

***Tubulanus* Renier, 1804**

***Tubulanus polymorphus* Renier, 1804**

(Bürger 1904; Wijnhoff 1912; Southern 1913; Friedrich 1936, 1958; Coe 1940; Gontcharoff 1955; Hylbom 1957; Melville 1986; Beckers *et al.* 2013)
Carinella polymorpha (Bürger, 1888, 1890, 1892, 1895; Joubin 1890; Riches 1893; Allen & Todd 1900; Sheldon 1901; Bergendal 1903; Punnett 1903)
Nemertes polymorpha (Örsted 1844)
Ophyocephalus polymorphus (Delle Chiaje 1829)
Tubulanus elegans (Blainville 1828)
Valencinia splendida (Quatrefages 1846; Diesing 1862)
For list of synonyms (Table S1)

Material examined:
Neotype designated here. FRANCE, Roscoff, sea grass beds of *Zostera marina* lower intertidal to shallow sub-intertidal zone in front of marine biological station (48°43'39.3"N 3°59'16.8"W), male specimen, tissue (posterior end) in ethanol (TP12/GNM Nemertinea 157, Genbank accession Number KX853120 (COI))

Voucher specimen. FRANCE, Roscoff, seagrass beds of *Zostera marina*, lower to shallow sub-intertidal zone in front of marine biological station (48°43'39.3"N 3°59'16.8"W), series of histological transverse sections, 98 slides (GNM Nemertinea 159, www.morphdbase.de/?D_Kraemer_20160921-S-8.)
Tissue in Ethanol (TP11/GNM Nemertinea 158, Genbank accession Number KX853119 (COI), KX853116 (16S)

Diagnosis. Endobenthic *Tubulanus* species, living in self-secreted parchment-like tubes among roots of *Zostera marina* in lower intertidal to shallow sublitoral; body coloration uniformly brick red, end of rhynchocoel/beginning of midgut region marked by abrupt change into darker red (fixation band); side organs laterally located within first 3rd of body; Body wall musculature thick, with thin layer of diagonal musculature connecting outer circular and longitudinal musculature; brain small in relation to body wall musculature; dorsal nerve present; medullary cords with inner neurilemma; lateral vessels small in relation to body wall musculature; cerebral organs: small epidermal pits; cephalic glands absent.

Habitat. Sublitoral zone close to Marine Biological Station of Roscoff, France. During low-tide, specimens situated in parchment-like tubes in sediment at 0.2-0.5 m depth between roots of sea grass (*Zostera marina* Linnaeus, 1753).

External characters. (For character checklist after Sundberg *et al.* 2016: Table S2) Neotype measured 65 mm from anterior end to side organs (Figure 4.1 a). Body width varying from 4 mm anteriorly to 6 mm in midgut region (Figure 4.1 a-c). Body coloration uniformly brick red (Figure 4.1). Cephalic lobe clearly demarcated from trunk, spatulate-shaped, measuring 4 mm at broadest point, wider than rest of body (Fig. 1a-c). Proboscis pore situated subterminally, ventrally (Figure 4.1 a). Mouth opening ventral, visible as long slit posterior to cephalic lobe (Figure 4.1 c). One pair of inverse-v-shaped cephalic furrows discernible dorsally, but not as clearly on ventral side at level of mouth opening (Figure 4.1 a, b, Appendix III: Supplementary Table 8). Extension of rhynchocoel (37 mm) discernible by light middorsal stripe and lighter body coloration. Beginning of intestinal region marked by abrupt change to darker red, corresponding to fixation band in formalin preserved specimens (Figure 4.1 a). Paired side organs visible

as small notches laterally located within in first 3rd of body (Figure 4.1 a, d, Appendix III: Supplementary Table 8).

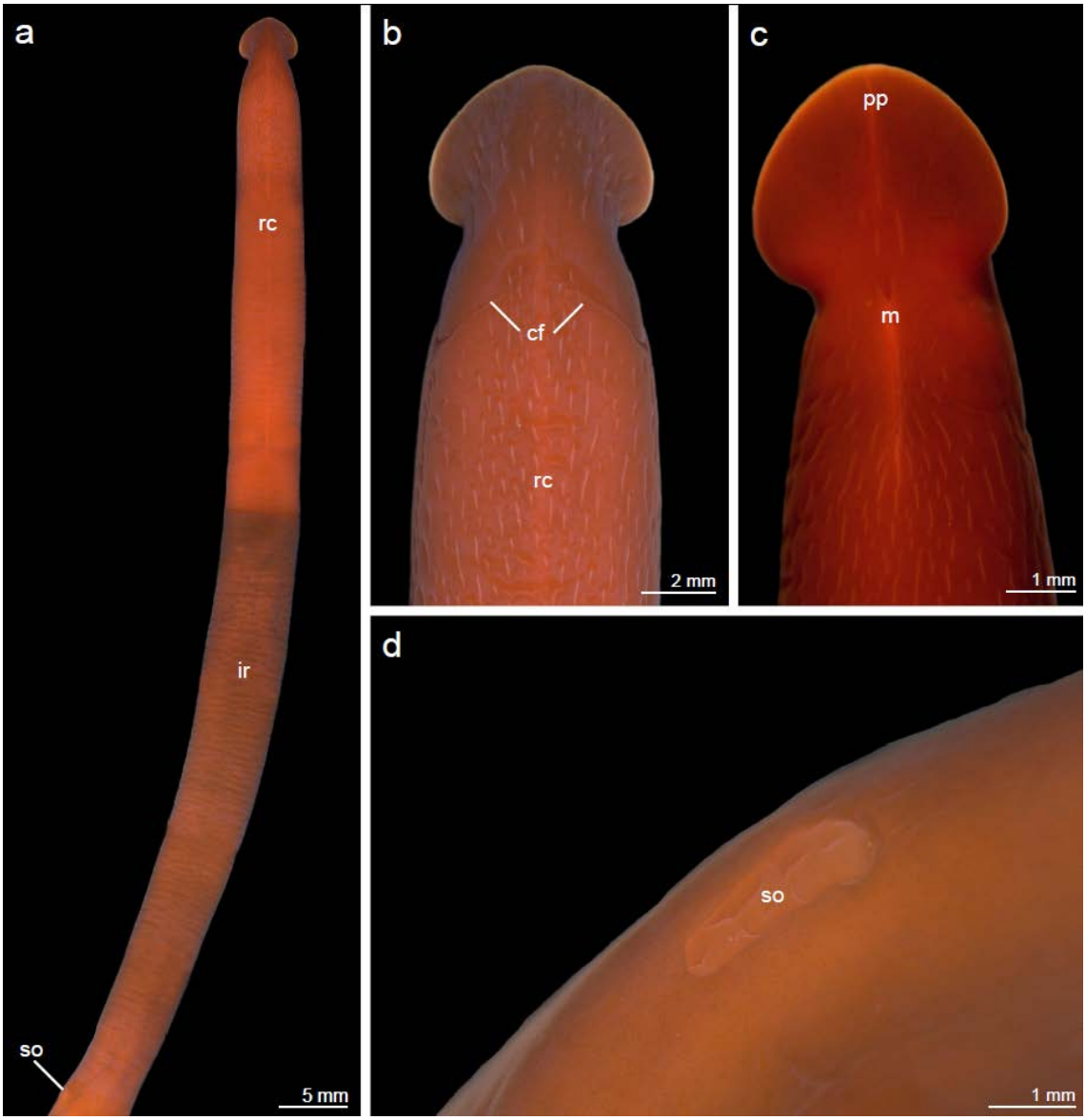

Figure 4.1. *Tubulanus polymorphus* neotype (TP12/GNM Nemertinea 157). Habitus images of living specimen. **(a)** Dorsal view of neotype showing, position of side organs and differentiated coloration in rhynchocoeal and midgut region**. (b)** Dorsal view of cephalic lobe showing one pair of cephalic furrows. **(c)** Ventral view of cephalic lobe showing position of proboscis pore and mouth opening. **(d)** Lateral view of side organs. Abbreviations: **cf**, cephalic furrows; **ir**, intestinal region; **m**, mouth; **pp**, proboscis pore; **rc**, rhynchocoel; **so**, side organ.

Body wall. Thick epidermis, almost as thick as body wall musculature, densely packed with gland cells, appearing pseudo-stratified. Basal lamina thick, with processes

extending dorso-ventrally into body wall musculature and into epidermis. Basal lamina followed by thin layer of outer circular musculature. Main part of body wall musculature constituted by prominent longitudinal musculature (Figure 4.2 a, d, f, g). Thin diagonal muscle layer present below outer circular musculature, connecting outer circular and longitudinal muscles (Figure 4.2 g). Layer of inner circular musculature surrounds alimentary canal and rhynchocoel. Inner and outer circular musculature interconnected by multiple muscle fibers (radial musculature) on each body side (Figure 4.2 f). Prominent layer of extracellular matrix surrounding alimentary canal and rhynchocoel from ventro-lateral. Longitudinal muscle plate present between alimentary canal and rhynchocoel, measuring same height as outer circular musculature of body wall (Figure 4.2 f).

Alimentary canal. Long, slit-like mouth opens posterior to brain lobes. Alimentary canal appearing unspecified throughout length of histological cross sections. Anteriorly, foregut epithelium enfolded and thick, measuring same height as epidermis. Dorsal part of epithelium slightly thinner and less enfolded than ventrally. In posterior course, alimentary canal increases in width becoming broader than rhynchocoel, whereas height of foregut epithelium decreases (Figure 4.2 f). Intestine (midgut) not in the range of the histological section series.

Nervous system. Sub epidermal position of nervous system: central and peripheral nervous system embedded in thick layer of extracellular matrix (basal lamina), situated between epidermis and outer circular musculature (sub-epidermal position) (Figure 4.2 a-g). Brain consisting of paired, equal-sized dorsal and ventral brain lobes, situated in juxtaposition to one another on dorso-lateral body side. Brain lobes dorso-ventrally interconnected by layer of continuous neurite-tracts, making neuropil of lobes barely distinguishable from one another (Figure 4.2 d, e). Lateral connection of lobes constituted by single prominent ventral and several, small, dorsal commissural tracts (Figure 4.2 e, g). Brain without inner neurilemma. Prominent outer neurilemma present giving rise to several bundles of extracellular matrix, traversing neuropil of brain. Small nerves protrude from brain lobes ventrally and laterally into epidermis (Figure 4.2 b-d).

Intra-epidermal nerve plexus present, visible as thin layer at basal part of epidermis (Figure 4.2 g).

Multiple cephalic nerves protrude to anterior-most part of cephalic lobe. Nerves distributed along each body side, appearing in higher number on ventral side (Figure 4.2 a). Ventral cephalic lobes confluent with lateral medullary (nerve) cords. Inner neurilemma present behind brain, separating neuronal cell somata from neuropil in lateral nerve cords (Figure 4.2 g). Scattered somata situated in periphery of neuropil, but most neuronal cell somata encircle neuropil in c-shaped manner exterior of inner neurilemma. Dorsal nerve present (Figure 4.2 f, g). Medullary cords and dorsal nerve regularly connected by small commissures on dorsal and ventral side (Figure 4.2 f, g). Lower dorsal nerve clearly discernible in foregut region, embedded between inner circular body wall and circular rhynchocoel musculature on dorsal side of rhynchocoel (Figure 4.2 f). Origin of lower dorsal nerve not detectable. Dorsal and lower dorsal nerve interconnected by barely distinguishable nerve fibers (Figure 4.2 f). Two esophageal nerves originate from ventral commissural tract, interconnected by thin commissural tract in front of mouth opening. Both nerves run ventro-laterally on each side of alimentary canal being barely distinguishable in posterior course. Gastrodermal nerve plexus present, visible as thin layer at basal part of gut epithelium (Figure 4.2 f). Paired proboscidial nerves arise from ventral commissural tract (Figure 4.2 e). Within proboscis (subepithelial position), nerves regularly interconnected by nerve plexus.

Vascular system. Cephalic lacuna reaching to anterior-most part of head, broadening with increasing width of cephalic lobe, irregularly traversed by dorso-ventrally and laterally arranged muscle bundles (Figure 4.2 a). Lateral blood vessels arise from lacuna behind proboscis insertion, likewise traversed by muscle bundles, therefore appearing subdivided into dorsal and ventral vessels (Figure 4.2 e, f). Lateral blood vessels situated below longitudinal musculature and appear overall small in relation to thick body wall musculature (Figure 4.2 f, g).

Proboscis apparatus. Prominently ciliated proboscis pore opens sub-terminally on ventral side of cephalic lobe (Figure 4.1 c). Rhynchodaeum extends to anterior part of brain (ventral commissural tract), anteriorly with small lumen surrounded by thick

glandular epithelium of same height as epidermis (Figure 4.2 a, c). In posterior course, rhynchodaeal epithelium decreases in height whereas rhynchodaeal lumen increases immensely. Rhynchocoel extends throughout first 3rd of the body (Figure 4.1 a). Rhynchocoel wall lined by layer of thin longitudinal musculature and outer circular musculature. Both layers become thicker posteriorly and appear more prominent on ventral side (Figure 4.2 e, f). Further posteriorly, longitudinal musculature decreases in thickness, becoming almost indiscernible in foregut region (Figure 4.2 f). Rhynchocoel ventrally encapsulated by prominent layer of connective tissue on level of mouth opening. Proboscis insertion located at level of ventral commissural tract of brain (Figure 4.2 e). In everted state, proboscis (palaeotype proboscis) layered as follows: Thick epithelium densely packed with gland cells, followed by barely distinguishable circular musculature and thick longitudinal musculature, measuring same height as proboscis epithelium (Figure 4.2 e, f). Proboscis nerves arise from ventral commissural tract and extend between epithelium and musculature (sub-epithelial position). Within proboscis, nerves located laterally, on opposite sides to each other. Posterior to proboscis insertion, both nerves subdivided into two nerves, fusing again in posterior course (Figure 4.2 e).

Excretory system. Not within range of histological cross section series.

Reproductive system. Sexes separate. Gonad arrangement not within range of histological cross section series.

Sense organs & cephalic glands. Eyes absent. Small cerebral organs, measuring half of epidermal height. Organs situated in juxtaposition to posterior margin of dorsal brain lobes. Canals of cerebral organs visible as epidermal pits, invaginating in posterior course. Canal surrounded by comparably thin, but densely packed layer of glandular cells. Cerebral organs connected via short nerve with dorsal brain lobes (Figure 4.2 b, c). Side organ visible exteriorly but not within range of histological cross sections (Figure 4.1 a, d).

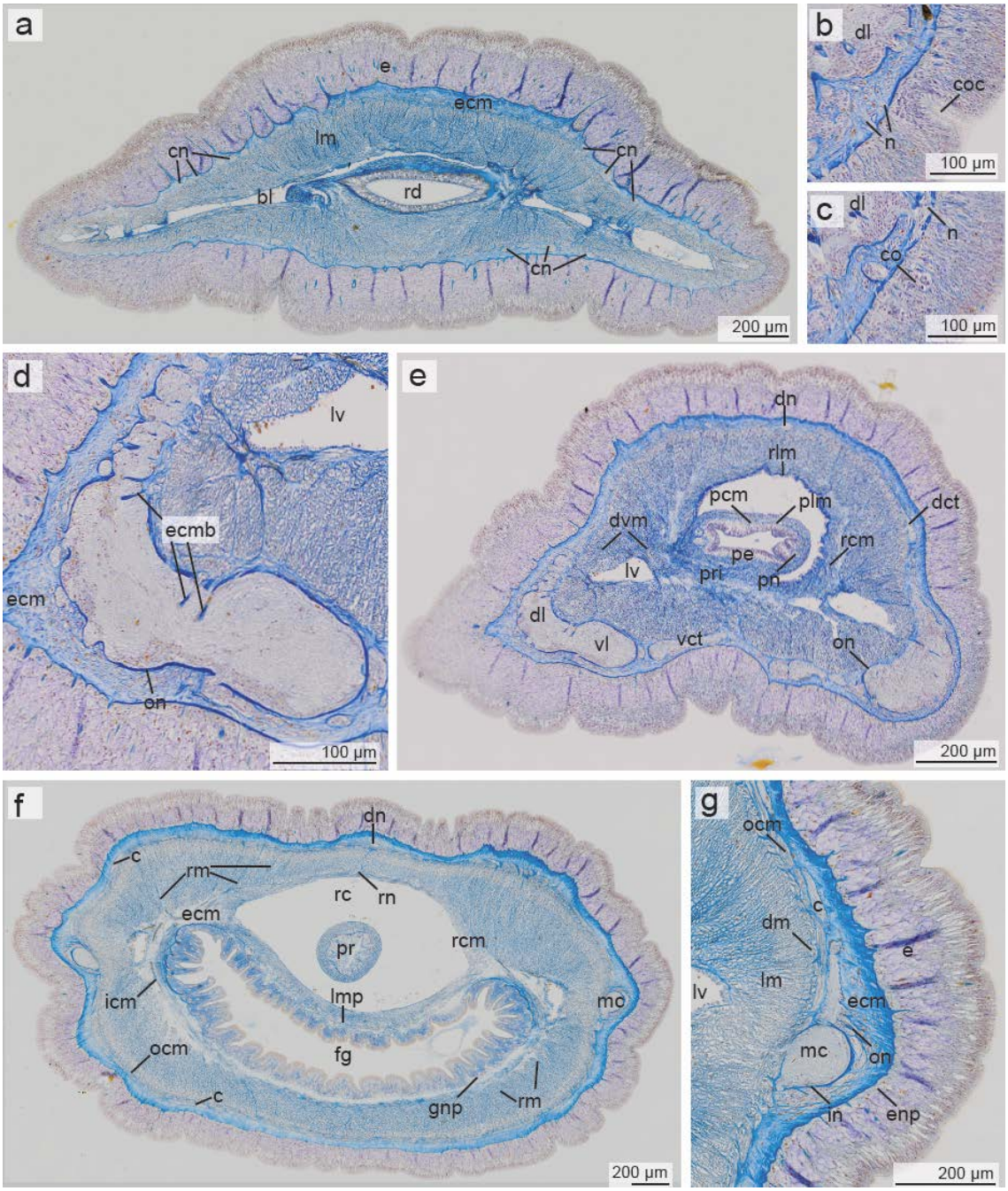

Figure 4.2 *Tubulanus polymorphus* voucher specimen (GNM Nemertinea 159, www.morphdbase.de/?D_Kraemer_20160921-S-8.1), cross sections, azan-stain. **(a)** Transverse section through cephalic lobe. **(b)** Transverse section through anterior part of the cerebral organ**. (c)** Transverse section throuch posterior part of the cerebral organ. **(d)** Magnified detail of brain **(e)** Transverse section at level of brain and proboscis insertion. **(f)** Transverse section through foregut region. **(g)** Magnified detail of transverse section through the foregut region showing the organization of the body wall and medullary cords. Abbreviations: **c**, connetive; **cm**, circular musculature; **cn**, cephalic nerve; **co**, cerebral organ; **coc**, canal of cerebral organ; **dct**, dorsal commissural tract; **dn**, dorsal nerve; **dm**, diagonal musculature; **dl**, dorsal lobe; **e**, epidermis; **ecb**, bundles of extracellular matrix traversing brain tissue; **ecm**, extra cellular matrix; **epn**, epidermal nerve plexus; **fg**, foregut; **gnp**, gastrodermal nerve plexus; **icm**, inner circular musculature; **in**, inner neurilemma; **lm**, longitundial musculature; **lmp**, longitudinal muscle

plate; **lv**, lateral vessel; **mc**, medullary cord; **ocm**, outer circular musculature; **on**, outer neurilemma; **pe**, proboscis epithelium; **pcm**, proboscidial circular musculature; **plm**, proboscidial longitudinal musculature; **pn**, proboscis nerve; **pr**; proboscis; **pri**, proboscis insertion; **rd**, ryhchodaeum; **rc**, rhynchocoel; **rcm**, rhynchocoeal circular musculature; **rm,** radial musculature connecting outer and inner circular musculature; **rn**, rhynchocoelic nerve; **vct**, ventral commissural tract; **vl**, ventral lobe.

***Tubulanus ruber* (Griffin, 1898) comb. nov.**

Carinella rubra (Griffin 1898; Coe 1904, 1905; Ricketts & Calvin 1948)

Carinella speciosa (Coe 1901, 1904)

Tubulanus polymorphus (Coe 1940; Corrêa 1964; Brusca & Brusca 1978; Melville 1986; Stricker 1987; Blake 1993; Stricker & Folsom 1998; Hochberg & Lunianski 1998; Stricker *et al.* 2001; von Döhren *et al.* 2010; Andrade *et al.* 2012; Beckers *et al.* 2013; Mulligan *et al.* 2014; Hiebert 2015)

For list of synonyms (Appendix III: Supplementary Table 6)

Material examined:

Neotype designated here. USA, Washington, San Juan Island, Cattle Point (48°26'56.2"N 122°57'55.1"W), male specimen: Anterior end: Series of histological cross sections, 59 slides (TR1/SBMHN465922, www.morphdbase.de/?D_Kraemer_20161104-S-9.1).

Tissue (posterior end) of same specimen in ethanol (TR1/SBMNH465922, GenBank accession number KX853121 (COI), KX853117 (16S);

Voucher specimen. USA, Washington, San Juan Island, Cattle Point **(**48°26'56.2"N 122°57'55.1"W), female specimen: Tissue (posterior end) of female specimen in Ethanol (TR4/SBMNH465923, GenBank KX853122 (COI), KX853118 (16S).

Other material. Same female specimen: anterior end: Series of histological cross sections, 65 slides at the Institute of Evolutionary Biology and Animal Ecology, University of Bonn (TR4: first 27 slides: www.morphdbase.de/?D_Kraemer_20161104-S-10.1).

Diagnosis. Epibenthic *Tubulanus* species in mid-intertidal; body coloration bright orange; body wall thin, layer of diagonal musculature absent; brain large in relation to body wall musculature, dorsal nerve absent; medullary cords without inner neurilemma; lateral blood vessels spacious in tip of head and foregut region in relation to body wall musculature; epidermal cerebral organs comparably large; extensive cephalic glands.

Habitat. During low-tide, specimens situated underneath rocks and small boulders in rocky mid-intertidal zone of Cattle Point on San Juan Island, Washington State.

External characters. (see also (Griffin 1898; Coe 1901, 1904, 1905; Corrêa 1964; Hiebert 2015) and character checklist after Sundberg et al. 2016: Appendix III: Supplementary Table 8). Neotype material not measured. Neotype and paratype characterized by bright, uniform orange coloration. Head spatulate-shaped, clearly demarcated from trunk, wider than rest of body. Proboscis pore opening subterminally at anterior-most tip of head. Mouth positioned ventrally, visible as long slit behind paired, lateral, transverse furrows (Coe 1901; Hiebert 2015). Rhynchocoel not visible through body wall.

Body wall. Epidermis thick, measuring same height as body wall musculature, densely packed with glandular cells (Figure 4.3 f, g). Thick basal lamina, followed by thin layer of outer circular musculature. Basal lamina doubling height of circular musculature (Figure 4.3 d, g). Longitudinal musculature prominent, appearing as main component of body wall, traversed by thick bundles of extracellular matrix (Figure 4.3 a, d, g). Rhynchocoel and alimentary canal surrounded by barely distinguishable inner layer of circular musculature (Figure 4.3 f). Radial musculature, connecting inner and outer circular musculature, not clearly discernible in section series. Longitudinal muscle plate barely discernible between alimentary canal and rhynchocoel (Figure 4.3 f).

Alimentary canal. No functional division of alimentary tract into esophagus or stomach discernible through histological cross section series. Long, slit-like mouth opens posterior to brain lobes into foregut. Anteriorly, ventral side of foregut epithelium folded and generally much thicker and richer in glands than flat dorsal side of alimentary canal (Figure 4.3 f). Folding, density of glands, and thickness of gut epithelium decrease in posterior course resulting in more homogenous epithelium.

Intestine discernible as simple tube with unfolded, thin epithelium. Epithelial cells bear multiple orange staining cell inclusions (www.morphdbase.de/?D_Kraemer_20161104-M-18.1).

Nervous system. (see also Beckers *et al.* 2013). Subepidermal position of nervous system: brain and medullary nerve cords embedded in layer of extracellular matrix (basal lamina) situated between epidermis and outer circular musculature (Figure 4.3 b-g). Brain consists of paired ventral and dorsal lobes, positioned ventro-laterally in juxtaposition to one another, surrounded by thick outer neurilemma (Figure 4.3 e). Several processes protrude from outer neurilemma and traverse neuropil of brain (Figure 4.3 d). Lobes interconnected by several thin, dorsal commissural tracts and one thick ventral commissural tract (Figure 4.3 d, e). Ventral brain lobes confluent with medullary cords. Neurites of medullary cords surrounded by somata in c-shaped manner ("c" opening towards lateral blood vessels) (Figure 4.3 f, g). Within posterior course, medullary cords interconnected by several commissures on dorsal and ventral body sides. Brain lobes and commissural tracts give rise to peripheral nervous system. Multiple cephalic nerves, situated below basal lamina, protrude to head tip, equally distributed on each body side (Figure 4.3 a). Cephalic nerves arise from anterior parts of dorsal and ventral commissural tracts and brain lobes. Two esophageal nerves originate from posterior margin of ventral brain lobes, running ventro-laterally along each side of alimentary canal. Esophageal nerves interconnected by commissural tract in front of mouth opening (Figure 4.3 c). Two proboscidial nerves arise from ventral commissural tract and innervate proboscis sub-epithelially in opposite positions. Both nerves interconnected by proboscidial nerve plexus. Paired rhynchodaeal nerves originate at posterior margin of ventral lobes and ventral commissural tract. Nerves innervate sub-epithelially in ventro-lateral positions. Nerves not discernible posterior to proboscis insertion. Epidermal- and gastrodermal nerve plexus present, visible as thin layer in basal part of epidermis and gut epithelium respectively (Figure 4.3 g).

Vascular system. Blood lacuna located in tip of head and extends 1/3 in length of rhynchodaeum. Lacuna irregularly traversed by dorso-ventral muscle bundles vessels

(Figure 4.3 a). Lateral blood vessels run inside of longitudinal body wall musculature (Figure 4.3 f, g). Vessels are voluminous in front of brain, appear thin on level of brain lobes and expand towards level of mouth opening, appearing extremely large in comparison to thickness of body wall musculature (Figure 4.3 a-f). Lateral blood vessels, irregularly traversed by muscle bundles arising from body wall musculature (Figure 4.3 a).

Proboscis apparatus. Due to fixation, proboscis partly everted and situated within rhynchodaeum. Thus, visible in everted and inverted state (Figure 4.3 a-e). In everted state proboscis (palaeotype proboscis) layered as follows: thick glandular epithelium, thin layer of extracellular matrix and circular musculature, followed by thicker longitudinal muscle layer (Figure 4.3 a, c-f). Anteriorly, longitudinal musculature measures two times the height of the circular layer. Thickness of both layers decreases posteriorly. Two proboscidial nerves located in sub-epithelial position on opposite sides of proboscis (Figure 4.3 a, e). Rhynchodaeum opens subterminally at tip of head via proboscis pore. Rhynchodaeum extends from anterior end to mouth opening. Rhynchodaeal lumen lined by epithelium, densely packed with glandular cells. Epithelium surrounded by thin layer of circular musculature (Figure 4.3 a). Quantity of glandular cells decreases towards proboscis insertion resulting in thinner epithelium, measuring same height as circular musculature surrounding rhynchodaeum. Proboscis inserts at level of mouth opening. Extension of proboscis and rhynchocoel not obtainable from serial sections. Rhynchocoel wall composed of longitudinal musculature, surrounded by thin, barely visible circular musculature. Both layers much thinner posteriorly. Lumen of rhynchocoel increases posteriorly, occupying ¾ of transverse section (Figure 4.3 f).

Excretory system. Not within range of histological cross section series.

Reproductive system. Sexes separate. Gonad arrangement not within range of histological cross section series.

Sense organs & cephalic glands. Without eyes. Cerebral organs present, located within epidermis, situated in juxtaposition and posterior to brain lobes, occupying 2/3 to full height of epidermis. Canal of cerebral organs anteriorly formed as epidermal pits. Pits

enclose posteriorly and lead as canal into basal part of epidermis. Canal surrounded by comparably thick layer of densely packed glandular cells (Figure 4.3 b, c). Cerebral organs innervated by one nerve, arising from dorsal brain lobe. Cephalic glands extend from tip of head and end shortly before brain. Glands surround blood lacuna and lateral vessels, being more prominent above the latter (Figure 4.3 a). Lateral organs not within range of the section series.

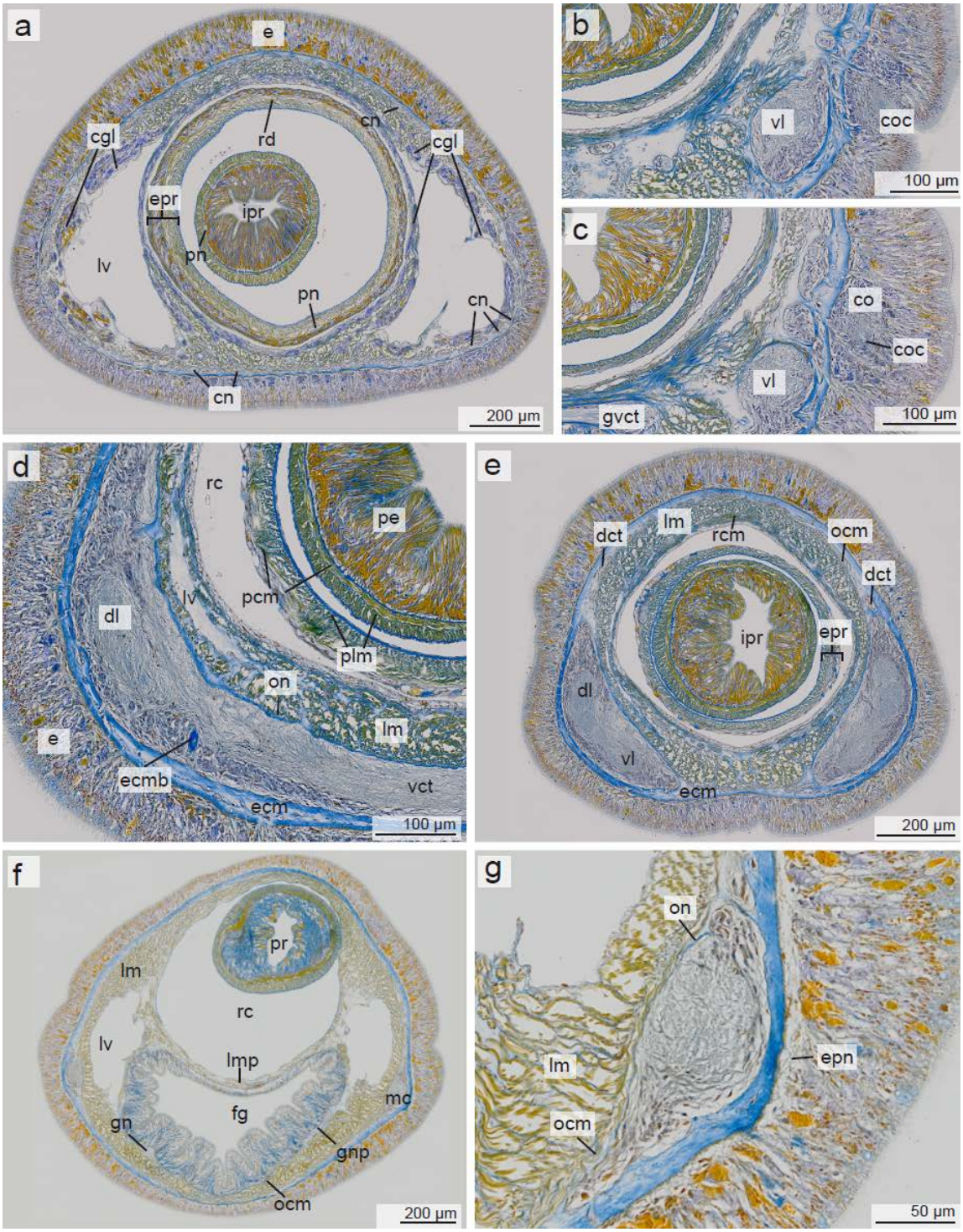

Figure 4.1 *Tubulanus ruber* comb. nov. neotype (TR1/SBMNH465922), cross sections, azan-stain. **(a)** Transverse section through cephalic lobe. **(b)** Transverse section through anterior part of the cerebral organ**. (c)** Transverse section throuch posterior part of the cerebral organ. **(d)** Magnified detail of brain. **(e)** Transverse section through brain region. **(f)** Transverse section through foregut region. **(g)** Magnified detail of foregut region showing structure of body wall and medullary cords. Abbreviations: **cgl**, cephalic gland; **cm**, circular musculature; **cn**, cephalic nerve; **co**, cerebral organ; **coc**, canal of cerebral organ: **dct**, dorsal commissural tract; **dl**, dorsal

lobe; **e**, epidermis; **ecb**, bundles of extracellular matrix traversing brain tissue **ecm**, extracellular matrix; **epr**, everted proboscis; **enp**, epidermal nerve plexus; **fg**, foregut; **gn**, gastric nerve; **gnp**; gastric nerve plexus; **gvct**, gastric ventral commissural tract; **icm**, innercircular musculature; **ipr**, inverted proboscis; **lm**, longitudinal musculature; **lmp**, longitudinal muscle plate; **lv**, lateral vessel; **ocm**, outer circular musculature; **on**, outer neurilemma; **pe**, proboscidial epithelium; **pcm**, proboscidial circular musculature; **plm**, proboscidial longitudinal musculature; **pn**, proboscis nerve; **rc**, rhynchocoel; **rd**, rhynchodaeum; **vct**, ventral commissural tract; **vl**, ventral lobe.

4.3.2 Phylogenetic analysis.

P-distance calculations based on the COI alignment support the separation of *T. polymorphus* from the European Atlantic Coast and *T. ruber* from the Pacific Coast of the United States into two species. Intraspecific variation is low in *T. polymorphus* (0.5%) and *T. ruber* (0.2-0.5%). Interspecific variation is comparably high between *T. polymorphus* and *T. ruber* ranging from 16.2% to 16.6%, and thus in the same interspecific distance range as to the remaining *Tubulanus* species (12.6-17.6%) (Table 4.1).

The concatenated data set of aligned COI (579nt) and 16S with removed uncertain positions (261nt) and the original 16S alignment used for maximum likelihood resulted in a length of 840nt and 979nt respectively. The resulting trees slightly differ in their topologies regarding the positions of *Tubulanus superbus*, *Tubulanus pellucidus*, *Callinera grandis*, *Cephalothrix bipunctata* and *Cephalothrix spiralis*. With uncertain positions in 16S removed, *T. pellucidus* groups with *C. grandis* (Bootstrap support: 60%) within the remaining *Tubulanus* species (43%), rendering the genus paraphyletic (Figure 4.4 a). The reduced set of nucleotides places *T. superbus* as sister to *T. polymorphus* (59%) (Figure 4.4 a)

When including uncertain positions within the analysis, *Tubulanus* appears monoyphyletic (90%) with *C. grandis* as sister taxon (78%). *Tubulanus superbus* appears as sister to *T. rhabodotus*, *T. sexlineatus* and *T. punctatus* and *T. pellucidus* groups with *T. ruber* and *T. annulatus* (60%) (Figure 4.4 b).

Otherwise, both analyses show the same topology with respect to *Carinoma hamanako* and *C. tremaphoros* as most basally branching palaeonemertean species, the monophyly of Cephalothricidae (gblocks: 85%/ original:100%), the position of *Carinina ochracea* (72%/84%) as basally branching species within Tubulanidae, and

the definite positions of the two *Tubulanus* species described above. The analyses indicate a subdivision of the genus *Tubulanus* into two clades, both of which are moderately supported (Figure 4.4 a, b). Clade 1 contains *T. sexlineatus, T. punctatus, T. rhabdotus, T. superbus,* and *T. polymorphus* (71%/98%), while the other (clade 2) comprises *T. annulatus, T. polymorphus* of Andrade *et al.* 2012 and *T. ruber* (80%/99%).

Table 4.1 Summary of uncorrected p-distances (%) based on COI.

	Tubulanus polymorphus	***Tubulanus ruber***
Tubulanus polymorphus	0.5	
Tubulanus ruber	16.2-16.6	0.2-0.5
Tubulanus superbus	14.3-14.5	16.1-16.2
Tubulanus pellucidus	17.1-17.4	16.1-16.2
Tubulanus annulatus	17.3-17.5	12.6-12-7
Tubulanus punctatus	15.5-16.1	17.5-17.6
Tubulanus sexlineatus	15.9-16.2	16.4-16.6
Tubulanus rhabdotus	15.5-15.7	15.2-15.4

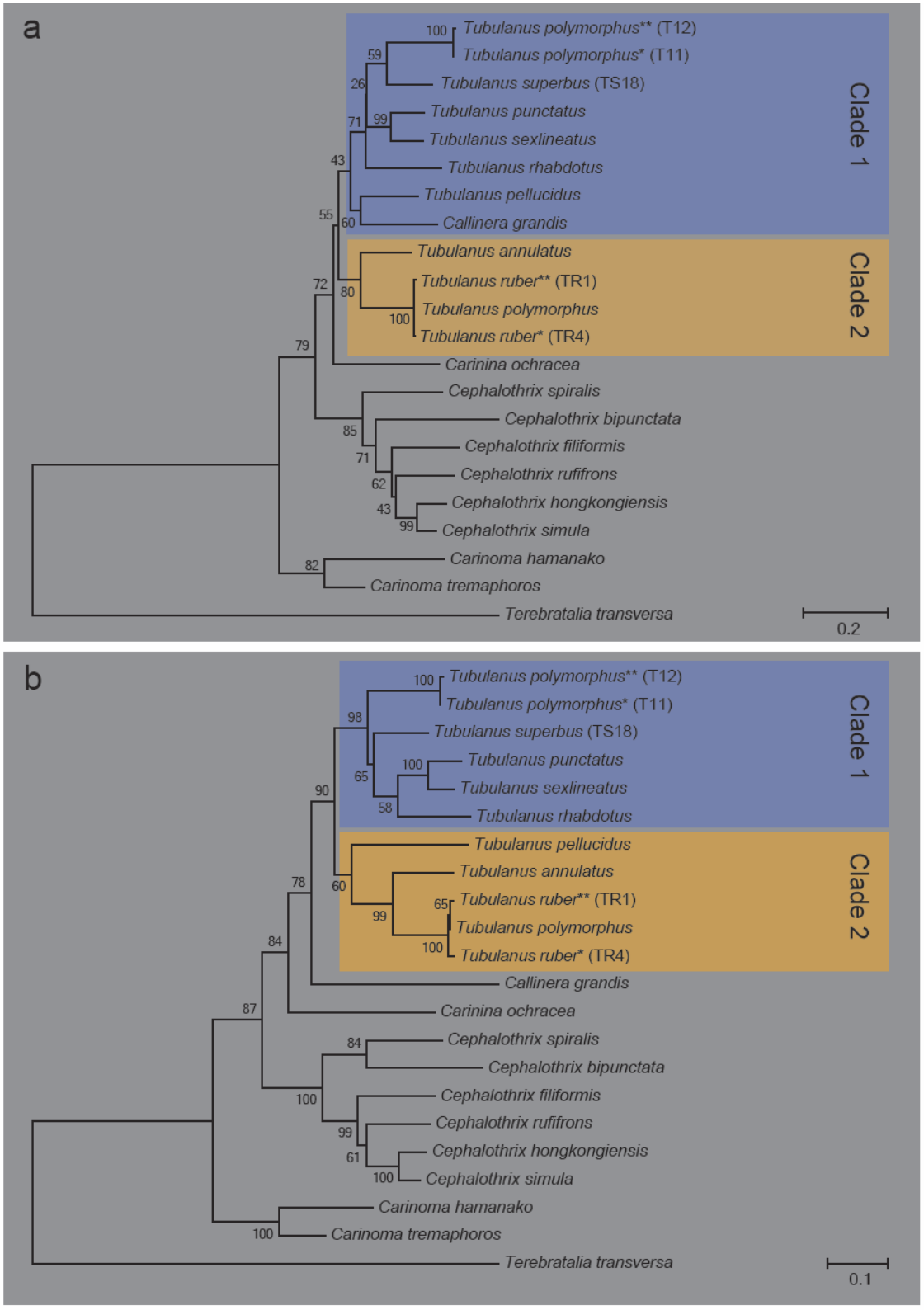

Figure 4.2 Phylogeny resulting from maximum likelihood analyses based on concatenated COI and 16S sequence data. *Terebratalia transversa* was used for out-group rooting. Numbers at branches indicate bootstrap support from 500 replicates. **(a)** Shows phylogeny based on the alignment excluding uncertain positions. **(b)** Shows phylogeny including uncertain positions. **

indicates neotype for *T. polymorphus* and *T. ruber*, * indicates voucher specimens for *T. polymorphus* and *T. ruber*.

4.4 Discussion

In recent decades, the systematics of several high ranking taxa (e.g. Annelida, Mollusca, and Nemertea) have experienced considerable revision, including the identification of a number of cryptic species. Thus, the long-held view of global distribution of some species has been challenged (Strand & Sundberg 2005b; Bleidorn *et al.* 2006; Barroso *et al.* 2009; Sundberg *et al.* 2009b, 2010; Jörger *et al.* 2012; Carmona *et al.* 2014; Leasi & Norenburg 2014; Kienberger *et al.* 2016). In the case of *Tubulanus polymorphus*, data on morphology provided in this study clearly enable a separation of the European specimens from the North American specimens. For the latter, we herein re-establish the species *Tubulanus ruber* (Griffin, 1898). It is characterized by bright orange coloration, comparably large epidermal cerebral organs (measuring 2/3 to full height of epidermis) and extensive cephalic glands. All characters are matching the descriptions of specimens collected from the North Pacific (Griffin 1898; Coe 1905; Corrêa 1964). Moreover, we observe a voluminous brain and lateral blood vessels relative to the thickness of the body wall musculature. A dorsal nerve, an inner circular musculature, and an inner neurilemma separating neuropil and cell somata within the lateral nerve cords, are absent.

Tubulanus polymorphus from the European west coast is characterized by a brick-red coloration, which is abruptly becoming darker posteriorly (corresponding to fixation band in formalin preserved specimens), small almost rudimentary cerebral organs, a layer of diagonal musculature interconnecting circular and longitudinal muscles, and the absence of cephalic glands. These are all characters matching the descriptions given by Bürger in 1892 and 1895 based on specimens collected from the Mediterranean Sea. Furthermore, we observe smaller brain and lateral blood vessels relative to the prominent body wall musculature. In contrast to *T. ruber*, a dorsal nerve and an inner neurilemma in the lateral nerve cords are present.

Both species can be further distinguished by their ecology, namely their different habitat preferences. Whereas *T. polymorphus* is found in parchment-like tubes in 0.2-0.5

m depth within sandy substrate between the roots of the sea grass *Zostera marina* on the Atlantic coast, *T. ruber* is found underneath stones in the rocky intertidal of the coast of the North Pacific. This is congruent with information given in the literature according to which *T. polymorphus* occurs among the rhizomes of *Posidonia oceanica* Delile, 1813, in the Mediterranean Sea (Bürger 1892, 1895), while *T. ruber* is reported to live in tubes attached to the bottom side of rocks (Coe 1943; Stricker 1987; Hiebert 2015).

We additionally observed differences concerning aspects of the reproductive biology i.e. gamete and larval morphology of both species. Whereas unfertilized oocytes of *T. ruber* measure 350 µm in diameter (Stricker 1987), egg size of *T. polymorphus* ranges between 90-100 µm (von Döhren, pers. observation). Newly hatched larvae of *T. polymorphus* measure approximately 110-120 mm in length and transit into a planktonic phase for more than nine days (von Döhren, pers. observation), whereas larva of *T. ruber* are not reported to undergo an extended planktonic phase (Stricker 1987). The length of the sperm cell soma (i.e. excluding the flagellum) also differs considerably between the two species: In *T. ruber* the sperm cell soma is approximately 1.5 times longer, while in *T. polymorphus* the sperm cell soma is about 1.5 times wider in its widest diameter (Stricker & Folsom 1998; von Döhren *et al.* 2010). Additionally, the sperm cells differ considerably in their ultrastructure between the two species. Sperm cells of *T. polymorphus* bear a flat bowl shaped acrosomal vesicle and a ring-shaped mitochondrion surrounding the centrioles (von Döhren & Bartolomaeus, in prep.). Sperm cells of *T. ruber* on the other hand, are characterized by a high acrosomal vesicle and a laterally situated mitochondrion, only partly encircling the nucleus (Stricker & Folsom 1998; von Döhren *et al.* 2010).

The molecular analyses further underpin the separation into two species. Even though based on only a few specimens, COI p-distance calculations reveal low intraspecific varation in both *T. polymorphus* (0.5%) and *T. ruber* (0.2-0.5%). Although the specimens of *T. polymorphus* were sampled in the same locality (Roscoff, France), the intraspecific variation is within the upper range of that observed in *T. ruber* species. We therefore consider it a sound estimate, notwithstanding the limited number and geographical range of the sample. In contrast to the intraspecific variation, interspecific variation between *T. polymorphus* and *T. ruber*, as well as other *Tubulanus* species is

high (12.6-17.5%) (Table 4.1). Therefore, we predict a pronounced barcoding gap between *T. polymorphus* and *T. ruber*.

The phylogenetic trees show that each species nests within one of two *Tubulanus* subclades, which had already been recovered in a previous analysis (Kajihara *et al.* 2015). Each of the resulting clades is supported by specific morphological characters, namely the differently developed cerebral organs and cephalic glands. The affiliation of *T. pellucidus*, which only possesses rudimentary cerebral organs (Coe 1905), to one or the other clade presently remains unresolved.

Based on the differences observed in all data sets, we decided to assign specimens as neotype material from the North American Pacific and the French Atlantic coast for *T. ruber* and *T. polymorphus* respectively since no type material is available from the original descriptions by Renier (1804) and Griffin (1898). Addtionally, formalin preserved voucher material for specimens collected from different localities in California, USA is catalogued under the name *T. polymorphus* by the Santa Barbara Natural History Museum (http://www.sbcollections.org/). However, the material does not enable successful DNA extractions and an assignment to the species described in this study (Norenburg, Geiger & Valentich-Scott, pers. communication).

We consider assigning *T. ruber* from Friday Harbor as reasonable since this site is located in close vicinity of the original type localities (Sitka in Alaska and Bremerton and Kilisut Harbor in the Pudget Sound Area in Washington State) (Griffin, 1898). In accordance with Sundberg *et al.* 2016, we regard assigning specimens from Roscoff as neotypes as generally unproblematic following the recently advocated practice of nemertean researchers regarding redescriptions (Hiebert & Maslakova 2015; Krämer *et al.* 2016; Sundberg *et al.* 2016). *T. polymorphus* was originally described from the Mediterranean Sea but the exact type locality was not recorded in the original description. Detailed descriptions by Bürger (Bürger 1892, 1895) are based on material collected from the Gulf of Naples but this appeared as one of last records of this species in this area. Subsequent publications do not report any findings of the species in the Mediterranean area but from the European Atlantic to North Sea coasts (Gontcharoff 1955; Sundberg & Hylbom 1994; Martínez *et al.* 2007; Herrera-Bachiller 2016). Roscoff is within the vicinity of the historically documented distribution range of the species (Joubin 1890; Bürger 1892; Wijnhoff 1912; Gontcharoff 1955).

4.5 Conclusions

With an integrative taxonomic approach used in this study we provide a broad set of data which enables a clear separation of *Tubulanus polymorphus* and *T. ruber* into two species. The deposition of material on publicly available databases (MorphDBase, GenBank), as well as information on sample sites enable an unambiguous reassignment of the broad spectrum of information published under the name *T. polymorphus* to either *T. ruber* (Stricker 1987; Stricker & Folsom 1998; Stricker *et al.* 2001; von Döhren *et al.* 2010; Andrade *et al.* 2012; Mulligan *et al.* 2014; Hiebert 2015) or *T. polymorphus* (Gontcharoff 1955; Sundberg & Hylbom 1994) (Appendix III: Supplementary Table 6). Regarding the data published by one of the co-authors of this paper (Beckers 2011; Beckers *et al.* 2013) the data acquired by classical histological methods refers to what we consider *T. ruber* (https://www.morphdbase.de?P_Beckers_20130201-M-11.1) while CLSM data and pictures showing external morphology were obtained from *T. polymorphus* (Appendix III: Supplementary Table 6).

Our phylogenetic analyses recover *Tubulanus* and Tubulanidae as either monophyletic or paraphyletic, depending on data set used. This incongruence might be the result of employing only two mitochondrial genes and/or insufficient taxon sampling. However, both phylogenic hypotheses reconstructed in this study are congruent with respect to the distinct positions of the two species within *Tubulanus*. Furthermore, results show that both species are not even close relatives.

Based on the assumed paraphyly of *Tubulanus* (Andrade *et al.* 2012; Kvist *et al.* 2014, 2015; Kajihara *et al.* 2015) recovered Kajihara *et al* (2015) suggested to keep the name *Tubulanus* for the group containing the type species (*T. polymorphus* of Andrade *et al*. 2012 which is, according to our data, *T. ruber* in the group we herein indicated as clade 2) and to rename the other tubulanid subclade (herein indicated as clade 1). In contrast, our data show that the specimens from Europe, representing the actual type species *T. polymorphus*, are nested within the clade (clade 1) that, according to Kajihara *et al* (2015), would have to be renamed. Therefore, a revision of the genus *Tubulanus* as intended by Kajihara *et al* (2015) would have been premature. The reassignment of the

type species *T. polymorphus* is the essential prerequisite for a future revision of the genus *Tubulanus*.

4.6 Acknowledgements

We are grateful to Terra Hiebert for providing pictures of *Tubulanus ruber*. We thank Kennet Lundin of the Göteborgs Naturhistorika Museum as well as Daniel Geiger and Paul Valentich-Scott of the Santa Barbara Natural History Musuem for the friendly and fast correspondences and for type material deposition. We are grateful to Christiane Wallnisch for technical assistance. We thank the staff of the Station Biologique de Roscoff in France and the Friday Harbor Laboratiories in WA, USA for facilities and accommodation during the collection trip.

Chapter 5

General Discussion

5.1 Morphological taxonomy

As of today, most descriptions include a section about external characters followed by detailed information on each organ system gained from histological sections. These morphological traits are compared to potential congeneric species in a subsequent systematic discussion (differential diagnosis) (Junoy & Gibson 1991; Norenburg 1993; Chernyshev 2002a; b, 2003a; Ritger & Norenburg 2006; Chapter 2 & 4).

However, the interpretation of histological data appears problematic for many reasons. First, it is difficult to obtain high-quality sections because preserving soft-bodied animals bears high risk of contraction and fixation artifacts (Sundberg 2015). Second, intraspecific variation might be misinterpreted as species or genus specific characters (Sundberg 1979). Third, many characters might share non-homologous similarities due to suspected convergent and parallel evolution rendering them less informative (Sundberg & Hylbom 1994; Strand *et al.* 2014; Sundberg 2015; Sundberg *et al.* 2016). Fourth, many characters lack a clear definition. The overall interpretation of morphological characters therefore lacks a widely applied standard approach and remains subjective (Sundberg 1989a; b, 2015; Vogt *et al.* 2010; Strand *et al.* 2014) (Sundberg 1989a; b; Strand *et al.* 2014 in Sundberg 2015). As a consequence, many nemertean species, genera, or even families are not sufficiently defined. This led to two extremes in nemertean taxonomy: new species are either assigned to “catch-all” groups that include vast numbers of likely-unrelated species or they are classified as new monotypic genera (Strand *et al.* 2014; Sundberg 2015). Examples of “catch-all” groups are the genera *Lineus*, *Amphiporus*, *Cerebratulus* or *Tetrastemma*. Many species were placed into these genera out of convenience or due to the lack of sufficient data suggesting an assignment to another genus (Strand & Sundberg 2005b; Sundberg 2015). Representatives of *Lineus*, for example, therefore appear on multiple unconnected branches of phylogenetic trees (Figure 5.1). Examples for monotypic genera are

especially found is less intensely studied groups, such as the polystiliferan hoplonemertean genera among Pelagica (Maslakova & Norenburg 2001). This results in histological-based genus and family diagnoses that do not reflect monophyletic groups. This is also shown by phylogenetic analyses in which relationships among species are not well resolved and several genera and families are rendered paraphyletic (Figure 5.1) (Thollesson & Norenburg 2003; Strand & Sundberg 2005a; Andrade *et al.* 2012; Kvist *et al.* 2014, 2015). As stated in Andrade *et al.* (2012) and Kvist *et al.* (2014) results gained from current phylogenies therefore demand the revision of several nemertean genera. As a consequence, current phylogenies do not necessarily present the required stable backbone, to assign an undescribed species to new or existing genera and families.

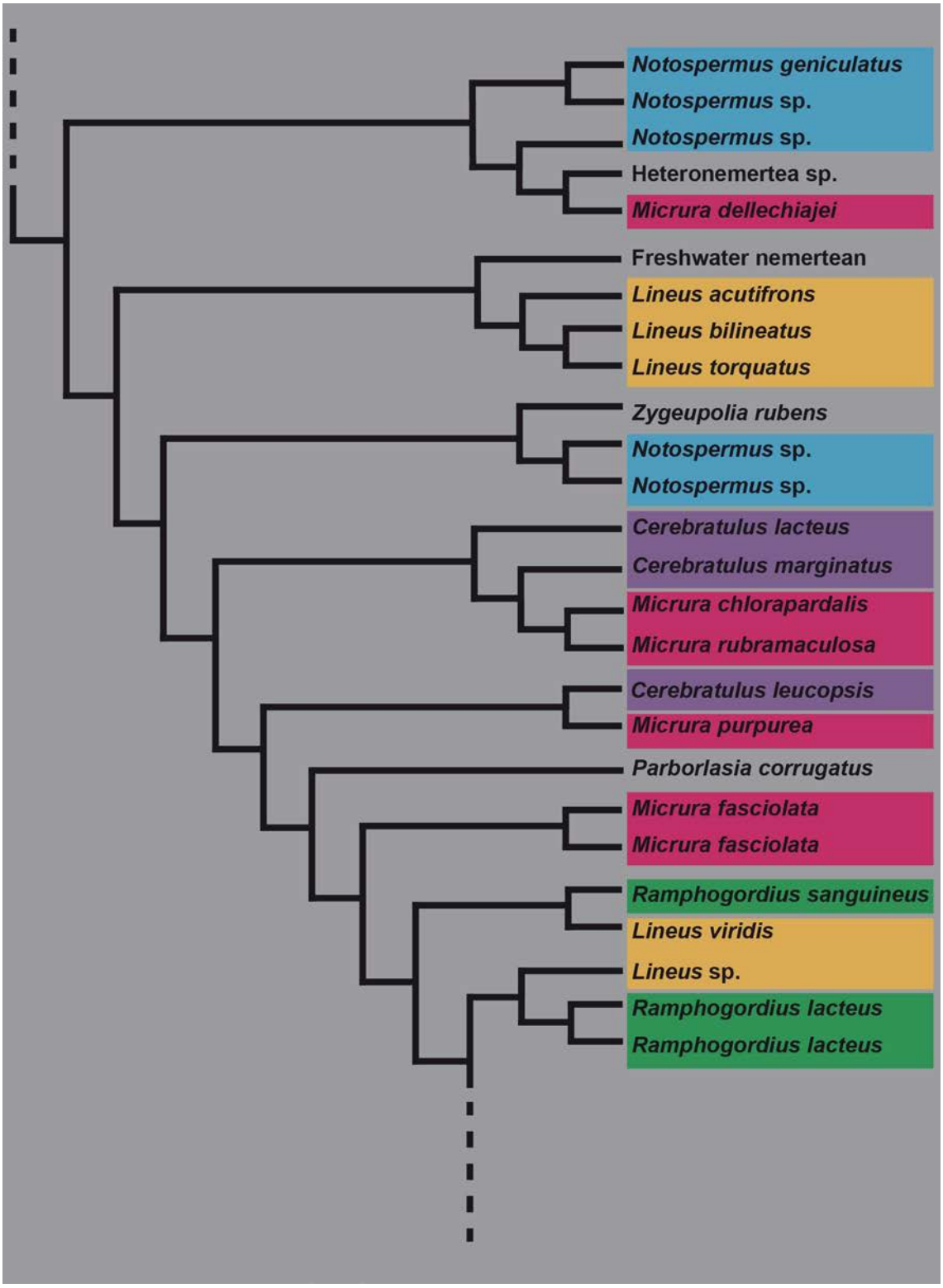

Figure 5.1 Internal relationships among heteronemerteans redrawn after results gained from maximum likelihood analysis conducted in Kvist. *et al*. 2015.

5.2 Molecular Taxonomy

Apart from reconstructing phylogenetic relationships among several animal phyla, sequence data are increasingly used to identify and delimitate species (Vogler & Monaghan 2006; Kvist 2013). By the employment of DNA barcoding, a short part of mitochondrial DNA (usually the cytochrome *c* oxidase subunit I (COI)) is used to identify an unknown specimen against a sequence database consisting of *a priori* identified specimens linked to a species name (Hebert *et al.* 2003, 2004; Tautz *et al.* 2003; Vogler & Monaghan 2006). In contrast to that, the more inclusive term DNA taxonomy represents different approaches to detecting species boundaries. Putative new species are identified or grouped into taxonomic units (Molecular operational taxonomic units (MOTUs) with the aid of so-called tree-based and non-tree-based-species delimitation methods. These aid to model or set potential species boundaries based on sequence alignments (Clement *et al.* 2000; Pons *et al.* 2006; Puillandre *et al.* 2012; Tang *et al.* 2012; Fujisawa & Barraclough 2013; Zhang *et al.* 2013; Chapter 3). The successful employment of DNA barcoding and DNA taxonomy relies on two important prerequisites: the presence of a high coverage of the target-taxon in barcode databases and the presence of a barcoding gap (which is the difference between the highest intraspecific variation and the lowest interspecific variation) (Kvist 2013). The barcoding gap therefore represents a threshold that allows the separatation of sequence data into clusters representing potential species (Vogler & Monaghan 2006; Fontaneto *et al.* 2015). Within the last decade, this served to detect several new but also cryptic nemertean species which would have remained hidden using morphology alone (Sundberg *et al.* 2009b, 2010; Chen *et al.* 2010; Strand & Sundberg 2011; Leasi & Norenburg 2014; Chapter 3).

Sequence data, especially COI data, represent a promising foundation to safely and quickly detect nemertean species (see Strand & Sundberg 2005a; Sundberg *et al.* 2009b, 2010; Chen *et al.* 2010; Leasi & Norenburg 2014). In all cases, however, identified species were not described, mainly because traditional nemertean taxonomy demands detailed histological-based descriptions. For almost a decade Sundberg and co authors (Sundberg *et al.* 2009b, 2010; Strand & Sundberg 2011; Strand *et al.* 2014; Sundberg 2015) have been advocating a DNA-based approach for describing and re-

describing nemertean species. They state that nemerteans can be identified and described based on external appearance, ecology, and molecular sequence data. They argue that internal morphology does not provide sufficient diagnostic characters and is therefore an unnecessary prerequisite for a species description to be accepted (Strand & Sundberg 2011; Strand *et al.* 2014; Sundberg 2015). Sundberg (2015) goes a step further, stating that in the course of assessing biodiversity, histology does not provide a time-efficient approach for identification. Apart from the general problem of identifying nemerteans, the difficulties related to histological work represent another reason why so many species remain unidentified in many marine surveys and are identified as "Nemertes sp." at best (Schander & Willassen 2005 in Sundberg 2015). The DNA-based approach contradicts the traditional way of describing nemertean species and was therefore not initially pursued. Moreover, the DNA-based approach was so largely criticized it still remains difficult to publish species descriptions without histological data (Sundberg 2015, publication procedure of Chapter 3).

However, the proposal of a DNA-based approach was accepted among the majority of active nemertean researchers at the beginning of 2016 (see list of authors of Sundberg *et al.* 2016). As stated in the proposal, species descriptions and re-descriptions are acceptable when information on external characters and ecology, as well as references to sequence data is included. Furthermore, a holotype and voucher material preserved in ethanol should be deposited in a public institution. Additionally, the authors account for another problem: Many old species descriptions do not explicitly state information on the *locus typicus* and for some type localities the access is strictly regulated by laws. By recommending the acceptance of re-descriptions based on material collected in the vicinity of the type locality, these problems can be circumvented. The "vicinity-concept" allows for quicker re-descriptions of problematic taxa, of which the identities have been confused for many years (Sundberg *et al.* 2016; Chapter 3 & 4).

Nevertheless, employing DNA barcodes as a tool for species delimitation and identification bears difficulties in nemerteans. As shown by Kvist in 2013 and Kvist *et al.* 2014, less than 20% of all recognized nemertean species are represented in barcode databases such as NCBI or BOLD. Many deposited sequences stem from misidentified specimens and are tied to an incorrect species name or to no name at all. Therefore, an

identification based on sequence data might be inconclusive (Meyer & Paulay 2005; Kvist 2013; see Chapter 2). Additionally, incomplete information does not allow for identification of a general barcoding gap in nemerteans (Kvist *et al.* 2014). To define a barcoding gap, a broad sample size of the species (or species group) in question is required to define the threshold between intraspecific and interspecific variation (Luo *et al.* 2015). While this is not a problem for highly abundant species such as *Lineus ruber*, *Lineus viridis*, and *Lineus clandestinus* (see Chapter 3, Appendix II: Supplementary Table 3) it can become problematic in cases where only a few individuals are found (see Chapter 2 and 4).

The overall functionality of DNA barcoding depends on a higher representation of accurately identified species in DNA databases. A sequence should therefore refer to a properly identified specimen which is, in the best case scenario, a type or a voucher specimen deposited in a public institution such as a museum collection (Kvist *et al.* 2010; Kvist 2013). These sequences would give a starting point for creating a "rigorous database of authoritative sequences" (Kvist *et al.* 2014: 304), which allow for more secure identification in the future.

5.3 Integrative taxonomy

Integrative taxonomy is defined as an multidisciplinary approach which integrates complementary sources of data to delimit, discover, and identify species and taxa at all levels (Dayrat 2005; Will *et al.* 2005; Yeates *et al.* 2011). This is somehow congruent with de Queiroz's (2007) idea of the unified species concept, which integrates criteria advocated by the different species concepts as circumstantial evidence for diverged species. Including data from multidisciplinary approaches allows the validation of species boundaries from multiple perspectives.

An integrative approach, including more than just one source of data, represents a promising methodology to safely identify species within Nemertea (see Maslakova & Norenburg 2008; Sundberg *et al.* 2009a; Kajihara *et al.* 2011, 2015; Chernyshev *et al.* 2015; Hiebert & Maslakova 2015; Chapter 2 & 4). It is obvious that in most cases, nemertean species can be safely delimited based on molecular data and external

characters and that these data will provide a solid basis for species identification in the future.

At this juncture, however, histological-based morphological data provide an informational background that is not yet given by molecular data in public repositories rendering a species description *sensu* Sundberg *et al.* (2016) problematic. Furthermore, within the last centuries, comparative morphology represented the dominating tool in species discovery (Padial *et al.* 2010). The majority of our taxonomic knowledge is therefore based on morphology. Combining traditional morphology with new molecular based methodologies therefore brings the traditional knowledge into the present day and prevents the loss of taxon specific information. This is essential for the re-description of species, especially when a species name represents synonymized lineages. Available old species names need to be tied to the specific lineages in question, before new species can described (Martinsson 2016). This prevents the unintentional description of a known species as a new one. In the case of *Tubulanus polymorphus* and *Tubulanus ruber* (Chapter 4), a separation into two species is possible based on only morphological or molecular data. By including internal morphology as a data source, the specimens collected from the Pacific and the European Atlantic could be assigned to the species descriptions by Griffin (1898), Renier (1804), and Bürger (1892, 1895) respectively. Although not included in the descriptive part of Chapter 4, additional information was gained by comparing ecology, gamete ultrastructure, and larval development with the respective published data (Stricker 1987; Stricker & Folsom 1998; Stricker *et al.* 2001). The integrative approach used in Chapter 4 therefore allowed for a more accurate delimitation of both species, and the reassignment of most published data under the name *T. polymorphus* to either *T. ruber* or *T. polymorphus* (Supplementary Table 6).

In the case of *Arenogigas armoricus* (Chapter 2), molecular data combined with external characters and ecological data provide an insufficient basis for the classification process itself. By focusing solely on external characters, important internal characters needed to classify the specimens would have remained unknown. Investigating internal structures reveals characters that are only shared by a small fraction of nemerteans assigned to Poseidonemertidae. Moreover, except for a few *Poseidonemertes* species, representatives of Poseidonemertidae are not well represented in molecular databases. A sole molecular-based approach would have only allowed an

assignment to the genus *Poseidonemertes*, which contradicts the morphological characters encountered through histology. Concerning *A. armoricus*, both molecular sequence data and information on external and internal morphology were necessary to provide a conclusive classification.

Concerning the delimitation of cryptic nemertean species, an integrative taxonomic approach might not lead to new insights. As shown in Chapter 3, the identification of *Lineus clandestinus*, *Lineus ruber*, and *Lineus viridis* was mainly based on molecular sequence data. Results gained from the morphological investigations were only of limited conclusiveness concerning the external morphology, or of no conclusiveness in case of the internal morphology.

5.4 Conclusions

I conclude that there is no clear advantage to either using molecular taxonomy or morphological taxonomy alone concerning the identification and delimitation of nemertean species. The species descriptions presented in this thesis show that, if one of the methods fails or is of limited conclusiveness, the application of the other approach can assist in succeeding to delimit species boundaries, allowing a good species description. In my point of view, molecular sequence data are of major importance and should always be included in a species description. In most cases, they provide a solid basis for identifying a species as shown in Chapters 3 and 4. Even if their applicability might be of limited use as shown in Chapter 2, sequence data will provide the reference for future identification by DNA-barcoding as they represent authoritative barcodes *sensu* Kvist *et al.* (2010). A species description *sensu* Sundberg *et al.* (2016) provides a pragmatic solution to many problems encountered in nemertean taxonomy. It allows for exploring nemertean diversity much quicker as species descriptions do not necessarily have to include detailed morphological descriptions. Taxonomic entanglements will be easier to solve as species re-descriptions do not have to rely on specimens collected from the type locality. Concerning re-descriptions, I suggest including other data sources such as histological-based morphology. These data provide a link to the traditional knowledge of nemertean taxonomy and prevent describing already known lineages as new species. At this point, histological-based data represent a degree of

information that is not yet provided by molecular data. Histological data or data gained from another methodological or biological background (i. e. ecology or life-history) should be included as long as they are informative in assessing species boundaries and whenever molecular data appear inconclusive in that regard.

References

Agapow PM, Bininda-Emonds ORP, Crandall KA, Gittleman JL, Mace GM, Marshall JC & Purvis A (2004) The Impact of Species Concept on Biodiversity Studies. *The Quarterly Review of Biology*, **79**, 161–179.

Alfaya JEF, Bigatti G, Kajihara H, Strand M, Sundberg P & Machordom A (2015) DNA barcoding supports identification of *Malacobdella* species (Nemertea: Hoplonemertea). *Zoological Studies*, **54**, 10. doi: 10.1186/s40555-014-0086-3

Allen, E.J. & Todd, R.A. (1900) The Fauna of the Salcombe Estuary. *Journal of the Marine Biological Association of the United Kingdom*, **6**, 152–217. doi: 10.1017/S0025315400006615.

Andrade SCS, Montenegro H, Strand M, Schwartz ML, Kajihara H, Norenburg JL, Turbeville JM, Sundberg P & Giribet G (2014) A Transcriptomic Approach to Ribbon Worm Systematics (Nemertea): Resolving the Pilidiophora Problem. *Molecular Biology and Evolution*, **31**, 3206–3215. doi:10.1093/molbev/msu253.

Andrade SCS, Strand M, Schwartz M, Chen H, Kajihara H, von Döhren J, Sun S, Junoy J, Thiel M, Norenburg JL, James M, Giribet G & Sundberg P (2012). Disentangling ribbon worm relationships : multi-locus analysis supports traditional classification of the phylum Nemertea. *Cladistics*, **27**, 1–19.

Appeltans W, Ahyong ST, Anderson G, Angel MV, Artois T, Bailly N, Bamber R, Barber A, Bartsch I, Berta, A, Błażewicz-Paszkowycz M, Bock P, Boxshall G, Boyko CB, Brandão SN, Bray RA, Bruce NL, Cairns SD, Chan TY, Cheng L, Collins AG, Cribb T, Curini-Galletti M, Dahdouh-Guebas F, Davie PJF, Dawson MN, De Clerck O, Decock W, De Grave S, de Voogd NJ, Domning DP, Emig CC, Erséus C, Eschmeyer W, Fauchald K, Fautin DG, Feist SW, Fransen CHJM, Furuya H, Garcia-Alvarez O, Gerken S, Gibson D, Gittenberger A, Gofas S, Gómez-Daglio L, Gordon DP, Guiry MD, Hernandez F, Hoeksema BW, Hopcroft RR, Jaume D, Kirk P, Koedam N, Koenemann S, Kolb JB, Kristensen RM, Kroh A, Lambert G, Lazarus DB, Lemaitre R, Longshaw M, Lowry J, Macpherson E, Madin LP, Mah C, Mapstone G, McLaughlin PA, Mees J, Meland K, Messing CG, Mills CE, Molodtsova TN, Mooi R, Neuhaus B, Ng PKL, Nielsen C, Norenburg JL, Opresko DM, Osawa M, Paulay G, Perrin W, Pilger JF, Poore GCB, Pugh P, Read GB, Reimer JD, Rius M, Rocha RM, Saiz-Salinas JI, Scarabino V, Schierwater B, Schmidt-Rhaesa A, Schnabel K E, Schotte M, Schuchert P, Schwabe E, Segers H, Self-Sullivan C, Shenkar N, Siegel V, Sterrer W, Stöhr S, Swalla B, Tasker ML, Thuesen EV, Timm T, Todaro MA, Turon X, Tyler S, Uetz P, van der Land J, Vanhoorne B, van Ofwegen LP, van Soest RWM., Vanaverbeke J, Walker-Smith G, Walter TC, Warren A, Williams GC, Wilson SP & Costello MJ (2012). The magnitude of global marine species diversity. *Current Biology*, **22**, 2189–202. doi: 10.1016/j.cub.2012.09.036.

Arnold G (1898) Zur Entwicklungsgeschichte des *Lineus gesserensis* O.F. Müller (*L. obscurus* Barrois). *Travaux de la Société Impériale des Naturalistes de St. Petersbourg*, 28, 1–30.

Balakrishnan R (2005) Species concepts, species boundaries and species identification: a view from the tropics. *Systematic biology*, **54**, 689–693. doi. 10.1080/10635150590950308.

Barrois J (1877) Memoire sur l'embryologie des Nemertes. *Annales des Scienes Naturelles*, **6**, 1–12.

Barroso R, Klautau M, Solé-Cava AM, Paiva PC (2009) *Eurythoe complanata* (Polychaeta: Amphinomidae), the "cosmopolitan" fireworm, consists of at least three cryptic species. *Marine Biology*, **157**, 69–80. doi. 10.1007/s00227-009-1296-9

Bartolomaeus T (1984) Zur Fortpflanzungsbiologie von *Lineus viridis*. *Helgoländer Meeresuntersuchungen*, **38**, 185–188.

Bartolomaeus T & von Döhren J (2010) Comparative morphology and evolution of the nephridia in Nemertea. *Journal of Natural History*, **44**, 2255–2286. doi: 10.1080/00222933.2010.503941.

Baum DA & Shaw KL (1995) Genealogical perspectives on the species problem. In: *Experimental and Molecular Approaches to Plant Biosystematics* (eds Hoch PC, Stephenson AG), pp. 289–303. Missouri Bontaical garden, St. Louis.

Beckers P (2011) Nemertean nervous system: a comparative analysis. Rheinische Friedrich-Wilhelms-Universität Bonn.

Beckers P & von Döhren J (2016) Nemertea (Nemertini). In: *Structure and Evolution of Invertebrate Nervous Systems* (eds Schmidt-Rhaesa A, Harzsch S & Purschke G), pp. 148–165. Oxford University Press, Oxford.

Beckers P, Faller S & Loesel R (2011) Lophotrochozoan neuroanatomy: An analysis of the brain and nervous system of *Lineus viridis* (Nemertea) using different staining techniques. *Frontiers in zoology*, **8**, 17. doi: 10.1080/00222933.2010.503941.

Beckers P, Loesel R & Bartolomaeus T (2013) The Nervous Systems of Basally Branching Nemertea (Palaeonemertea). *PLoS ONE*, **8**, e66137. doi: 10.1371/journal.pone.0066137.

Bergendal D (1903) Till kännedomen om de nordiska Nemertinerna. 4. Förteckning öfver vid Sveriges vestkust iakttagna Nemertiner. *Arkiv för Zoologi*, **1**, 85–156.

Blainville (1828) Dictionnaire des sciences naturelles, dans lequel on traite mé thodiquement des différens être de la nature, considérés soit en eux-mêmes, d'aprè s l'é tat actuel de nos connoissances, soit relativement a l'utilité qu'en peuvent retirer la mé decine, l'ag. In: *Suivi d'une biographie des plus célèbres naturalistes* (ed Levrault FG), pp. 365–625. Paris.

Blake JA (1993) Phylum Nemertea. In: *Taxonomic Atlas of the Benthic Fauna of the Santa Maria Basin and Western Santa Barbara Channel Vol 1 Introduction, Benthic Ecology, Oceanology, Platyhelminthes, and Nemertea* (eds Blake JA & Lissner A), pp. 95–132. Santa Barbara Museum of Natural History, Santa Barbara

Bleidorn C, Kruse I, Albrecht S & Bartolomaeus T (2006) Mitochondrial sequence data expose the putative cosmopolitan polychaete *Scoloplos armiger* (Annelida, Orbiniidae) as a species complex. *BMC evolutionary biology*, **6**, 47. doi: 10.1186/1471-2148-6-47.

Bleidorn C, Podsiadlowski L, Zhong M, Eeckhaut I, Hartmann S, Halanych KM & Tiedemann R (2009) On the phylogenetic position of Myzostomida: Can 77 genes get it wrong? *BMC Evolutionary Biology*, **9**, 150. doi: 10.1186/1471-2148-9-150.

Brusca GJ & Brusca RC (1978) A naturalist's seashore guide: common marine life of the northern California coast and adjacent shores. Mad River Press Inc, Eureka, California, 205 pp.

Bucklin A, Steinke D & Blanco-Bercial L (2011) DNA barcoding of marine metazoa. *Annual review of marine science*, **3**, 471–508. doi: 10.1146/annurev-marine-120308-080950.

Bürger O (1888) Beiträge zur Kenntnis des Nervensystems der Nemertinen. *Nachrichten von der Königl. Gesellschaft der Wissenschaften und der Georg-Augusts-Universität zu Göttingen*, **1888**, 479–482.

Bürger O (1890) Untersuchungen über die Anatomie und Histologie der Nemertinen nebst Beiträgen zur Systematik. *Zeitschrift für Wissenschaftliche Zoologie*, **50**, 1–277.

Bürger O (1892) Zur Systematik der Nemertinenfauna des Golfs von Neapel. *Nachrichten von der Königlichen Gesellschaft der Wissenschaften und der Georg-Augusts-Universität zu Göttingen*, **5**, 137–178.

Bürger, O. (1895) Fauna und Flora des Golfes von Neapel und der angrenzenden Meeresabschnitte. R. Friedländer und Sohn, Berlin, pp. 743.

Bürger O (1904) Nemertini. In: (ed Schultze, FE) *Das Tierreich*, pp. 1–151. R. Friedlander und Sohn, Berlin..

Bürger O (1897-1907) Nemertini (Schnuwürmer). In: *H. G. Bronns's Klassen und Ordnungen des Tierreichs*, pp. 1–542. C.F. Winter'sche Verlagshandlung, Leipzig.

Cantell CE (1975) Anatomy, taxonomy, and biology of some Scandinavian heteronemertines of the genera *Lineus*, *Micrura*, and *Cerebratulus*. *Sarsia*, **58**, 89–122.

Caplins SA, Turbeville JM & Street WC (2011) The Occurrence of *Ramphogordius sanguineus* (Nemertea , Heteronemertea) in the Intertidal Zone of the Atlantic Coast of Virginia and New Observations on its Feeding Behavior. **38**, 65–70.

Carmona L, Lei BR, Pola M, Gosliner TM, Valdés Á & Cervera JL (2014) Untangling the *Spurilla neapolitana (*Delle Chiaje, 1841) species complex: A review of the genus *Spurilla* Bergh, 1864 (Mollusca: Nudibranchia: Aeolidiidae). *Zoological Journal of the Linnean Society*, **170**, 132–154. doi: 10.1111/zoj.12098.

Castresana J (2000) Selection of Conserved Blocks from Multiple Alignments for Their Use in Phylogenetic Analysis. *Molecular Biology and Evolution*, **17**, 540–552. doi: 10.1093/oxfordjournals.molbev.a026334.

Chen H, Strand M, Norenburg JL, Sun S, Kajihara H, Chernyshev AV, Maslakova SA & Sundberg P (2010) Statistical parsimony networks and species assemblages in Cephalotrichid nemerteans (Nemertea). *PloS One*, **5**, e12885. doi. 371/journal.pone.0012885.

Chernyshev AV (2002a) Description of a new species of the genus *Poseidonemertes* (Nemertea, Monostilifera) with establishment of the family Poseidonemertidae. *Zoologicheskiy Zhurnal*, **81**, 909–916.

Chernyshev AV (2002b) A New Nemertean, *Callinera zhirmunskyi* sp . n ., from the Pacific Coast of Canada with a Special Reference to Callineridae Taxonomy. *Russian*, **28**, 132–135.

Chernyshev A V (2003a) Classification System of the Higher Taxa of Enoplan Nemerteans (Nemertea, Enopla). *Invertebrate Zoology*, **29**, S57–S65.

Chernyshev AV (2003b) A new species of *Tetrastemma* from the Sea of Japan and redescription of *Tetrastemma laminariae* Uschakov, 1928 (Nemertea: Tetrastemmidae). *Zoological Institute St. Petersburg*, **12**, 19–22.

Chernyshev AV (2003c) New species of the genus *Hubrechtella* (Nemertea, Anopla) from the Sea of Japan and validation of the family Hubrechtellidae. *Russian Journal of Marine Biology*, **29**, 333–336.

Chernyshev AV (2004) Problems of taxonomy of the "*Lineus ruber*" heteronemertean complex (Nemertea, Anopla). *Zoologicheskiy Zhurnal*, **83**, 788–794.

Chernyshev AV (2005) System of Families of enoplan Nemerteans of the Order Eumonostilifera (Nemertea:Enopla). *Russian Journal of Marine Biology*, **31**, S27–S33.

Chernyshev AV (2013) Two new species of deep-sea nemerteans from the SoJaBio expedition in the Sea of Japan. *Deep-Sea Research II*, **86–87**, 148–155. doi: 10.1016/j.dsr2.2012.07.041.

Chernyshev AV, Abukawa S & Kajihara H (2015) *Sonnenemertes cantelli* gen. et sp. nov. (Heteronemertea)—A new Oxypolella-like nemertean from the abyssal plain adjacent to the Kuril–Kamchatka Trench. *Deep Sea Research II*, **111**, 119–127. doi: 10.1016/j.dsr2.2014.07.014.

Clement M, Posada D & Crandall KA (2000) TCS: a computer program to estimate gene genealogies. *Molecular ecology*, **9**, 1657–1659. doi: 10.1016/j.ijgo.2006.12.004.

Coe WR (1901) Papers from the Harriman Alaska Expedition XX. The Nemerteans. *Proceedings of the Washington Academy of Sciences*, **3**, 1–110.

Coe WR (1904) Nemerteans. In: *Harriman Alaska Series Volume XI* (ed Merriam CH), pp.111–220. Doubleday, Page & Company, New York.

Coe, W.R. (1905) Nemerteans of the West and Northwest coasts of America. *Bulletin of the Museum of comaparative Zoology at Harvard College*, **47**, 1–318.

Coe, W.R. (1940) Revision of the nemertean fauna of the Pacific coasts of North, Central, and northern South America. *Allan Hancock Pacific Expeditions*, **2**, 247–323.

Coe WR (1943) Biology of the nemerteans of the Atlantic coast of North America. *Transactions of the Connecticut Academy of Arts and Sciences*, **35**, 129–328.

Coe WR (1944) A new species of hoplonemertean (*Paranemertes biocellatus*) from the Gulf of Mexico. *Journal of the Washington Academy of Sciences*, **34**, 407–409.

Corrêa DD (1964) Nemerteans from California and Oregon. *Proceedings of the California Academy of Sciences*, **31**, 515–558.

Cracraft J (1983) Species Concepts and Speciation Analysis. In: *Current Ornithology* (ed Johnston RF), pp. 159–187. Springer US, Boston, MA.

Darwin C (1859) On the Origin of Species by Means of Natural Selection. D. Appleton and company, New York.

Dayrat B (2005) Towards integrative taxonomy. *Biological Journal of the Linnean Society*, **85**, 407–415. doi: 10.1111/j.1095-8312.2005.00503.x.

Delle Chiaje S (1829) *Memorie sulla storia e notomia degli animali senza vertebre del regno di Napoli*. Societa Tipografia, Napoli.

Diesing KM (1862) Revision der Turbellarien. Abtheilung: Dendrocoelen. K.K. Hof-uund Staatsdruckerei,Wien.

von Döhren J (2011) The fate of the larval epidermis in the Desor-larva of *Lineus viridis* (Pilidiophora, Nemertea) displays a historically constrained functional shift from planktotrophy to lecithotrophy. *Zoomorphology*, **130**, 189–196. doi: 10.1007/s00435-011-0131-2.

von Döhren J (2015) Nemertea. In: *Evolutionary Developmental Biology of Invertebrates 2* (ed Wanninger A), pp. 155–192. Springer, Wien.

von Döhren J & Bartolomaeus T (2006) Ultrastructure of sperm and male reproductive system in *Lineus viridis* (Heteronemertea, Nemertea). *Zoomorphology*, **125**, 175–185. doi: 10.1007/s00435-006-0024-y.

von Döhren J & Bartolomaeus T (2007) Ultrastructure and development of the rhabdomeric eyes in *Lineus viridis* (Heteronemertea, Nemertea). *Zoology*, **110**, 430–438. doi: 10.1016/j.zool.2007.07.006.

von Döhren J, Beckers P & Bartolomaeus T (2010) Comparative Sperm Ultrastructure in Nemertea. *Journal of Morphology*, **271**, 793–813. doi: 10.1002/jmor.10834.

von Döhren J, Beckers P & Bartolomaeus T (2012) Life history of *Lineus viridis* (Müller, 1774) (Heteronemertea, Nemertea). *Helgoland Marine Research*, **66**, 243–252. doi: 10.1007/s10152-011-0266-z.

Donoghue MJ (1985) A critique of the biological species concept and recommendations for a phylogenetic alternative. *Bryologist*, 172–181.

Dunn CW, Giribet G, Edgecombe GD & Hejnol A (2014) Animal Phylogeny and Its Evolutionary Implications. *The Annual Review of Ecology, Evolution, and Systematics*, **45**, 371–395.

Edgecombe GD, Giribet G, Dunn CW, Hejnol A, Kristensen RM, Neves RC, Rouse GW, Worsaae K & Sørensen MV (2011) Higher-level metazoan relationships: Recent progress and remaining questions. *Organisms Diversity and Evolution*, **11**, 151–172. doi:10.1007/s13127-011-0044-4.

Faasse MA & Turbeville JM (2015) The first record of the north-west Pacific nemertean *Cephalothrix simula* in northern Europe. *Marine Biodiversity Records*, **8**, e17. doi: 10.1017/S1755267214001523.

Fernández-Álvarez FÁ & Machordom A (2013) DNA barcoding reveals a cryptic nemertean invasion in Atlantic and Mediterranean waters. *Helgoland Marine Research*, **67**, 599–605. doi: 10.1007/s10152-013-0346-3.

Folmer O, Black M, Hoeh W, Lutz R & Vrijenhoek R (1994) DNA primers for amplification of mitochondrial cytochrome c oxidase subunit I from diverse metazoan invertebrates. *Molecular marine biology and biotechnology*, **3**, 294–9.

Fontaneto D, Flot JF & Tang CQ (2015) Guidelines for DNA taxonomy, with a focus on the meiofauna. *Marine Biodiversity*, **45**, 433–451. doi: 10.1007/s12526-015-0319-7.

Friedrich H (1935) Studien zur Morphologie, Systematik und Ökologie der Nemertinen der Kieler Bucht. Archiv für Naturgeschichte, **4**, 293-371.

Friedrich H (1936) Nemertini. In: *Tierwelt Nord-und Ostsee* (eds Grimpe G & Wagler E), pp. 1–68. Leipzig.

Friedrich H (1958) Nemertini. *The Zoology of Iceland*, **2**, 1–24.

Friedrich H (1979) Nemertini. In: *Morphogenese der Tiere* (ed Seidel F), pp. 1–136. Gustav Fischer, Jena.

Frutos I, Montalvo S & Junoy J (1998) A new species of *Prosorhochmus* (Hoplonemertea, Monostilifera) from the Chafarinas Islands (western Mediterranean). *Journal of Zoology*, **245**, 293–298.

Fujisawa T & Barraclough TG (2013) Delimiting species using single-locus data and the generalized mixed yule coalescent approach: A revised method and evaluation on simulated data sets. *Systematic Biology*, **62**, 707–724. doi: 10.1093/sysbio/syt033.

Funk DJ & Omland KE (2011) Species-Level Paraphyly and Polyphyly:Frequency, Causes, and Consequences, with Insights from Animal Mitochondrial DNA. *Annual Review of Ecology, Evolution, and Systematics*, **34**, 397–423. doi: 10.1146//annurev.ecolsys.34.011802.132.

Gibson R (1967) Occurrence of the entocommensal rhynchocoelan, *Malacobdella grossa*, in the oval piddock, *Zirfaea crispata*, on the Yorkshire coast. *Journal of the Marine Biological Association of the United Kingdom*, **47**, 301–317.

Gibson R (1972) Nemerteans. Hutchinson & CO Ltd, London.

Gibson R (1982) British nemerteans. Cambridge University Press, Cambridge.

Gibson R (1985) The need for a standard approach to taxonomic descriptions of nemerteans. *Integrative and Comparative Biology*, **25**, 5–14.

Gibson R (1995) Nemertean genera and species of the world: an annotated checklist of original names and description citations, synonyms, current taxonomic status, habitats and recorded zoogeographic distribution. *Journal of Natural History*, **29**, 271–561.

Gibson, R. (2005). *Lineus gesserensis* (O.F. Müller, 1774). In: Norenburg, J.; Gibson, R. (2016). World Nemertea database. Accessed through: World Register of Marine Species at http://www.marinespecies.org/aphia.php?p=taxdetails&id=177633 on 2016-11-01

Gibson R & Jennings JB (1969) Observations on the diet, feeding mechanisms, digestion and food reserves of the entocommensal rhynchocoelan Malacobdella grossa. *Journal of the Marine Biological Association of the United Kingdom*, **49**, 17–32.

Giribet G (2015) Morphology should not be forgotten in the era of genomics-a phylogenetic perspective. *Zoologischer Anzeiger*, **256**, 96–103. doi: 10.1016/j.jcz.2015.01.003.

Gontcharoff M (1951) Biologie de la régéneration et de la reproduction chez Quelques Lineidae de France. *Annales des Scienes Naturelles*, **11**, 149–235.

Gontcharoff M (1955) Nemertes-Tuniciers, Inventaire de la faune marine de Roscoff. *suppl aux Travaux de la Station Biologique de Roscoff*, **7**, 1–15.

Gontcharoff M (1959) Rearing of certain nemerteans (Genus *Lineus). Annals New York Academy of Sciences*, **77**, 93–95.

Gontcharoff M (1960) Le développement post-embryonnaire et la croissance chez *Lineus ruber* et *Lineus viridis* (Némertes Lineidae). *Annales des Scienes Naturelles*, **2**, 225–279.

González VL & Giribet G (2015) A multilocus phylogeny of archiheterodont bivalves (Mollusca, Bivalvia, Archiheterodonta). *Zoologica Scripta*, **44**, 41–58. doi: 10.1111/zsc.12086.

Griffin BB (1898) Description of some marine nemerteans of Pudget Sound and Alaska. *Annals New York Academy of Sciences*, **10**, 193–217.

Hailer F, Kutschera VE, Hallström BM, Klassert D, Fain SR, Leonard JA, Arnason U & Janke A (2012) Nuclear genomic sequences reveal that polar bears are an old and distinct bear lineage. *Science*, **336**, 344–347. doi: 10.1126/science.1216424.

Hall TA (1999) BioEdit: a user-friendly biological sequence alignment editor and analysis program for Windows 95/98/NT. *Nucleic Acids Symposium*, **41**, 95–98.

Hallas JM & Gosliner TM (2015) Family matters: The first molecular phylogeny of the Onchidorididae Gray, 1827 (Mollusca, Gastropoda, Nudibranchia). *Molecular Phylogenetics and Evolution*, **88**, 16–27. doi: 10.1016/j.ympev.2015.03.015.

Hao Y, Kajihara H, Chernyshev AV, Okazaki RK & Sun SC (2015) DNA Taxonomy of *Paranemertes* (Nemertea:Hoplonemertea) with Spirally Fluted Stylets. *Zoological science*, **32**, 571–578.

Hart MW & Sunday J (2007) Things fall apart: biological species form unconnected parsimony networks. *Biology letters*, **3**, 509–512. doi: 10.1098/rsbl.2007.0307.

Haszprunar G (1996) The Mollusca: Coelomate turbellarians or mesenchymate annelids? In: *The Mollusca: Coelomate turbellarians or mesenchymate annelids?* (ed Taylor J), pp. 1–28. Oxford University Press, London.

Hebert PDN, Ratnasingham S & deWaard JR (2003) Barcoding animal life: cytochrome c oxidase subunit 1 divergences among closely related species. *Proceeding of the Royal Society B* , **270,** S96–S99.

Hebert PDN, Stoeckle MY, Zemlak TS & Francis CM (2004) Identification of Birds through DNA Barcodes. *PLoS biology*, **2**, 1657–1663. doi: 10.1371/journal.pbio.0020312

Hejnol A, Obst M, Stamatakis A, Ott M, Rouse GW, Edgecomve GD, Martinez P, Baguña J, Bailly X, Jondelius U, Wiens M, Müller WEG, Seaver E, Wheeler WC, Martindale MQ, Giribet G & Dunn CW (2009) Assessing the root of bilaterian animals with scalable phylogenomic methods. *Proceedings of the Royal Society B*, **276**, 4261–4270. doi: 10.1098/rspb.2009.0896.

Herrera-Bachiller A (2016) Los Nemertinos de Espana Y Portugal. Universidad de Alcalá.

Hiebert TC (2015) *Tubulanus polymorphus* an orange ribbon worm. In: *Rudys'Illustrated Guide to Common Spcedies* (eds Hiebert TC, Butler BA & Shanks AL), pp. 1–3. Charleston, Oregon.

Hiebert TC & Maslakova SA (2015) Integrative Taxonomy of the *Micrura alaskensis* Coe, 1901 Species Complex (Nemertea: Heteronemertea), with Descriptions of a New Genus *Maculaura* gen. nov. and Four New Species from the NE Pacific. *Zoological Science*, **32**, 615–637. doi: 10.2108/zs150011.

Hochberg FG & Lunianski DN (1998) Nemertean collections at the Santa Barbara Museum of Natural History: type specimens and vouchers for Wesley R. Coe's 1940 publication. *Hydrobiologia*, **365**, 291–300.

Hubrecht AAW (1886) Contributions to the embryology of the Nemertea. *Quarterly Journal of Microscopical Science*, **26**, 417–448.

Hylbom R (1957) Studies on palaeonemerteans of the Gullmar Fjord area (west coast of Sweden). *Arkiv för Zoologi*, **10**, 539–582.

Jörger KM, Norenburg JL, Wilson NG & Schrödl M (2012) Barcoding against a paradox? Combined molecular species delineations reveal multiple cryptic lineages in elusive meiofaunal sea slugs. *BMC evolutionary biology*, **12**, 245. doi: 10.1186/1471-2148-12-245.

Jörger KM & Schrödl M (2013) How to describe a cryptic species? Practical challenges of molecular taxonomy. *Frontiers in Zoology*, **10**, 59. doi: 10.1186/1742-9994-10-59.

Joubin L (1890) Recherches sur les Tubellarié des côtes de France (Némertes). *Archives de zoologie expérimentale et générale, Série 2*, **5**, 61–90.

Junoy J & Gibson R (1991) A New Species of *Procephalothrix* (Anopla, Archinemertea) from North-Western Spain (Nemertea). *Zoologischer Anzeiger*, **226**, 185–194.

Kajihara H, Chernyshev AV, Sun SC, Sundberg P & Crandall FB (2008) Checklist of Nemertean Genera and Species Published between 1995 and 2007. *Species Diversity*, **13**, 245–274.

Kajihara H, Gibson R & Mawatari SF (2001) A new genus and species of monostiliferous hoplonemertean (Nemertea : Enopla : Monostilifera) from Japan. *Hydrobiologia*, **456**, 187–198.

Kajihara H, Gibson R & Mawatari SF (2003) *Potamostoma shizunaiense* gen. et sp. nov. (Nemertea: Hoplonemertea: Monostilifera): a new brackish-water nemertean from Japan. *Zoological science*, **20**, 491–500. doi: 10.2108/zsj.20.491.

Kajihara H, Kakui K, Yamasaki H & Hiruta SF (2015) *Tubulanus tamias* sp. nov. (Nemertea: Palaeonemertea) with Two Different Types of Epidermal Eyes. *Zoological science*, **32**, 596–604.

Kajihara H, Olympia M, Kobayashi N, Katoh T, Chen HX, Strand M & Sundberg P (2011) Systematics and phylogeny of the hoplonemertean genus *Diplomma* (Nemertea) based on molecular and morphological evidence. *Zoological Journal of the Linnean Society*, **161**, 695–722. 10.1111/j.1096-3642.2010.00650.x.

Kang XX, Fernández-Álverez FA, Alfaya JEF, Machordom A, Strand M, Sundberg P & Sun SC (2015) Species Diversity of *Ramphogordius sanguineus/Lineus ruber*-like Nemerteans (Nemertea: Heteronemertea) and Geographic Distribution of *R. sanguineus*. *Zoological science*, **32**, 579–589.

Katoh K &Standley DM (2013) MAFFT multiple sequence alignment software version 7: improvements in performance and usability. *Molecular Biology and Evolution*, **30**, 772–80. doi: 10.1093/molbev/mst010.

Kienberger K, Carmona L, Pola M, Padula V, Gosliner TM & Cervera JL (2016) *Aeolidia papillosa* (Linnaeus, 1761) (Mollusca: Heterobranchia: Nudibranchia), single species or a cryptic species complex? A morphological and molecular study. *Zoological Journal of the Linnean Society*, **177**, 481–506. doi: 10.1111/zoj.12379.

Kirsteuer E (1974) Description of *Poseidonernertes caribensis* sp.n., and discussion of other taxa of Hoplonemertini Monostilifera with divided longitudinal musculature in the body wall. *Zoologica Scripta*, **3**, 153–166.

Krämer D & von Döhren J (2015) *Arenogigas armoricus* , a New Genus and Species of a Monostiliferous Hoplonemertean (Nemertea) from the North-West Coast of France. *Zoological Science*, **32**, 605–614. doi: 10.2108/zs140266.

Krämer D, Schmidt C, Podsiadlowski L, Beckers P, Horn L & von Döhren J (2016) Unravelling the *Lineus ruber/viridis* species complex (Nemertea, Heteronemertea). *Zoologica Scripta*, 1–16. doi: 10.1111/zsc.12185.

Kremer JR, Mastronarde DN & McIntosh JR (1996) Computer visualization of three-dimensional image data using IMOD. *Journal of structural biology*, **116**, 71–76.

Kvist S (2013) Molecular Phylogenetics and Evolution Barcoding in the dark ?: A critical view of the sufficiency of zoological DNA barcoding databases and a plea for broader integration of taxonomic knowledge. *Molecular phylogenetics and evolution*, **69**, 39–45. doi: 10.1016/j.ympev.2013.05.012.

Kvist S, Chernyshev AV & Giribet G (2015) Phylogeny of Nemertea with special interest in the placement of diversity from Far East Russia and northeast Asia. *Hydrobiologia*, **760**, 105–119. doi: 10.1007/s10750-015-2310-5.

Kvist S, Laumer CE, Junoy J & Giribet G (2014) New insights into the phylogeny, systematics and DNA barcoding of Nemertea. *Invertebrate Systematics*, **28**, 287–309. doi: 10.1071/IS13061.

Kvist S, Oceguera-Figueroa A, Siddall ME & Erséus C (2010) Barcoding, types and the Hirudo files: using information content to critically evaluate the identity of DNA barcodes. *Mitochondrial DNA*, **21**, 198–205.

Laumer CE, Bekkouche N, Kerbl A, Goetz F, Neves RC, Sørensen MV, Kristensen RM, Hejnol A, Dunn CW, Giribet G & Worsaae K (2015) Spiralian Phylogeny Informs the Evolution of Microscopic Lineages. *Current Biology*, **25**, 2000–2006. doi: 10.1016/j.cub.2015.06.068.

Leasi F & Norenburg JL (2014) The necessity of DNA taxonomy to reveal cryptic diversity and spatial distribution of meiofauna, with a focus on nemertea. *PLoS ONE*, **9**, e104385. doi: 10.1371/journal.pone.0104385

Linnaeus C (1753) Species plantarum. Laurentii Salvii, Stockhom.

Linnaeus C (1758) Systema naturae. Laurentii Salvii, Stockholm.

Luo A, Lan H, Ling C, Zhang A, Shi L, Ho SYW & Zhu C (2015) A simulation study of sample size for DNA barcoding. *Ecology and Evolution*, **5**, 5869–5879. doi: 10.1002/ece3.1846.

Martín-Durán JM, Vellutini BC & Hejnol A (2015) Evolution and development of the adelphophagic, intracapsular Schmidt's larva of the nemertean Lineus ruber. *EvoDevo*, **6**, 28. doi: 10.1186/s13227-015-0023-5.

Martínez J, Adarraga I & Ruiz JM (2007) Tipificación de poblaciones bentónicas de los fondos blandos de la plataforma continental de Guipúzcoa (sureste del golfo de Vizcaya). *Boletín Instituto Español de Oceanografía*, **23**, 85–110.

Martinsson S (2016) Exploring the species boundaries in terrestrial clitellates (Annelida: Clitellata). Göteborgs Universitet.

Maslakova SA & Norenburg JL (2001) Phylogenetic study of pelagic nemerteans (Pelagica, Polystilifera). *Hydrobiologia*, **456**, 111–132. doi: 10.1023/A:1013048419113.

Maslakova SA & Norenburg JL (2008) Revision of the smiling worms, genus *Prosorhochmus* Keferstein, 1862, and description of a new species, *Prosorhochmus belizeanus* sp. nov. (Prosorhochmidae, Hoplonemertea, Nemertea) from Florida and Belize. *Journal of Natural History*, **42**, 1219–1260. 10.1080/00222930801995747.

Maslakova SA, Thiel M, Vásquez N & Norenburg JL (2005) The smile of *Amphiporus nelsoni* Sanchez, 1973 (Nemertea : Hoplonemertea : Monostilifera : Amphiporidae) leads to a redescription and a change in family. *Proceedings of the Biological Society of Washington*, **118**, 483–498.

Mayden RL (1997) A hierarchy of species concepts: the denouement in the saga of the species problem. In *Species: The units of biodiversity* (eds Claridge MF, Dawah HA & Wilson MR), pp. 381–423. Chapman & Hall, London.

Mayr E (1942) Systematics and the Origin of Species from the Viewpoint of a Zoologist. Columbia University Press, New York.

Mayr E (1943) Criteria of subspecies, species and genera in ornithology. *Annals of the New York Academy of Sciences*, **44**, 133–139.

Mayr E (1969) Principles of Systematic Zoology. McGraw-Hill, Inc, New York.

McDermott JJ (2001) Status of the Nemertea as prey in marine ecosystems. *Hydrobiologia*, **456**, 7–20.

McDermott JJ, Roe P (1985) Food , Feeding Behavior and Feeding Ecology of Nemerteans. *American Zoologist*, **25**, 113–125.

Meier R & Willmann R (2000) The Hennigian Species Concept. In: *Species Concepts and Phylogenetic Theory: A debate* (eds Wheeler & Meier R), pp. 30–43. Columbia University Press, New York.

Melo-Ferreira J, Boursot P, Suchentrunk F, Ferrand N & Alves PC (2005) Invasion from the cold past: Extensive introgression of mountain hare (*Lepus timidus*) mitochondrial DNA into three other hare species in northern Iberia. *Molecular Ecology*, **14**, 2459–2464. doi: 10.1111/j.1365-294X.2005.02599.x.

Melville RV (1986) *Tubulanus* Renier, [1804] and *T. polymorphus* Renier [1804] (Polychaeta): Proposed reinstatement under the plenary powers. Z.N.(S.) 1094. *The Bulletin of zoological nomenclature* ., **43**, 112–114.

Menéndez M & Woodworth PL (2010) Changes in extreme high water levels based on a quasi-global tide-gauge data set. *Journal of Geophysical Research*, **115**, 1–15. doi: 10.1029/2009JC005997.

Meyer CP & Paulay G (2005) DNA barcoding: Error Rates Based on Comprehensive Sampling. *PLoS biology*, **3**, 2229–2239. doi: 10.1371/journal.pbio.0030422.

Mishler BD (1985) The morphological, developmental, and phylogenetic basis of species concepts in bryophytes. *Bryologist*, 207–214.

Müller OF (1774) Vermivm terrestrium et fluviatilium, seu animalium infusoriorum, helminthicorum et testaceorum, non marinorum, succincta historia. Vol. 1, Part 2. Copenhagen, Leipzig: Heineck and Faber.

Mulligan KL, Hiebert TC, Jeffery NW & Gregory TR (2014) First estimates of genome size in ribbon worms (phylum Nemertea) using flow cytometry and Feulgen image analysis densitometry. *NRC Research Press*, **851**, 847–851. doi:10.1139/cjz-2014-0068.

Nei M & Kumar S (2000) Molecular evolution and phylogenetics. Oxford University Press, London.

Nelson G & Platnick NI (1981) Systematics and biogeography. Columbia University Press, New York.

Nesnidal MP, Helmkampf M, Meyer A, Witek A, Bruchhaus I, Ebersberger I, Hankeln H, Lieb B, Struck TH & Hausdorf B (2013) New phylogenomic data support the monophyly of Lophophorata and an Ectoproct-Phoronid clade and indicate that Polyzoa and Kryptrochozoa are caused by systematic bias. *BMC evolutionary biology*, **13**, 253. doi: 10.1186/1471-2148-13-253.

Nixon KC & Wheeler QD (1990) An amplification of the phylogenetic species concept. *Cladistics*, **6**, 211–223.

Norenburg JL (1985) Structure of the Nemertine Integument with Consideration of Its Ecological and Phylogenetic Significance. *American Zoologist*, **51**, 37–51.

Norenburg JL (1993) *Riserius pugetensis* gen. n., sp. n. (Nemertina: Anopla), a new mesopsammic species, and comments on phylogenetics of some anoplan characters. *Hydrobiologia*, **266**, 203–218.

Nusbaum J & Oxner M (1913) Die Diovogonie oder die Entwicklung eines Embryo aus zwei Eiern bei der Nemertine *Lineus ruber* Müll . *Archiv für Entwicklungsmechanik der Organismen*, **36**, 342–352.

Nylander JAA (2004) MrModeltest v2, Program distributed by the author.

Örsted AS (1844) Entwurf einer systematischen Entheilung und speciellen Beschreibung der Plattwürmer auf microscopschen Untersuchungen. Verlag von C. A. Reitzel, Universitäts-Buchhändler, Copenhagen.

Padial JM, Miralles A, De la Riva I & Vences M (2010) The integrative future of taxonomy. *Frontiers in Zoology*, **7**, 16. doi: 10.1186/1742-9994-7-16.

Palumbi SR (1996) Nucleic acids II: the polymerase chain reaction. In: *Molecular systematics* (eds Hillis DM, Moritz DMC, Mable BK), pp. 205–247. Sinauer Associates, Inc., Sunderland, Massachusetts.

Pedersen KJ (1968) Some morphological and histochemical aspects of nemertean connective tissue. *Zeitschrift für Zellforschung*, **90**, 570–595. doi: 10.1007/BF00339505.

Podsiadlowski L, Braband A, Struck TH, von Döhren J & Bartolomaeus T (2009) Phylogeny and mitochondrial gene order variation in Lophotrochozoa in the light of new mitogenomic data from Nemertea. *BMC genomics*, **10**, 364. doi: 10.1186/1471-2164-10-364.

Pons J, Barraclough TG, Gomez-Zurita J, Cardose A, Duran DP, Hazell S, Kamoun S, Sumlin W & Vogler AP (2006) Sequence-Based Species Delimitation for the DNA Taxonomy of Undescribed Insects. *Systematic Biology*, **55**, 595–609. doi: 10.1080/10635150600852011.

Puillandre N, Lambert A, Brouillet S & Achaz G (2012) ABGD, Automatic Barcode Gap Discovery for primary species delimitation. *Molecular Ecology*, **21**, 1864–1877. doi: 10.1111/j.1365-294X.2011.05239.x.

Punnett RC (1903) On the Nemerteans of Norway. *Bergens museums årbog*, **2**, 1–35.

Quatrefages A (1846) Études sur les types inférieurs de l'embranchement des annelés. Mémoire sur la famille des Némertiens (Nemertea). *Annales des Scienes Naturelles Zoologie, Sèrie 3*, **6**, 173–303.

De Queiroz K (2005) Ernst Mayr and the modern concept of species. *Proceedings of the National Academy of Sciences of the United States of America*, **102**, 6600–6607. 10.1073/pnas.0502030102.

De Queiroz K (2007) Species concepts and species delimitation. *Systematic Biology*, **56**, 879–886. doi: 10.1080/10635150701701083.

Riches TH (1893) A list of the nemertines of Plymouth Sound. *Journal of the Marine Biological Association of the United Kingdom (New Series)*, **3**, 1–29.

Ricketts E, Calvin J (1948) *Between Pacific tides*. Stanford University press, Standford.

Ritger R &Norenburg JL (2006) *Tubulanus riceae* new species (Nemertea: Anopla: Palaeonemertea: Tubulanidae), from South Florida, Belize and Panama. *Journal of Natural History*, **40**, 931–942. doi: 10.1080/00222930600833867.

Rogers AD, Junoy J, Gibson R & Thorpe JP (1993) Enzyme electrophoresis, genetic identity and description of a new genus and species of heteronemertean (Nemertea, Anopla) from northwestern Spain and North Wales. *Hydrobiologia*, **266**, 219–238.

Rogers AD, Thorpe JP & Gibson R (1995) Genetic evidence for the occurrence of a cryptic species with the littoral nemerteans *Lineus ruber* and *L. viridis* (Nemertea : Anopla). *Marine Biology*, **122**, 305–316.

Rosen DE (1979) Fishes from the uplands and intermontane basins of Guatemala: revisionary studies and comparative geography. *Bulletin of the American Museum of Natural History*, **162**, 267-376.

Ross HA, Murugan S & Li WLS (2008) Testing the reliability of genetic methods of species identification via simulation. *Systematic biology*, **57**, 216–230. doi: 10.1080/10635150802032990.

Rubinoff D, Cameron S & Will K (2006) A genomic perspective on the shortcomings of mitochondrial DNA for "barcoding" identification. *Journal of Heredity*, **97**, 581–594. doi: 10.1093/jhered/esl036.

Sanger F, Nicklen S & Coulson AR (1977) DNA sequencing with chain-terminating inhibitors. *Proceedings of the National Academy of Sciences of the United States of America*, **74**, 5463–5467.

Schander C & Willassen E (2005) What can biological barcoding do for marine biology? *Marine Biology Research*, **1**, 79–83. doi: 10.1080/17451000510018962.

Schmidt GA (1946) Genetic and ecological relations of littoral nemerteans of the genus *Lineus*. *Proceedings of the USSR Academy of Sciences*, **51**, 405–407.

Schmidt GA (1964) Embryonic development of littoral nemertines *Lineus desori* and *Lineus ruber* (O.F. Mülleri, 1774, G. A. Schmidt, 1945) in connection with ecological relation changes of mature individuals when forming the new species Lineus ruber. *Zoologica Poloniae*, **14**, 75–122.

Schultze MS (1853) Zoologische Skizzen. *Zeitschrift für wissenschaftliche Zoologie*, **4**, 178–195.

Schwartz ML (2009) Untying a Gordian knot of worms : systematics and taxonomy of the Pilidiophora (phylum Nemertea) from multiple data sets. The George Washington University.

Schwartz ML & Norenburg JL (2001) Can we infer heteronemertean phylogeny from available morphological data? *Hydrobiologia*, **456**, 165–174.

Sheldon L (1901) Nemertines. In: *The Cambridge Natural History* (eds Harmer SF & Shipley AE), pp. 99–120. Macmillan and Co., Ltd, New York.

Simpson GG (1961) Principles of animal taxonomy. Columbia University Press, New York.

Southern R (1913) Nemertinea. *Proceedings of the Royal Irish Acamdey. Section B.*, **31**, 1–20.

Stamatakis A (2006) Phylogenetic models of rate heterogeneity: a high performance computing perspective. *Proceedings 20th IEEE International Parallel & Distributed Processing Symposium*, 1–8.

Stamatakis A (2014) RAxML version 8: a tool for phylogenetic analysis and post-analysis of large phylogenies. *Bioinformatics*, **30**, 1312–1313.

Stiasny-Wijnhoff G (1923) *On Brinkmann's system of the Nemertea Enopla and Siboganemertes weberi, n.g.n.sp*. Leiden.

Strand M, Herrera-Bachiller A, Nygren A & Kånneby T (2014) A new nemertean species: what are the useful characters for ribbon worm descriptions? *Journal of the Marine Biological Association of the United Kingdom*, **94**, 317–330. doi: 10.1017/S002531541300146X.

Strand M & Sundberg P (2005a) Delimiting species in the hoplonemertean genus *Tetrastemma* (phylum Nemertea): Morphology is not concordant with phylogeny as evidenced from mtDNA sequences. *Biological Journal of the Linnean Society*, **86**, 201–212. doi: 10.1111/j.1095-8312.2005.00535.x.

Strand M & Sundberg P (2005b) Genus *Tetrastemma* Ehrenberg, 1831 (Phylum Nemertea)- a natural group? Phylogenetic relationships inferred from partial 18S rRNA sequences. *Molecular phylogenetics and Evolution*, **37**, 144–52. doi: 10.1016/j.ympev.2005.02.006.

Strand M & Sundberg P (2011) A DNA-based description of a new nemertean (phylum Nemertea) species. *Marine Biology Research*, **7**, 63–70. doi: 10.1080/17451001003713563.

Stricker SA (1987) Phylum Nemertea. In: *Reproduction and development of marine invertebrates of the northern Pacific coast: data and methods for the study of eggs, embryos, and larvae* (ed Strathmann MF), pp. 129–137. University of Washington Press, Washington.

Stricker SA & Folsom MW (1998) A comparative ultrastructural analysis of spermatogenesis in nemertean worms. *Hydrobiologia*, **365**, 55–72.

Stricker SA, Smythe TL, Miller L & Norenburg JL (2001) Comparative biology of oogenesis in nemertean worms. *Acta Zoologica*, **82**, 213–230.

Struck TH & Fisse F (2008) Phylogenetic position of nemertea derived from phylogenomic data. *Molecular Biology and Evolution*, **25**, 728–736. doi: 10.1093/molbev/msn019.

Sun SC, Kajihara H & Chernyshev AV (2015) Special Issue: Proceedings of the 8th International Conference on nemertean Biology. *Zoological Science*, **32**, 499–500.

Sundberg P (1979) Statistical analysis of variation in characters in *Tetrastemma laminariae* (Nemertini), with a redescription of the species. *Journal of Zoology*, **189**, 39–56.

Sundberg P (1989a) Phylogeny and cladistic classification of terrestrial nemerteans: the genera *Pantinonemertes* Moore & Gibson and *Geonemertes* Semper. *Zoological journal of the Linnean Society*, **95**, 363–372.

Sundberg P (1989b) Phylogeny and cladistic classification of the paramonostiliferous family Plectonemertidae (phylum Nemertea). *Cladistics*, **5**, 87–100.

Sundberg P (2015) Thirty-five Years of Nemertean (Nemertea) Research - Past, Present, and Future. *Zoological Science*, **32**, 501–506.

Sundberg P, Andrade SCS, Bartolomaeus T, Beckers P,von Döhren J, Krämer D, Gibson R, Giribet G, Herrera-Bachiller A, Junoy J, Kajihara H, Kvist S, Kånneby T, Sun SC, Thiel M, Turbeville JM. & Strand M (2016) The future of nemertean taxonomy (phylum Nemertea) – a proposal. *Zoologica scripta*, **45**, 579-582. doi: 10.1111/zsc.12182.

Sundberg P, Chernyshev A V., Kajihara H, Kånneby T & Strand M (2009a) Character-matrix based descriptions of two new nemertean (Nemertea) species. *Zoological Journal of the Linnean Society*, **157**, 264–294. doi: 10.1111/j.1096-3642.2008.00514.x.

Sundberg P & Hylbom R (1994) Phylogeny of the Nemertean Sublass Palaeonemertea (Anopla, Nemertea). *Cladistics*, **10**, 347–402.

Sundberg P & Saur M (1998) Molecular phylogeny of some European heteronemertean (Nemertea) species and the monophyletic status of *Riseriellus*, *Lineus*, and *Micrura*. *Molecular phylogenetics and evolution*, **10**, 271–80.

Sundberg P & Strand M (2007) Genetics do not reflect habitat differences in Riseriellus occultus (Heteronemertea, Nemertea) from Spain and Wales. *Marine Biology Research*, **3**, 117–122. doi: 10.1080/17451000601182619.

Sundberg P & Strand M (2010) Nemertean taxonomy – time to change lane? *Journal of Zoological Systematics and Evolutionary Research*, **48**, 283–284. 10.1111/j.1439-0469.2010.00568.x.

Sundberg P & Svensson M (1994) Homoplasy, character function, and nemertean systematics. *Journal of Zoology*, **234**, 253–263.

Sundberg P, Thuroczy Vodoti E & Strand M (2010) DNA barcoding should accompany taxonomy - the case of Cerebratulus spp (Nemertea). *Molecular ecology resources*, **10**, 274–81. doi:10.1111/j.1755-0998.2009.02774.x.

Sundberg P, Turbeville JM & Lindh S (2001) Phylogenetic relationships among higher Nemertean (Nemertea) Taxa inferred from 18S rDNA sequences. *Molecular phylogenetics and evolution*, **20**, 327–334.

Sundberg P, Vodoti ET, Zhou H & Strand M (2009b) Polymorphism hides cryptic species in *Oerstedia dorsalis* (Nemertea, Hoplonemertea). *Biological Journal of the Linnean Society*, **98**, 556–567. doi: 10.1111/j.1095-8312.2009.01310.x.

Tamura K, Peterson D, Peterson N, Stecher G, Nei M & Kumar S (2011) MEGA5: Molecular Evolutionary Genetics Analysis Using Maximum Likelihood, Evolutionary Distance, and Maximum Parsimony Methods. *Molecular biology and evolution*, **28**, 2731–9. doi: 10.1093/molbev/msr121.

Tang CQ, Leasi F, Obertegger U Kieneke, A, Barraclough TG & Fontaneto D (2012) The widely used small subunit 18S rDNA molecule greatly underestimates true diversity in biodiversity surveys of the meiofauna. *Proceedings of the National Academy of Sciences*, **109**, 16208–16212. 10.1073/pnas.1209160109.

Tautz D, Arctander P, Minelli A, Thomas RH & Vogler AP (2003) A plea for DNA taxonomy. *Trends in Ecology and Evolution*, **18**, 70–74.doi: 10.1016/S0169-5347(02)00041-1.

Templeton AR, Crandall KA & Sing F (1992) Cladistic Analysis of Phenotypic Associations With Haplotypes Inferred From Restriction Endonuclease Mapping and DNA Sequence Data. III. Cladogram Estimation. *Genetics*, **132**, 619–633.

Thiel M (1998) Nemertines as predators on tidal flats – High Noon at low tide. *Hydrobiologia*, **365**, 241–250.

Thiel M & Kruse I (2001) Status of the Nemertea as prey in marine ecosystems. *Hydrobiolgia*, **456**, 21–32.

Thiel M & Reise K (1993) Interaction of nemertines and their prey on tidal flats. *Netherlands journal of sea research*, **31**, 163–172.

Thollesson M & Norenburg JL (2003) Ribbon worm relationships: a phylogeny of the phylum Nemertea. *Proceedings of the Royal Society/ Biological Sciences*, **270**, 407–415. doi: 10.1098/rspb.2002.2254.

Turbeville JM (1991) Nemertinea. In: *Microscopic Anatomy of Invertebrates Volume 3 Plathelminthes and Nemertinea* (eds Harrison FW & Bogitsh BJ), pp. 285–328. Wiley-Liss, New York.

Turbeville JM (2002) Progress in nemertean biology: development and phylogeny. *Integrative and comparative biology*, **42**, 692–703.

Turbeville JM (2007) 2 Enopla. In: *Spezielle Zoologie Teil 1: Einzeller und Wirbellose* (eds Westheide W & Rieger R), p. 297. Elsevier Spektrum Akademischer Verlag.

Turbeville JM, Field KG & Raff RA (1992) Phylogenetic position of phylum Nemertini, inferred from 18S rRNA sequences: molecular data as a test of morphological character homology. *Molecular biology and evolution*, **9**, 235–249.

Turbeville J & Ruppert E (1985) Comparitive ultrastructure and the evolution of Nemertines. *American Zoologist*, **71**, 53–71.

van Valen L (1976) Ecological species, multispecies, and oaks. *Taxon*, **25**, 233–239.

Vogler AP & Monaghan MT (2006) Recent advances in DNA taxonomy. *Journal of Zoological Systematics and Evolutionary Research*, **45**, 1–10. doi: 10.1111/j.1439-0469.2006.00384.x

Vogt L, Bartolomaeus T, Giribet G (2010) Cladistics and the standardization of morphological data. *Cladistics*, **26**, 301–325. doi: 10.1111/j.1096-0031.2009.00286.x.

Weigert A, Helm C, Meyer M, Nickel B, Arendt D, Hausdorf B, Santos SR, Halanych KM, Purschke G, Bleidorn C & Struck TH (2014) Illuminating the base of the Annelid tree using transcriptomics. *Molecular Biology and Evolution*, **31**, 1391–1401. doi: 10.1093/molbev/msu080.

Wheeler QD (2004) Taxonomic triage and the poverty of phylogeny. *Philosophical transactions of the Royal Society of London. Series B, Biological sciences*, **359**, 571–583. doi: 10.1098/rstb.2003.1452.

Whelan N V., Kocot KM, Santos SR & Halanych KM (2014) Nemertean Toxin Genes Revealed through Transcriptome Sequencing. *Genome Biology and Evolution*, **6**, 3314–3325. doi: 10.1093/gbe/evu258.

Wickham DE (1979) Predation by the nemertean Carcinonemertes errans on eggs of the Dungeness crab Cancer magister. *Marine Biology*, **55**, 45–53.

Wickham DE (1980) Aspects of the life history of *Carcinonemertes errans* (Nemertea:Carcinonemertidae), an egg predator of the carb Cancer magister. *The Biological Bulletin*, **159**, 247–257.

Wijnhoff G (1912) List of nemerteans collected in the neighbourhood of Plymouth from May-September, 1910. *Journal of the Marine Biological Association of the United Kingdom*, **9**, 407–434.

Wijnhoff GS (1936) Die Polystilifera der Siboga-Expedition. *Siboga Expedition*, **22**, 1-214.

Will KW, Mishler BD & Wheeler QD (2005) The Perils of DNA Barcoding and the Need for Integrative Taxonomy. *Systematic Biology*, **54**, 844–851. doi: 10.1080/10635150500354878.

Wilson EO (1985) Time to Revive Systematics. *Science*, **230**, 4731. 10.1126/science.230.4731.1227

Yao H, Song J, Liu C, Luo K, Han J, Li Y, Pang X, Xu H, Zhu Y, Xiao P & Chen S (2010) Use of ITS2 region as the universal DNA barcode for plants and animals. *PLoS ONE*, **5**. doi: 10.1371/journal.pone.0013102.

Yeates DK, Seago A, Nelson L *et al.* (2011) Integrative taxonomy, or iterative taxonomy? *Systematic Entomology*, **36**, 209–217. doi: 10.1111/j.1365-3113.2010.00558.x.

Zhang J, Kapli P, Pavlidis P & Stamatakis A (2013) A general species delimitation method with applications to phylogenetic placements. *Bioinformatics*, **29**, 2869–2876. doi: 10.1093/bioinformatics/btt499.

Appendix

I. Supplementary material Chapter 2

Supplementary Table 1 List of primers used in the present study

Target	Primer	Primer sequence	Reference
COI mtDNA	LCO1490	5'-GGTCAACAAATCA TAAAGATATTGG-3'	Folmer *et al*. 1994
	HCO1298	5'-TAAACTTCAGGGT GACCAAAAAATCA-3'	Folmer *et al*. 1994
16S rRNA	ar-L	5'-CGCCTGTTTATC AAAAACAT-3	Palumbi 1996
	br-H	5'-CCGGTCTGAACTC AGATCACGT-3'	Palumbi 1996
28S rRNA	28S (+)	5'-AGTAAGCGGAGGA AAAGAAACTAACCAG-3'	Sadler 2010 unpublished
	28S (-)	5'-GAATCGCTACGGA CCTCCACCAG-3'	Sadler 2010 unpublished

Supplementary Table 2. List of nemertean species included in the phylogenetic analysis, their GenBank accession numbers and references.

Species	**COI**	**16S**	**28S**
Amphiporus imparispinosus Griffin, 1989	HQ848612 (Andrade *et al*. 2012)	AJ436788 (Thollesson & Norenburg 2003)	HQ856878 (Andrade *et al*. 2012)
Amphiporus lactifloreus (Johston, 1828)	HQ848611 (Andrade *et al*. 2012)	JF277617 (Andrade *et al*. 2012)	HQ856876 (Andrade *et al*. 2012)
Prosorhochmus americanus Gibson *et al*. 1986	HQ848595 (Andrade *et al*. 2012)	EF157576 (Maslakova & Norenburg 2008)	HQ856879 (Andrade *et al*. 2012)
***Prosorhochmus claparedii* Keferstein, 1862**	**KP203862 (present study)**	**KP203860 (present study)**	**KP203861 (present study)**
Prosorhochmus nelsoni Sánchez, 1973	HQ848606 (Andrade *et al*. 2012)	JF277604 (Andrade *et al*. 2012)	HQ856891 (Andrade *et al*. 2012)

Species	COI	16S	28S
Geonemertes pelaensis Semper, 1863	HQ848592 (Andrade *et al*. 2012)	JF277610 (Andrade *et al*. 2012)	HQ856888 (Andrade *et al*. 2012)
Malacobdella grossa (Müller, 1776)	HQ848591 (Andrade *et al*. 2012)	JF277614 (Andrade *et al*. 2012)	HQ856882 (Andrade *et al*. 2012)
Carcinonemertes carcinophila (Kölliker, 1845)	HQ848619 (Andrade *et al*. 2012)	JF277603 (Andrade *et al*. 2012)	HQ856893 (Andrade *et al*. 2012)
Gononemertes parasita Bergendal, 1900	HQ848607 (Andrade *et al*. 2012)	JF277606 (Andrade et al. 2012)	HQ856889 (Andrade *et al*. 2012)
Emplectonema buergeri Coe, 1901	HQ848600 (Andrade *et al*. 2012)	JF277616 (Andrade *et al*. 2012)	HQ856880 (Andrade *et al*. 2012)
Emplectonema gracile (Johnston, 1837)	HQ848620 (Andrade *et al*. 2012)	JF277621 (Andrade *et al*. 2012)	HQ856883 (Andrade *et al*. 2012)
Nipponemertes pulcher (Johston, 1837)	HQ848597 (Andrade *et al*. 2012)	JF277625 (Andrade *et al*. 2012)	HQ856871 (Andrade *et al*. 2012)
Zygonemertes virescens (Verrill, 1879)	HQ848590 (Andrade *et al*. 2012)	JF277615 (Andrade *et al*. 2012)	HQ856885 (Andrade *et al*. 2012)
Protopelagonemertes beebei Coe, 1936	HQ848602 (Andrade *et al*. 2012)	JF277629 (Andrade *et al*. 2012)	HQ856873 (Andrade *et al*. 2012)
Argonemertes australiensis (Dendy, 1892)	HQ848601 (Andrade *et al*. 2012)	JF277605 (Andrade *et al*. 2012)	HQ856892 (Andrade *et al*. 2012)
Nemertopsis bivittata (Delle Chiaje, 1841)	HQ848608 (Andrade *et al*. 2012)	JF277609 (Andrade *et al*. 2012)	HQ856877 (Andrade *et al*. 2012)
Ototyphlonemertes correae Envall, 1996	HQ848613 (Andrade *et al*. 2012)	JF277612 (Andrade *et al*. 2012)	HQ856884 (Andrade *et al*. 2012)
Ototyphlonemertes macintoshi Bürger, 1895	HQ848605 (Andrade *et al*. 2012)	JF277613 (Andrade *et al*. 2012)	HQ856886 (Andrade *et al*. 2012)
Paranemertes sp. Coe, 1901	AJ436916 (Thollesson & Norenburg 2003)	AJ436806 (Thollesson & Norenburg 2003)	AJ436861 (Thollesson & Norenburg 2003)
Paranemertes sanjuanensis Stricker, 1982	AJ436917 (Thollesson & Norenburg 2003)	AJ436807 (Thollesson & Norenburg 2003)	AJ436862 (Thollesson & Norenburg 2003)
Paranemertes peregrina Coe, 1901	AJ436915 (Thollesson & Norenburg 2003)	AJ436805 (Thollesson & Norenburg 2003)	AJ436860 (Thollesson & Norenburg 2003)

Species	COI	16S	28S
Poseidonemertidae 2011 Chernyshev, 2002	**KP203859 (present study)**	**KP203857 (present study)**	**KP203858 (present study)**
Poseidonemertes sp. 508 Kirsteuer, 1967	AJ436918 (Thollesson & Norenburg 2003)	AJ436808 (Thollesson & Norenburg 2003)	AJ436863 (Thollesson & Norenburg 2003)
Poseidonemertes sp. 349	AJ436906 (Thollesson & Norenburg 2003)	AJ436796 (Thollesson & Norenburg 2003)	AJ436851 (Thollesson & Norenburg 2003)
Poseidonemertes collaris Roe & Wickham, 1984	AJ436919 (Thollesson & Norenburg 2003)	AJ436809 (Thollesson & Norenburg 2003)	AJ436864 (Thollesson & Norenburg 2003)
Arenogigas armoricus	**KP119170 (present study)**	**KP119167 (present study)**	**KP119169 (present study)**
Paradrepanophorus crassus (Quatrefages, 1846)	HQ848603 (Andrade *et al*. 2012)	JF277628 (Andrade *et al*. 2012)	HQ856867 (Andrade *et al*. 2012)
Cephalothrix rufifrons (Johnston, 1837)	HQ848604 (Andrade *et al*. 2012)	JF277529 (Andrade *et al*. 2012)	HQ856841 (Andrade *et al*. 2012)
Baseodiscus unicolor Stiasny-Wijnhoff, 1925	KF935505 (Kvist *et al*. 2014)	KF935452 (Kvist *et al*. 2014)	KF935341 (Kvist *et al*. 2014)
Lineus longissimus (Gunnerus, 1770)	GU392023 (Strand & Sundberg 2011)	DQ911377 (Sundberg & Strand 2007)	AJ436880 (Thollesson & Norenburg 2003)
Hubrechtella dubia Bergendahl, 1902	HQ848631 (Andrade *et al*. 2012)	JF277630 (Andrade *et al*. 2012)	HQ856897 (Andrade *et al*. 2012)

II. Supplementary material Chapter 3

Supplementary Table 3 List of collected specimens with Museum collection number/specimen IDs, sampling locality, GenBank accession numbers for COI, 16S, ITS, and collection date. Specimens are ordered by morphospecies: *Lineus viridis*, *Lineus clandestinus*, *Lineus ruber*, *Ramphogordius sanguineus*, and *Riseriellus occultus*.

Morphospecies	Specimen ID	Localitiy	COI	16S	ITS	Collection date
Lineus viridis	Lv2Hl10	Helgoland	KM878335	-	-	November 2010
	Lv3Hl10	Helgoland	KM878336	-	-	November 2010
	Lv53Sy11	Sylt	KM878337	-	-	February 2011
	Lv38Sy11	Sylt	KM878338	-	-	February 2011
	Lv25Sy11	Sylt	KM878339	-	-	February 2011
	Lv45Sy11	Sylt	KM878340	-	-	February 2011
	Lv10Hl10	Helgoland	KM878341	-	-	November 2010
	Lv34Sy11	Sylt	KM878342	-	-	February 2011
	Lv44Sy11	Sylt	KM878343	-	-	February 2011
	Lv50Sy11	Sylt	KM878344	-	-	February 2011
	Lv8Hl10	Helgoland	KM878345	KM878511	KM878526	November 2010
	Lv42Sy11	Sylt	KM878346	-	-	February 2011
	Lv31Sy11	Sylt	KM878347	-	-	February 2011
	Lv6Rsc10	Roscoff	KM878348	-	-	May 2010
	Lv47Sy11	Sylt	KM878349	-	-	February 2011
	Lv3Rsc10	Roscoff	KM878350	-	-	May 2010
	Lv23SSy11	Sylt	KM878351	-	-	February 2011
	Lv37Sy11	Sylt	KM878352	-	KM878521	February 2011
	Lv40Sy11	Sylt	KM878353	-	-	February 2011
	Lv8Rsc10	Roscoff	KM878354	-	-	May 2010
	Lv15Sy11	Sylt	KM878355	-	-	February 2011
	Lv4Rsc11	Roscoff	KM878356	-	-	April 2011
	Lv4Rsc10	Roscoff	KM878357	-	-	May 2010

Morphospecies	Specimen ID	Localitiy	COI	16S	ITS	Collection date
	Lv5Sy11	Sylt	KM878358	-	-	February 2011
	Lv16Sy11	Sylt	KM878359	-	-	February 2011
	Lv6Sy11	Sylt	KM878360	-	-	February 2011
	Lv17Sy11	Sylt	KM878361	-	-	February 2011
	Lv18Sy11	Sylt	KM878362	-	-	February 2011
	Lv22Sy11	Sylt	KM878363	-	-	February 2011
	Lv9Sy11	Sylt	KM878364	-	-	February 2011
	Lv19Sy11	Sylt	KM878365	-	-	February 2011
	Lv10Sy11	Sylt	KM878366	-	-	February 2011
	Lv20Sy11	Sylt	KM878367	-	-	February 2011
	Lv9Hl10	Helgoland	KM878368	-	-	November 2010
	Lv12Sy11	Sylt	KM878369	-	-	February 2011
	Lv1Sy11	Sylt	KM878370	-		February 2011
	Lv13Sy11	Sylt	KM878371	KM878514	KM878520	February 2011
	Lv3Sy11	Sylt	KM878372	-	-	February 2011
	Lv4Sy11	Sylt	KM878373	-	-	February 2011
	Lv14Sy11	Sylt	KM878374	-	-	February 2011
	Lv8Sy11	Sylt	KM878375	-	-	February 2011
	Lv29Sy11	Sylt	KM878376	-	-	February 2011
	Lv6Hl10	Helgoland	KM878377	-	-	November 2010
	Lv46Sy11	Sylt	KM878378	-	-	February 2011
	Lv48Sy11	Sylt	KM878379	-	-	February 2011
	Lv49Sy11	Sylt	KM878380	-	-	February 2011
	Lv51Sy11	Sylt	KM878381	-	-	February 2011
	Lv52Sy11	Sylt	KM878382	-	-	February 2011
	Lv39Sy11	Sylt	KM878383	-	-	February 2011
	Lv4Hl10	Helgoland	KM878384	KM878512	KM878523	November 2010

Morphospecies	Specimen ID	Localitiy	COI	16S	ITS	Collection date
	Lv54Sy11	Sylt	KM878385	-	-	February 2011
	Lv5Hl10	Helgoland	KM878386	-	-	November 2010
	Lv2Rsc10	Roscoff	KM878387	-	-	May 2010
	Lv5Rsc10	Roscoff	KM878388	-	-	May 2010
	Lv3Con11	Concarneau	KM878390	-	-	September 2011
	Lv11Sy11	Sylt	KM878391	-	-	February 2011
	GNM Nem.146/ Lv1Rsc10	**Roscoff**	**KM878392**	**-**	**-**	**May 2010**
	Lv2Con11	Concarneau	KM878393	-	-	September 2011
	Lv2Rsc11	Roscoff	KM878394	-	-	April 2011
	Lv1Rsc11	Roscoff	KM878395	-	-	April 2011
	GNM Nem.144/ Lv6Wi12	**Wimereux**	**KM878396**	**-**	**-**	**November 2012**
	GNM Nem.145/ Lv7Wi12	**Wimereux**	**KM878397**	**-**	**-**	**November 2012**
	Lv2Wi12	Wimereux	KM878398	-	-	November 2012
	GNM Nem.143/ Lv1Wi12	**Wimereux**	**KM878399**	**KM878513**	**KM878522**	**November 2012**
	Lv5Wi13	Wimereux	KM878400	-	-	October 2013
	Lv7Wi13	Wimereux	KM878401	-	-	October 2013
	Lv2Wi13	Wimereux	KM878402	-	-	October 2013
	Lv3Wi13	Wimereux	KM878403	-	-	October 2013
	Lv8Wi13	Wimereux	KM878404	-	-	October 2013
	Lv6Wi13	Wimereux	KM878405	-	-	October 2013
	Lv10Wi13	Wimereux	KM878406	-	-	October 2013
	Lv9Wi13	Wimereux	KM878407	-	-	October 2013
	Lv11Wi13	Wimereux	KM878408	-	-	October 2013

Morphospecies	Specimen ID	Localitiy	COI	16S	ITS	Collection date
Lineus clandestinus	Lv27Rsc10	Roscoff	KM878409	KM878517	KM878524	May 2010
	Lv9Rsc10	Roscoff	KM878410	-	-	May 2010
	Lv1Con11	Concarneau	KM878411	-	-	September 2011
	Lv5Rsc11	Roscoff	KM878412	-	-	April 2011
	Lv2Con13	Concarneau	KM878413	KM878515	KM878519	March 2013
	Lv1Wi13	Wimereux	KM878414	-	-	October 2013
	Lv7Rsc10	Roscoff	KM878415	-	-	May 2010
	GNM Nem.142/ Lv2Rsc12	**Roscoff**	**KM878416**	**-**	**-**	**September 2012**
	Lv71Sy11	Sylt	KM878417	-	-	February 2011
	Lv1Sy10	Sylt	KM878418	-	-	January 2010
	Lv28Sy11*	Sylt	KM878419	KM878498	KM878530	February 2011
	Lv62Sy11	Sylt	KM878420	-	-	February 2011
	Lv55Sy11	Sylt	KM878421	-	-	February 2011
	Lv2Sy10	Sylt	KM878422	-	-	January 2010
	Lv63Sy11	Sylt	KM878423	-	-	February 2011
	GNM Nem.154/ Lv56Sy11	**Sylt**	**KM878424**	**-**	**-**	**February 2011**
	Lv30Sy11	Sylt	KM878425	-	-	February 2011
	Lv64Sy11	Sylt	KM878426	-	-	February 2011
	Lv41Sy11	Sylt	KM878427	-	-	February 2011
	Lv21Sy11	Sylt	KM878428	-	-	February 2011
	Lv7Sy11	Sylt	KM878429	-	-	February 2011
	Lv65Sy11	Sylt	KM878430	-	-	February 2011
	Lv32Sy11	Sylt	KM878431	-	-	February 2011
	Lv4Con13*	Concarneau	KM878432	KM878503	KM878527	March 2013
	Lv57Sy11	Sylt	KM878433	-	-	February 2011

Morphospecies	Specimen ID	Localitiy	COI	16S	ITS	Collection date
	Lv66Sy11	Sylt	KM878434	-	-	February 2011
	Lv58Sy11	Sylt	KM878435	KM878500	KM878531	February 2011
	Lv67Sy11	Sylt	KM878436	-	-	February 2011
	Lv24Sy11	Sylt	KM878437	-	-	February 2011
	GNM Nem.151/ Lv7Idg12	**Île de Groix**	**KM878438**	**KM878499**	**KM878528**	**September 2012**
	Lv59Sy11	Sylt	KM878439	-	-	February 2011
	Lv68Sy11	Sylt	KM878440	-	-	February 2011
	Lv35Sy11	Sylt	KM878441	-	-	February 2011
	Lv6Idg12	Île de Groix	KM878442	-	-	September 2012
	Lv69Sy11	Sylt	KM878443	-	-	February 2011
	Lv26Sy11	Sylt	KM878444	-	-	February 2011
	Lv5Idg12	Île de Groix	KM878445	-	-	September 2012
	Lv60Sy11	Sylt	KM878446	-	-	February 2011
	Lv70Sy11	Sylt	KM878447	-	-	February 2011
	Lv27Sy11	Sylt	KM878448	-	-	February 2011
	Lv61Sy11	Sylt	KM878449	-	-	February 2011
	Lv1Idg12	Île de Groix	KM878450	-	-	September 201
	Lv43Sy11	Sylt	KM878451	-	-	February 201
	Lv7Hl10	Helgoland	KM878452	KM878502	KM878532	November 20120
	Lv3Sy10	Sylt	KM878453	-	-	January 2010
	GNM Nem.150/ Lv5Wi12	**Wimereux**	**KM878454**	**KM878501**	**KM878533**	**November 2012**
	GNM Nem.152/ Lv28Rsc10	**Roscoff**	**KM878455**	**KM878504**	**KM878529**	**May 2010**
	Lv33Sy11	Sylt	KM878456	-	-	February 2011

Morphospecies	Specimen ID	Localitiy	COI	16S	ITS	Collection date
Lineus ruber	**GNM Nem.153/ Lv3Rsc12**	**Roscoff**	**KM878457**	**-**	**-**	**September 2012**
	Lr7Idg12	Île de Groix	KM878458	-	-	September 2012
	Lr8Idg12	Île de Groix	KM878459	-	-	September 2012
	Lr4Idg12	Île de Groix	KM878460	-	-	September 2012
	Lr1Idg12	Île de Groix	KM878461	KM878506	-	September 2012
	Lr1Rsc10	Roscoff	KM878462	-	-	May 2010
	Lr1Con13	Concarneau	KM878463	KM878510	KM878538	March 2013
	GNM Nem.148/ Lr4Rsc12	**Roscoff**	**KM878464**	**-**	**-**	**September 2012**
	Lr3Rsc12	Roscoff	KM878465	-	-	September 2012
	Lr7Rsc11	Roscoff	KM878466	KM878505	KM878534	April 2011
	Lr8Rsc10	Roscoff	KM878467	KM878507	KM878535	May 2010
	Lr21Rsc10	Roscoff	KM878468	-	-	May 2010
	Lr9Rsc10	Roscoff	KM878469	-	-	May 2010
	Lr23Rsc10	Roscoff	KM878470	-	-	May 2010
	Lr1Rsc11	Roscoff	KM878471	-	-	April 2011
	Lr24Rsc10	Roscoff	KM878472	-	-	May 2010
	Lr12Rsc11	Roscoff	KM878473	KM878509	KM878537	April 2011
	Lr2Rsc11	Roscoff	KM878474	-	-	April 2011
	Lr15Rsc10	Roscoff	KM878475	-	-	May 2010
	Lr5Rsc11	Roscoff	KM878476	-	-	April 2011
	Lr17Rsc10	Roscoff	KM878478	-	-	May 2010
	Lr18Rsc10	Roscoff	KM878479	-	-	May 2010
	Lr3Rsc10	Roscoff	KM878480	-	-	May 2010
	Lr19Rsc10	Roscoff	KM878481	-	-	May 2010

Morphospecies	Specimen ID	Localitiy	COI	16S	ITS	Collection date
	GNM Nem.147/ Lr7Rsc12	Roscoff	KM878482	-	-	September 2012
	Lr2Rsc12	Roscoff	KM878483	-	-	September 2012
	Lr1Rsc12	Roscoff	KM878484	-	-	September 2012
	Lr20Rsc10	Roscoff	KM878485	-	-	May 2010
	Lr25Rsc10	Roscoff	KM878486	-	-	May 2010
	Lr7Wi13	Wimereux	KM878487	-	-	October 2013
	Lr1Wi13	Wimereux	KM878488	-	-	October 2013
	Lr4Wi12	Wimereux	KM878489	KM878508	KM878536	November 2012
	Lr11Wi13	Wimereux	KM878490	-	-	October 2013
	Lr12Wi13	Wimereux	KM878491	-	-	October 2013
	Lr4Wi13	Wimereux	KM878492	-	-	October 2013
	Lr13Rsc10	Roscoff	KM878493	-	-	May 2010
	Lr11Rsc10	Roscoff	KM878494	-	-	May 2010
Ramphogordius sanguineus	Rs1Con12	Concarneau	KM878495	KM878497	-	September 2012
Riseriellus occultus	Ro1Con11	Concarneau	KM878496	KM878518	KM878539	April 2011

Supplementary Table 4 List of primer pairs used in this study.

Target	Primer Name	Primer sequence	Reference
COI	LCO1490	5'-GGTCAACAAATCATAAAGATATTGG-3'	Folmer *et al.* 1994
	HCO1298	5'-TAAACTTCAGGGTGACCAAAAAATCA-3'	Folmer *et al,* 1994
16S	ar-L	5'-CGCCTGTTTATCAAAAACAT-3	Palumbi *et al*. 1996
	br-H	5'-CCGGTCTGAACTCAGATCACGT-3'	Palumbi *et al*. 1996
ITS	ITS-28S-*Lineus*	5'-TTTTCAACTTTCCCTCACGG-3'	This study
	ITS-18S-*Lineus*	5'-CATTTGAGGAAGTAAAAGTCGTAAC-3'	This study

Supplementary Table 5 List of GenBank specimens used for the maximum likelihood analyses based on COI mtDNA and 16S rRNA with Genbank accession numbers, sampling locality (country) and references. Specimens are ordered by morphospecies: *Lineus viridis*, *Lineus clandestinus*, *Lineus ruber*, and *Ramphogordius sanguineus*. CL, Chile; DE, Germany; SE, Sweden; UK, United Kingdom; USA, Maine, United States of America.

Morphospecies	Species	Localitiy	COI	16S	Reference
Lineus viridis	*L. viridis*	DE	HQ848579	JF277582	Andrade *et al*. 2012
	L. viridis	DE	FJ839919	-	Podsiadlowski *et al*. 2009
	L. viridis	USA	EF124974	EF124886	Schwartz & Norenburg 2006
	L. viridis	USA	AJ436936	AJ436826	Thollesson & Norenburg 2003
	L. viridis	UK	KC812597	-	Strand *et al*. 2014
	L. viridis	UK	KC812596	-	Strand *et al*. 2014
	L. ruber/viridis	SE	GU392024	-	Strand & Sundberg 2011
	L. ruber	USA	EF124970	EF124883	Schwartz & Norenburg 2006
	L. ruber	SE	-	AF103759	Sundberg & Saur 1998
Lineus clandestinus	*L. ruber*	SE	-	AF103758	Sundberg & Saur 1998
	L. viridis	UK	-	AF103760	Sundberg & Saur 1998
Lineus ruber	*L. ruber*	UK	KC812602	-	Strand *et al*. 2014
	L. ruber	UK	-	AF103757	Sundberg & Saur 1998
Ramphogordius sanguineus	*L. ruber*	UK	DQ911370	DQ911371	Sundberg & Strand 2007
	L. ruber	CL	KC812595	-	Strand *et al*. 2014

III. Supplementary material Chapter 4

Supplementary Table 6 List of synonyms and references for *Tubulanus polymorphus* and *Tubulanus ruber*

	***Tubulanus polymorphus* described/mentioned as:**	***Tubulanus ruber* described/mentioned as:**
Renier 1804	*Tubulanus polymorphus*	
Delle Chiaje 1829	*Ophyocephalus polymorphus*	
Oersted 1844	*Nemertes polymorpha*	
Quatrefages 1846	*Valencinia splendida*	
Diesing 1862	*Valencinia splendida*	
Bürger 1888	*Carinella polymorpha*	
Bürger 1890	*Carinella polymorpha*	
Bürger 1892	*Carinella polymorpha*	
Bürger 1895	*Carinella polymorpha*	
Bürger 1897-1907	*Carinella polymorpha*	
Bürger 1904	*Tubulanus polymorphus*	
Griffin 1898		*Carinella rubra*
Joubin 1890	*Carinella polymorpha*	
Riches 1893	*Carinella polymorpha*	
Allen & Todd 1900	*Carinella polymorpha*	
Sheldon 1901	*Carinella polymorpha*	
Coe 1901		*Carinella speciosa*
Bergendahl 1903	*Carinella polymorpha*	
Punnet 1903	*Carinella polymorpha*	
Coe 1904		*Carinella speciosa*, *Carinella rubra*
Coe 1905		*Carinella rubra*
Wijnhoff 1912	*Tubulanus polymorphus*	
Southern 1913	*Tubulanus polymorphus*	
Friedrich 1936	*Tubulanus polymorphus*	
Coe 1940	*Tubulanus polymorphus*	*Tubulanus polymorphus*
Gontcharoff 1955	*Tubulanus polymorphus*	
Ricketts & Calvin 1956		*Carinella rubra*
Hylbom 1957	*Tubulanus polymorphus*	
Friedrich 1958	*Tubulanus polymorphus*	
Corrêa 1964		*Tubulanus polymorphus*
Brusca & Brusca 1973		*Tubulanus polymorphus*
Melville 1986	*Tubulanus polymorphus*	*Tubulanus polymorphus*
Stricker 1987		*Tubulanus polymorphus*
Blake 1993		*Tubulanus polymorphus*

	***Tubulanus polymorphus* described/mentioned as:**	***Tubulanus ruber* described/mentioned as:**
Stricker & Folsom 1998		*Tubulanus polymorphus*
Stricker et al. 2001		*Tubulanus polymorphus*
von Döhren *et al*. 2010		*Tubulanus polymorphus*
Andrade *et al*. 2012		*Tubulanus polymorphus*
Beckers 2013	*Tubulanus polymorphus*	*Tubulanus polymorphus*
Mulligan 2014		*Tubulanus polymorphus*
Hiebert 2015		*Tubulanus polymorphus*

Supplementary Table 7 List of GenBank specimens used for phylogenetic analyses based on COI and 16S. ** indicates neotype *T. polymorphus* and *T. ruber*, * indicates voucher specimens for *T. polymorphus* and *T. ruber*.

Taxa	COI	16S	Reference
Callinera grandis Bergendahl, 1903	HQ848626	JF277570	Andrade *et al*. 2012
Carinina ochracea Sundberg et al., 2009	HQ848627	JF277631	Andrade *et al*. 2012
Carinoma hamanako Kajihara et al., 2011	HQ848628	JF277600	Andrade *et al*. 2012
Carinoma tremaphoros Thompson, 1900	HQ848630	JF277602	Andrade *et al*. 2012
Cephalothrix bipunctata Bürger, 1892	KF935591	KF935447	Kvist *et al*. 2014
Cephalothrix filiformis (Johnston, 1828)	HQ848617	JF277593	Andrade *et al*. 2012
Cephalothrix honkongiensis Sundberg et al., 2003	HQ848615	JF277590	Andrade *et al*. 2012
Cephalothrix rufifrons (Johnston, 1837)	HQ848604	JF277592	Andrade *et al*. 2012
Cephalothrix simula (Iwata, 1952)	AJ436945	AJ436836	Thollesson & Norenburg 2003
Cephalothrix spiralis Coe, 1930	AJ436946	AJ436837	Thollesson & Norenburg 2003
Tubulanus annulatus (Montagu, 1804)	HQ848622	JF277599	Andrade *et al*. 2012
Tubulanus pellicidus (Coe, 1895)	HQ848625	JF277595	Andrade *et al*. 2012
***Tubulanus ruber*/TR1/SBMNH465922** (Griffin, 1828)**	**KX853121**	**KX853117**	**This study**
Tubulanus ruber*/TR4/SBMNH465922 (Griffin, 1828)**	**KX853122**	**KX853118**	**This study**
Tubulanus polymorphus Renier, 1904	HQ848621	JF277598	Andrade *et al*. 2012

Taxa	COI	16S	Reference
Tubulanus polymorphus*/TP12/GNM Nemertinea 157 Renier, 1904*	**KX853120**		**This study**
Tubulanus polymorphus*/TP11/GNM Nemertinea 158 Renier, 1904	**KX853119**	**KX853116**	**This study**
Tubulanus punctatus (Takakura, 1898)	HQ848624	JF277597	Andrade *et al*. 2012
Tubulanus rhabdotus Corrêa, 1954	AJ436948	AJ436839	Thollesson & Norenburg 2003
***Tubulanus superbus*/TS8 (Kölliker, 1845)**	**KX857632**	**KX857631**	**This study**
Terebratalia transversa	JF509715	JF509720	Andrade *et al*. 2012

Supplementary Table 8 Character checklist after Sundberg *et al*. 2016

Character	***Tubulanus polymorphus***	***Tubulanus ruber***
1. Biology	0 (Free-living)	0 (Free-living)
2. Habitat	0 (Marine)	0 (Marine)
3. Benthic divisions	2 (Sublittoral)	1 (Littoral)
4. (Pelagic divisions)	0 (Epipelagic)	0 (Epipelagic)
5. Habitat	1 (Infaunal)	2 (Epibenthic)
6. Substratum	1 (Sand)	2 (Rock/boulders)
7. Behavior when mechanically disturbed	6 (Spontaneous fragmentation)	unknown
8. Cephalic furrows/slits	1 (one pair)	1 (one pair)
9. Distribution of anterior cephalic furrows/slits	1 (Dorsal)	4 (Ventral and dorsal)
10. Shape of anterior (dorsal) cephalic furrows (viewed with tip of head directing forwards)	0 (V-sphape or oblique)	0 (V-sphape or oblique)
11. Shape of posterior (dorsal) cephalic furrows (viewed with tip of head directing forwards) Constrictions at posterior of cephalic slits	N/A	N/A
12. Head clearly demarcated from body	1 (Head wider than trunk)	1 (Head wider than trunk)
13. Position of cephalic furrows	1 (If single pair in front of brain lobes)	1 (If single pair in front of brain lobes)

Character	*Tubulanus polymorphus*	*Tubulanus ruber*
14. Shape of head/cephalic lobe	5/10 (Spatulate/ shield-shaped)	5/10 (Spatulate/ shield-shaped)
15. Head viewed laterally	0 (without extensions)	0 (without extensions)
16. Cross section shape of body	1 (Dorsally-ventrally flattened)	0 (Rounded-cylindrical)
17. Shape of posterior tip	N/A	N/A
18. Eyes	0 (absent)	0 (absent)
19. Eye distinctiveness	N/A	N/A
20. Eye morphology	N/A	N/A
21. Relative eye size	N/A	N/A
22. Eye position relative to brian lobes	N/A	N/A
23. General body color	1 (Dark)	2 (Pale/light)
24. Primary dorsal body color	0 (red)	6 (orange)
25. Color pattern	0 (absent)	0 (absent)
26. Color of blood	3 (not applicaple)	3 (not applicable)
27. Proboscis armature	0 (absent)	0 (absent)
28. Number of accessory stylet pouches	N/A	N/A
29. Number of stylets in each accessory stylet pouch)	N/A	N/A
30. Stylet: basis/stylet ratio	N/A	N/A
31. Stylet shaft	N/A	N/A
32. Shape of stylet basis	N/A	N/A
33. Median waist of stylet basis	N/A	N/A
34. Proboscis used for locomotion	0 (unknown)	0 (unknown)
35. Proboscis pore	1 (subterminal, ventral)	1 (subterminal, ventral)
36. Position of mouth	2 (Just behind brain)	2 (just behind brain)
37. Shape of mouth	1 (elongate slit)	1 (elongate slit)
38. Lateral margins	1 (no distinction in coloration)	1 (no distinction in coloration)
39. Distribution of bristles/cirri	0 (not seen)	0 (not seen)

IV. Publikationen & Tagungsbeiträge

Publikationen

Daria Krämer, Patrick Beckers, & Jörn von Döhren (submitted). Redescription of *Tubulanus polymorphus* Renier, 1804 (Palaeonemertea, Nemertea) leads to the re-establishment of *Tubulanus* (*Carinella*) *ruber* (Griffin, 1898).

Daria Krämer; Christian Schmidt; Lars Podsiadlowski; Patrick Beckers; Lisa Horn; Jörn von Döhren (2016). Unravelling the *Lineus ruber*/*viridis* species complex (Nemertea, Heteronemertea). Zoologica Scripta. doi:10.1111/zsc.12185.

Daria Krämer & Jörn von Döhren (2015). *Arenogigas armoricus*, a new genus and species of a monostiliferous hoplonemertean (Nemertea) from the North-West coast of France. Zoological Science 32: 605-614. doi:10.2108/zs140266.

Per Sundberg; Sónia C. S. Andrade; Thomas Bartolomaeus; Patrick Beckers; Jörn von Döhren; **Daria Krämer**; Ray Gibson; Gonzalo Giribet; Alfonso Herrera-Bachiller; Juan Junoy; Hiroshi Kajihara; Sebastian Kvist; Tobias Kånneby; Shi-Chun Sun; Marthin Thiel; James M. Turbeville; Malin Strand (2016). The future of nemertean taxonomy (phylum Nemertea) – a proposal. Zoologica Scripta. doi:10.1111/zsc.12182.

Marion Schneider; Benjamin Klein; **Daria Krämer**, Kristina Knezevic; Lydia Tiflova; Solveigh Vogt; Anna Rauhaus; Karin Van der Straeten; Ditlev Karbe; Ralph Sommerlad & Thomas Ziegler (2014). First observations on the coutship, mating, and nest visit behaviour of the Philippine crocodile (*Crocodylus mindorensis*) at the Cologne Zoo. jzar - Journal of Zoo and Aquarium Research **2**(4): 123-129.

Tagungsbeiträge

Symposium “Systematics and Biodiversity Research in the Era of Genomics” (2015) in Oslo, Norwegen, organisiert von “The Norwegian Academy of Sciences and Letters and the Editors of Zoologica Scripta”. **Teilnahme**.

Daria Krämer, Christian Schmidt; Thomas Bartolomaeus; Lisa Horn; Jörn von Döhren (2015) Nemertean diversity was likely underestimated in the past – the case of the *Lineus ruber*/*viridis*-species complex (Nemertea: Heteronemertea). **Vortrag**: DZG Graduate Meeting Zoological Systematics Bonn 2015 – Cryptic speciation, Challenges to modern taxonomy.

Daria Krämer; Thomas Bartolomaeus; Jörn von Döhren (2015). A new monostiliferan species (Nemertea:Hoplonemertea) from the Mediterranean Sea in Italy. **3. Posterpreis für Poster Präsentation**: 16. Jahrestagung der Gesellschaft für Biologische Systematik (GfBS) in Bonn.

Jörn von Döhren; **Daria Krämer**; Thomas Bartolomaeus (2015) Analysis of a comprehensive data set on *Tubulanus polymorphus* Renier, 1804 leads to a separation of the species and to re-establishment of *Tubulanus* (*Carinella*) *ruber* (Griffin, 1898) **Poster Präsentation**: 16. Jahrestagung der Gesellschaft für Biologische Systematik (GfBS) in Bonn.

Daria Krämer, Christian Schmidt; Thomas Bartolomaeus; Lisa Horn; Jörn von Döhren (2014) Nemertean diversity was likely underestimated in the past – the case of the *Lineus ruber*/*viridis*-species complex (Nemertea: Heteronemertea). **Vortrag**: 107th Annual Meeting of the German Zoological Society in Göttingen
Daria Krämer; Thomas Bartolomaeus; Christian Schmidt; Lisa Horn; Jörn von Döhren (2014) Taking traditional knowledge to the future – a standard for reconciling morphology and barcodes in the *Lineus ruber*/*viridis* - species complex (Nemertea). **Poster Präsentation**: International Congress on Invertebrate Morphology (ICIM3) in Berlin.

Daria Krämer; Christian Schmidt;Thomas Bartolomaeus; Lisa Horn; Patrick Beckers; Jörn von Döhren (2014)Taking traditional knowledge to the future – a standard for reconciling morphology and barcodes in the *Lineus ruber*/*viridis* - species complex (Heteronemertea) **Vortrag**: 8th International Conference on Nemertean Biology in Qingdao, China.

Daria Krämer; Thomas Bartolomaeus; Patrick Beckers; Jörn von Döhren (2014) An undescribed Monostiliferan species (Nemertea: Hoplonemertea) from the Northwest Atlantic Coast of France. **Poster Präsentation**: 8th International Conference on Nemertean Biology in Qingdao, China.

Jörn von Döhren; **Daria Krämer**; Patrick Beckers; Thomas Bartolomaeus (2014) New Standards in the Taxonomy of Nemertea. **Poster Präsentation**: 8th International Conference on Nemertean Biology in Qingdao, China.

Daria Krämer; Jörn von Döhren; Thomas Bartolomaeus (2014) An undescribed Monostiliferan species (Nemertea: Hoplonemertea) from the Northwest Atlantic Coast of France. **Poster Präsentation**: 15. Jahrestagung der Gesellschaft für Biologische Systematik (GfBS) in Dresden.